Transglutaminase 2 is required for the survival and tumorigenicity of colorectal cancer cells through its transamidase activity by blocking p53 signaling

Transglutaminase ist für das Überleben und Tumorigenität von Darmkrebszellen durch das Blockieren des p53 Signalweges über seine Transaminase-Aktivität verantwortlich

Dissertation zur Erlangung des Doktorgrades

der Naturwissenschaften

vorgelegt beim Fachbereich Biowissenschaften (FB 15)

der Johann Wolfgang Goethe-Universität in Frankfurt am Main

von

Ilaria Lunger, aus Meran

Frankfurt am Main 2019

GOETHE
UNIVERSITÄT
FRANKFURT AM MAIN

Vom Fachbereich Biowissenschaften (FB 15) der

Johann Wolfgang Goethe-Universität als Dissertation angenommen

Dekan: Prof. Dr. Sven Klimpel

Gutachter: Prof. Dr. Amparo Acker-Palmer

Prof. Dr. Michael A. Rieger

Datum der Disputation:

Erklärung

Ich erkläre hiermit, dass ich mich bisher keiner Doktorprüfung im mathematisch- naturwissenschaftlichen Bereich unterzogen habe.

Frankfurt am Main, den ………………………………………
…………………………………………
(Unterschrift Ilaria Lunger)

Versicherung

Ich erkläre hiermit, dass ich die vorgelegte Dissertation über „Transglutaminase 2 is required for the survival and tumorigenicity of colorectal cancer cells through its transamidase activity by blocking p53 signaling" selbständig angefertigt und mich anderer Hilfsmittel als der in ihr angegebenen nicht bedient habe, insbesondere, dass alle Entlehnungen aus anderen Schriften mit Angabe der betreffenden Schrift gekennzeichnet sind. Ich versichere, die Grundsätze der guten wissenschaftlichen Praxis beachtet und nicht die Hilfe einer kommerziellen Promotionsvermittlung in Anspruch genommen zu haben.

Frankfurt am Main, den ………………………………………
…………………………………………
(Unterschrift Ilaria Lunger)

Table of Contents

II

Figures and tables

Summary

Worldwide, 14 million people suffer from cancer and 8.8 million people succumb to their disease every year. In Germany, the incidence is 480,000 new cases and 233,753 cancer-related deaths per year. About one in eight diagnosed cancers in Germany affects the gut. Almost 40% of patients die within the first 5 years after diagnosis of colorectal cancer. Therefore, a deeper understanding of colorectal cancer biology is needed to ensure further progress in finding novel treatment strategies and therefore improve quality of life. This applies to both, early and advanced tumor stages.

The aim of the present project was the identification of molecules that are involved in the development and progression of colon cancer, and to characterize their function in colon cancer cells. The identification of such molecules offers the opportunity to selectively target them by using selective drugs. Novel targeted therapies are immensely important to develop innovative options for the treatment of colorectal cancer.

Based on the expression strength of the surface marker protein CD133, that allows the enrichment for an aggressive cell subpopulation, a screening was established that allowed comparative protein expression analyzes between an aggressive and a highly aggressive tumor-cell-subpopulation. This enabled the identification of molecules that contribute to a particularly aggressive tumor growth and the potentially associated treatment failure. Among them, the multifunctional and bivalent enzyme tissue transglutaminase 2 (TGM2) was identified. The enzyme TGM2 belongs to the family of tissue transglutaminases (TGases) and has both transamidase and GTPase properties. Due to its diverse enzymatic activities, TGM2 has been implicated in a variety of diseases, including cancer. The first step in this work was to test, whether TGM2 was enriched in colon cancer tissue from patients. It could be demonstrated, that the protein expression level of TGM2 in tumor epithelial cells was significantly upregulated compared to the corresponding normal tissue. In addition, a significant increase in enzymatic transamidase activity was detectable. To further substantiate the hypothesis that TGM2 plays a central role in colon cancer, the influence of TGM2 expression on colorectal cancer cells were investigated by loss-of-function studies using gene engineering methods. With two independent shRNAs and CRISPR / Cas9 lentiviral vector systems, TGM2 expression was genetically reduced or completely deleted. Using either method, colon cancer cells showed an immediate inhibition of cell growth and expansion compared to control cells. Similarly, tumorigenicity and stem cell activity in 2D cultures were nearly abolished after loss of TGM2. Importantly, the same results were also observed in vivo. After TGM2 expression was reduced

in colon cancer cells by shRNAs and injected subcutaneously into NOD / SCID mice, their ability to form tumors was very much diminished compared to control animals.

To evaluate TGM2 inhibition for future clinical applications, preclinical xenograft models were established. The pharmacological inhibition of TGM2 in xenotransplantation models led to a significant delay in tumor initiation as well as to a considerable inhibition of tumor growth during the observation period. Furthermore, almost complete stagnation of tumor growth was achieved by inhibitor treatment of already established tumors in an animal xenograft model. In tumor-spheroid cultures of patient-derived tumor tissues, the treatment of primary tumor cells with tested drugs resulted in a significant reduction in tumor-spheroid formation and hence tumorigenicity.

To clarify whether a specific TGM2 isoform or enzymatic activity of TGM2 plays a predominant role in the development of colon cancer, various TGM2 constructs were generated for lentiviral gain-of-function studies. These experiments showed that the TGM2 transamidase activity of isoform 1 is crucial for the survival of tumor cells; Transaminase-inactive TGM2 variants were unable to rescue cells from cell death after loss of endogenous TGM2. Time-lapse microscope analysis and flow cytometry-based methods clarified the cell fate decision causing the growth disadvantage of colon cancer cells after loss of TGM2. TGM2 knockdown cells showed a massive induction of apoptosis following TGM2 knockdown with shRNAs compared to the control cells with functional TGM2. In addition, a significant increase of apoptotic cells and activation of caspase 3 were found. RNA-Seq data and protein-protein interaction analyzes support a link between TGM2 and signaling pathways that are critical for cancer development and progression. Mechanistically, TGM2 forms heteromeric compounds with the tumor suppressor gene p53 and thus directly influences the activity of p53. When TGM2 in colorectal cancer cells is inhibited by gene knock-down or pharmacological treatment, TGM2-mediated p53 inhibition is abolished, and phosphorylated p53 activates caspase 3 leading subsequently to apoptosis in colon cancer cells.

        The present study demonstrates for the first time the direct interaction and thus regulation of TGM2 and p53 in the pathophysiology of colorectal cancer. The transaminase activity of TGM2 is essential and potentially leads to covalently bound TGM2-p53 heterodimers. This prevents activation of p53 and leads to deregulated p53 signaling. In addition, it has been shown here that TGM2 transaminase activity and protein expression are highly upregulated in primary colorectal cancer tissue. Taken together, these results suggest that TGM2 plays a crucial role in the survival of colon cancer cells and that its targeted inhibition can effectively and sustainably reduce cell survival and tumorigenicity. Thus, TGM2 represents a promising target molecule that can contribute to the improvement of intestinal cancer targeted therapy.

Zusammenfassung

Weltweit erkranken jährlich 14 Millionen Menschen an Krebs und 8,8 Millionen Menschen erliegen ihrer Krankheit. In Deutschland liegt die Inzidenz bei 480.000 Neuerkrankungen und 233.753 krebsbezogener Todesfälle pro Jahr. Fast jede achte diagnostizierte Krebserkrankung in Deutschland betrifft den Darm, wobei Männer mit 33.100 Darmkrebserkrankten etwas häufiger betroffen sind als Frauen mit 27.900. Bezieht man diese Zahlen auf die Gesamtbevölkerung in Deutschland, erkrankt im Durchschnitt jeder 15. Mann und jede 18. Frau im Laufe ihres Lebens an Darmkrebs. Die relative 5-Jahres-Überlebensrate für Darmkrebspatienten liegt sowohl für Männer als auch für Frauen bei ca. 63 %. Umgekehrt bedeutet dies, dass fast 40 % der Patienten an den Folgen ihrer Krankheit innerhalb der ersten 5 Jahre nach der Diagnose sterben.

Obwohl eine zunehmende Anzahl von fortgeschrittenen Operationstechniken und etablierten Chemotherapien zu einer verbesserten Prognose für Patienten führte, ist ein tieferes Verständnis der Darmkrebsbiologie zwingend erforderlich, um einen weiteren Fortschritt in den benötigten Behandlungsstrategien zu gewährleisten und die Lebensqualität sowie die Lebenserwartung zu verbessern. Dies gilt sowohl für frühe Stadien der Tumorerkrankung als auch im späteren Verlauf.

Die neoplastische Veränderung des Darmgewebes ist die Folge eines mehrstufigen Prozesses, der genetische Veränderungen beinhaltet, welche oft in einer sequenzspezifischen Weise auftreten. Diese Akkumulation von Mutationen wurde erstmals von Vogelstein 1988 beschrieben und als Adenom-zu-Karzinom-Sequenz bezeichnet. Die Zellen, die im Laufe ihrer Lebenszeit einige solcher Mutationen angehäuft haben, erwerben selektive Vorteile gegenüber anderen Zellen, können sich unkontrolliert vermehren und sind unempfindlich gegenüber Kontrollmechanismen wie zum Beispiel Signalen, die einen programmierten Zelltod (Apoptose) einleiten. Die genetischen Veränderungen sind besonders beutend für eine kleine Subpopulation von Zellen, den sogenannten Tumor-induzierenden Zellen (TIZ), oder sogenannten Tumorstammzellen, welche vor mehr als 10 Jahren im Darmkrebs beschrieben wurden. Bisher bleiben viele Fragen zu den molekularen Mechanismen, die zur Entstehung von malignen tumorinduzierenden Zellen führen, unbeantwortet.

Ziel des vorliegenden Projektes war die Charakterisierung von Molekülen, welche maßgeblich bei der Entstehung und Progression von Darmkrebs beteiligt sind und Darmkrebszellen spezifisch kennzeichnen. Die Identifizierung solcher Moleküle bietet die Möglichkeit, jene mittels selektiver Wirkstoffe gezielt anzugreifen. Diese sogenannten Zielmoleküle besitzen ein hohes therapeutisches Potential und sind immanent wichtig, um alternative Therapien zur Behandlung von Darmkrebs zukünftig entwickeln zu können.

Basierend auf der Expressions-Stärke von CD133, einem Oberflächen-Markerprotein, das eine Anreicherung aggressiver Zellsubpopulationen mit hoher TIZ-Dichte ermöglicht, wurde ein Screening etabliert, das vergleichende Proteinexpressionsanalysen zwischen einer aggressiven (CD133+) und einer hoch aggressiven (CD133high) Darmkrebszellen-Subpopulation ermöglichte[10]. Die Untersuchung der Proteinexpressionssignaturen dieser CD133high Zellsubpopulation ermöglichte die Identifizierung von Molekülen, die zu einem besonders aggressiven Tumorwachstum und dem damit potentiell verbundenen Therapieversagen beitragen. Darunter befand sich auch das multifunktionale und bivalente Enzym „Tissue Transglutaminase 2" (TGM2), das in der fortlaufenden Studie im Detail untersucht wurde.

Das Enzym TGM2 gehört zur Familie der Gewebetransglutaminasen (TGasen). Wie alle enzymatisch aktiven TGasen besitzt TGM2 eine aktive katalytische Triade und katalysiert eine Ca^{2+} abhängige, posttranslationale Modifikation von Proteinen. Neben der gut charakterisierten Transaminase-Aktivität besitzt TGM2 zusätzlich die Fähigkeit, weitere enzymatische Reaktionen zu katalysieren, u.a. kann TGM2 als GTPase fungieren und eine G-Protein-gekoppelte Rezeptor-ähnliche Signalweiterleitung induzieren. Diese beiden unterschiedlichen Enzym-Aktivitäten schließen sich gegenseitig aus und werden durch Konformationsänderungen durch Bindung von Ca^{2+} bzw. ATP/GTP reguliert. Aufgrund seiner vielfältigen enzymatischen Aktivitäten wurde TGM2 mit einer Vielzahl von Krankheitsprozessen wie Entzündungen, Wundheilung, neurodegenerativen Erkrankungen und Krebs in Verbindung gebracht. Interessanterweise werden dem Molekül auch konträre Eigenschaften zugesprochen. So konnte eine erhöhte TGM2-Expression in verschiedenen Krebsarten beobachtet und mit dem Fortschreiten der Krankheit und der Metastasierung in Zusammenhang gebracht werden. Gleichzeitig gibt es jedoch zahlreiche Studien, die TGM2 eine tumorsuppressive Rolle zuschreiben. Bezüglich der Funktion von TGM2 in Darmkrebs ist wenig bekannt, daher soll in dieser Arbeit die Rolle von TGM2 in Darmkrebs kontextspezifisch entschlüsselt werden.

Zuerst wurde überprüft, ob TGM2 auch im primären Tumorgewebe und korrespondierenden Normalgewebe von Darmkrebs-Patienten differenziell exprimiert wird. Dafür wurde eine Strategie entwickelt, um primäre, humane Epithelzellen von nicht-epithelialen Zellpopulationen, einschließlich

Stromazellen, zu isolieren und aufzureinigen, um gezielt die Expression von TGM2 im Darmepithelzellen zu untersuchen, und Ergebnisverfälschungen durch nicht-epithelialen Zellen aus der unmittelbaren Tumor-Umgebung zu vermieden.

Es konnte gezeigt werden, dass auf Proteinebene das Expressionsniveau von TGM2 in Tumorepithelzellen im Vergleich zum korrespondierenden normalen Gewebe signifikant hochreguliert war. Darüber hinaus war auch eine signifikante Erhöhung der Transaminase-Aktivität mit einem Enzym-Test nachweisbar. Diese Daten zeigten einen proportionalen Zusammenhang zwischen einer hohen TGM2-Expression und Transaminase-Aktivität. Um die Hypothese, dass TGM2 eine zentrale Funktion bei der Entstehung und Progression von Darmkrebs spielt, weiter zu untermauern, sollte der Einfluss von TGM2 auf Darmkrebszellen mittels gentechnologischen Methoden untersucht werden. In zwei gut beschriebenen Darmkrebs-Ziellinien – SW480 und HCT116 – wurde mit Hilfe zweier unabhängiger shRNAs- bzw. CRISPR/Cas9-lentiviralen Vektorsystemen, die TGM2-Expression genetisch vermindert bzw. komplett ausgeschaltet. Mit beiden Methoden zeigten Darmkrebszellen eine sofortige Hemmung des Zellwachstums und Expansion im Vergleich zu Kontrollzellen.

In einem weiteren Schritt wurde der Einfluss von TGM2 auf die Tumorsphärenbildung untersucht. Die Fähigkeiten von Zellen, Tumorsphären zu bilden, ist ein Hinweis für vorhandene Stammzellaktivität. Da nur Stammzellen bzw. TIZ in der Lage sind, Tumore zu induzieren, ist es von wesentlichem Interesse, diesen Zellen therapeutisch anzugreifen. Mit beiden shRNAs gegen TGM2 konnte sowohl in SW480 als auch in HCT116 Zellen die Tumorigenität in 2D-Kulturen nahezu aufgehoben werden. Dasselbe Ergebnis war auch in vivo zu beobachten. Nachdem in SW480 Zellen die TGM2-Expression mittels shRNAs fast vollständig reduziert wurde, zeigte die subkutane Injektion der Zellen in die Flanke von NOD/SCID Mäusen, dass deren Fähigkeit zur Tumorbildung annähernd eliminiert wurde im Vergleich zu Kontrollen.

Um diese funktionellen Analysedaten auf ihre Übertragbarkeit in die klinische Anwendung zu überprüfen, wurden präklinische Xenograft-Modelle etabliert. Die pharmakologische Hemmung von TGM2 durch zwei selektive TGM2 Inhibitoren - Tyrphostin 47 and LDN-27219 - in präklinischen Transplantationsmodellen führte sowohl zu einer signifikanten Verzögerung der Tumorinitiierung als auch zu einer deutlichen Hemmung des Tumorwachstums im Verlauf des Beobachtungszeitraumes. Des Weiteren wurden in einem Tier-Xenograft-Modell bereits etablierte Tumore in vivo mit oben genannten Inhibitoren behandelt. Dabei konnte mit dem Inhibitor LDN-27219 eine deutliche Hemmung des Tumorwachstums erreicht werden.

Um diese Ergebnisse auf primäre Patientenzellen zu übertragen, wurden Tumorsphärenkulturen aus humanem Tumorgewebe von Darmkrebs-Patienten etabliert und deren Reaktion auf die TGM2-spezifische Inhibitoren beobachtet. Auch hier führte die Behandlung von primären Tumorzellen mit oben genannten Wirkstoffen zu einer signifikanten Reduktion der Tumorsphärenbildung und somit ihrer Tumorigenität.

Im primären, humanen Tumorepithelgewebe konnte in dieser Arbeit eine signifikant höhere Transaminase-Aktivität im Vergleich zum Normalgewebe nachgewiesen werden, daher war es von zentraler Bedeutung die Rolle der Enzymaktivitäten von TGM2 im Darmkrebs im Detail zu untersuchen. Darüber hinaus war bekannt, dass TGM2 Isoformen in verschiedenen Krebsentitäten differenziell reguliert sein können. Um zu klären, ob eine bestimmte Isoform bzw. eine spezifische Enzymaktivität von TGM2 eine vorherrschende Rolle in der Entstehung und Entwicklung von Darmkrebs spielt, wurden verschiedene TGM2 Konstrukte in lentivirale Expressionsvektoren kloniert. Diese Studien mit unterschiedlichen TGM2-Isoformen und mit mutierten TGM2 mit eingeschränkter Enzymaktivitäten belegten, dass die TGM2-Transaminierungsreaktion der Isoform 1 für das Überleben von Tumorzellen entscheidend ist; Transaminase-inaktive TGM2-Varianten waren nicht in der Lage, Zellen vor dem Zelltod nach Verlust von endogenem TGM2 zu bewahren.

Die gewonnenen Erkenntnisse lassen eine wesentliche Rolle von TGM2 in der pathologischen Schicksalsentscheidung von Darmkrebszellen vermuten. Welches Zellschicksal von TGM2 vermittelt wird, wurde durch Zeitraffer-Mikroskop-Aufnahmen beantwortet. Der Wachstumsnachteil von Darmkrebs-Zellen beim Verlust von TGM2 kann durch zwei verschiedene Szenarien erklärt werden; entweder führt der TGM2-Knockdown zu einem Wachstumsstillstand (Zellzyklusarrest) in Darmkrebszellen, oder er hemmt das Überleben von Krebszellen und induziert Apoptose. Zeitraffer-Mikroskop-Aufnahmen von Zellen nach TGM2-Knockdown zeigten eine massive Induktion von Apoptose im Vergleich zu den Kontrollzellen mit funktionsfähiger TGM2 auf Einzelzellebene. Dieses Ergebnis konnte auch mit Hilfe von durchflusszytometrisch-gestützten Methoden reproduziert werden. Auf Basis dieser Analysemethoden konnte zusätzlich zum signifikanten Anstieg von apoptotischen Zellen eine starke Aktivierung von Caspase 3 festgestellt werden. Um zu verstehen welche molekularen Mechanismen und Interaktionspartner in der TGM2-vermittelten Apoptose in Darmkrebszellen involviert sind, wurden biochemische Studien, Genexpressionsanalysen und lentivirale Vektor-Systeme herangezogen. Mit Hilfe dieser Analysen konnte eine Verbindung zwischen TGM2 und der Regulation von Genen hergestellt werden, welche für die Krebsentwicklung und Progression von entscheidender Bedeutung sind. Gestützt durch durchflusszytometrisch-basierten Studien und Protein-Protein-Interaktionsanalysen konnte gezeigt werden, dass TGM2 mit dem Tumorsuppressorgen p53 Heteromere bildet und somit die Aktivität von p53 direkt beeinflusst. Wird die Expression von TGM2 in Darmkrebszellen mittels shRNAs gemindert, so wird die von TGM2 vermittelte p53-Inhibition aufgehoben. Phosphoryliertes p53 aktiviert Caspase 3 und induziert in Folge die Apoptose in Darmkrebszellen.

Die vorliegende Studie konnte erstmalig die direkte Interaktion und somit Regulation von TGM2 und p53 in der Pathophysiologie von Darmkrebs zeigen. Die Transaminase-Aktivität von TGM2 ist hierbei

entscheidend und führt potentiell zu kovalent gebundenen TGM2-p53-Heterodimeren. Dies verhindert die Aktivierung von p53 und führt zu einer deregulierten p53-Signalübertragung. Letztendlich wird die Aktivierung von pro-apoptotischen Signalwegen, wie die Aktivierung von Caspase 3 verhindert. Außerdem konnte gezeigt werden, dass die TGM2-Transaminase-Aktivität und Proteinexpression in primärem Darmkrebsgewebe stark hochreguliert ist. Zusammenfassend legen diese Ergebnisse nahe, dass TGM2 eine entscheidende Rolle im Überleben von Darmkrebszellen spielt und seine zielgerichtete Hemmung das Zellüberleben und die Tumorigenität wirksam und nachhaltig reduzieren kann. Somit stellt TGM2 ein vielversprechendes Zielmolekül dar, das zur Verbesserung der Darmkrebstherapie beitragen kann.

1. Introduction

1.1 Colon Cancer

Approximately 14 million new cancer cases and 8.8 million cancer-related deaths can be reported worldwide every year [2]. 480,000 new incidences and 233,753 cancer deaths are counted in Germany per year. Among them, 33,100 men and 27,900 women suffered from colorectal cancer (CRC) in 2014 [3]. In the course of life, one out of 15 men and one out of 18 women will acquire CRC. The relative 5-year survival rates in CRC are only 62 % for women and men [4]. Although a growing number of advanced surgical techniques and established chemotherapy regimens lead to a better outcome for patients who are suffering from CRC, it is obvious that a deeper understanding of CRC biology and an advance in treatment strategies is needed to improve the survival outcome of patients with early and advanced CRC.

1.1.1 Intestinal stem cells and organization of the intestinal epithelium

The intestinal tissue fulfills complex functions, while digestion and food absorbance, it also maintains an effective barrier against potentially lethal microorganism and deleterious agents. Due to daily exposition to aggressive luminal context the rate of supersede cells is remarkably high. To ensure a life-long functionality a conversion rate of up to 10^{11} epithelial cells (~200g) [11] occurs every day. This enormous feat is only driven by a small population of adult intestinal stem cells (ISCs) that reside within specialized niches. These niches are located at the bottom of crypts of Lieberkühn. At least six of Lieberkühn crypts encircle an intestinal villus, together they build the smallest anatomical and functional unit of the adult intestinal epithelium. Although the cellular organization varies in the different gut sections, the general cell composition remains identical. ISCs which are located at the bottom of crypts give rise to their direct progeny - transit-amplifying (TA) cells. They spend approximately two days in the crypt before they migrate upwards and terminally differentiate into the specialized intestinal epithelial cell types, goblet cells, enteroendocrine cells, Paneth cells and enterocytes [12,13].

In the last 50 years, great efforts have been made to identify ISCs, to examine their function and location. Cheng and Bjerknes suggest a stem cell zone model, hypothesizing that the columnar cells at the base of the crypt, which are intercalated with Paneth cells, are the resident stem cells [14]. Crypt basal columnar cells (CBC) are proposed to give rise to the four major cell lineages in the intestinal epithelium [15–19]. This was found due to lineage tracing experiments labeled cells are migrating upward the crypt, during gradual

differentiation from immature to mature intestinal epithelial cells. At the same time, another ISC model referred to as the +4 model was described. This model claims that cells with stem cell attributes are located at the fourth position from the crypt base, above the Paneth cell compartment [20,21,22]. However, there is conflicting data concerning the correctness of these stem cell models, therefore the identity of the ISC remains a controversial discussion. To be able to specifically characterize ISCs for a prospective isolation and further characterization or analysis, implies the identification of ISC markers. The search for ISC markers has been the subject of many investigations [23–27]. The first described valid marker for intestinal cells with stem cell like properties was the Leu-rich repeat-containing G protein-coupled receptor 5 (Lgr5). Lgr5 is a WNT target gene selectively expressed at the base of adult intestinal crypts [23,28] which marks around 14-16 proliferative, undifferentiated CBC cells. Since then a wide range of putative CBCs or +4 ISCs markers were described. Based on the Lgr5$^+$ expression a CBC stem cells signature, using gene expression and proteome profiling revealed a pattern of approximately 500 stem cell enriched genes [29]. These and additional gene expression studies together with lineage tracing experiments lead to the definition of further CBC marker including *Smoc2* [29], *Musashi1* [30], *Promin-1* (CD133) [31], *Olfm4* [32,33] and *Ascl2* [34,35]. Bmi1$^+$ was the first investigated +4 stem cell (+4SC) marker [24,36]. Bmi1$^+$ cells are able to regenerate Lrg5$^+$, therefore this relative quiescent +4SC have been considered as reserve stem cells in case of damage to the active CBC stem cells [37–39]. Other markers identified for the +4SC pool like Tert, Hopx, lrig1 and Dcamkl1 also label for cells at the +4 position which are slow cycling and capable to give rise to Lrg5+ CBC cells [26,27,40–42]. Although the intensive search for stem cell marker has greatly increased our knowledge of the role and function of ISCs, many questions remain unclear, as does the relationship between +4SCs and CBCs.

1.1.3 Signaling pathways in intestinal homeostatic self-renewal

The manifold tasks of the intestinal tissue and its high turnover require a tight regulation and a complex communication between ISCs and surrounding tissue. One of the best studied signaling pathways is the WNT/β-Catenin pathway, which is also the driving force behind cell proliferation in the intestinal epithelium. In general the WNT/β-Catenin pathway is highly conserved throughout the animal kingdom [43]. WNT is known to act as a morphogen, therefore it must be secreted to the outside of the cell. For this purpose, WNT is transported to the outside with the help of the 7-transmembrane protein Wntless (WLS) [44,45]. Another 7-pass-transmembrane protein called Fizzled (Fz) acts as a WNT receptor and upon WNT binding Fz cooperates with a single-pass transmembrane molecule of the Low Density Lipoprotein Receptor-related Protein (LRP) family (LRP5-6) [46–48]. After the Fz/LRP complex is formed, it activates the WNT canonical signaling pathway. Subsequently, Dishevelled (Dsh), a cytoplasmatic

protein upstream of glycogen synthase 3 (GSK3), is phosphorylated which in turn induces the phosphorylation of LRP by GSK3β. LRP phosphorylation leads to the recruitment of Axin away from the destruction complex and as a consequence β-catenin is stabilized and translocate into the nucleus were it activates WNT target genes [49,50]. Axin is a central part of the cytoplasmatic destruction box as it acts as a scaffold protein for CK1, GSK3α/β and Adenomatous-polyposis-coli-Protein (APC) – the other protein elements of the destruction box, bringing them into close proximity. Recruitment of Axin to LRP leads to disintegration of the destruction box and stabilization of β-catenin. When WNT receptors are not engaged, Axin stabilizes the destruction box, β-catenin is phosphorylated by CK1 and GSK3α/β, further ubiquitinated and degraded [51,52]. β-catenin is a key player for the homeostatic maintenance and proliferation of ISCs, which could be shown by numerous studies. [53–57].

An exclusively paracrine signaling pathway is the vertebrate hedgehog (Hh) signaling pathway, secreted by enterocytes. Hedgehog signals are morphogenic events, bidirectional between epithelium and mesenchyme to orchestrate embryonic and adult epithelial development and homeostasis in the intestine [58,58]. In adults, Hh is expressed in the epithelium, whereas Hh receptors and downstream components reside in the mesenchyme [59,60]. Sonic hedgehog (SHh) or Indian hedgehog (IHh) are both members of the hedgehog family, bind on their cell-surface receptors, Patched 1 and 2 (PTCH1 and PTCH2) and induce internalization. Upon hedgehog binding the transmembrane protein Smoothened (SMO) is no longer inhibited by PTCH, SMO in turn, activates Serin/threonine kinase 36 (STK36) which inhibits the assembly of GLI degradation complex, consisting of protein kinase A (PKA) and glycogen synthase 3 (GSK3). Without Hh binding the PKA/GSK3 complex mediates phosphorylation of the GLI family members Gli1, 2 and 3 to mediate their degradation [61,62]. During gut morphogenesis it could be found that bone morphogenetic proteins (BMPs) are one of the major targets for Hh signaling [63,64,59] which are members of the transforming-growth-factor-β (TGF-β) superfamily. BMP2 and BMP4 transmit signals from the mesenchyme back to the epithelium via their epithelial receptor BMPR1, which subsequently lead to phosphorylation of Smad 1, 5 or 8 proteins and heterodimerization with Smad4 and gene transcription [58]. BMP signaling is mostly active in the epithelium of villi, due to the expression of its antagonists noggin, Gremlin1 and 2 or Chordin-like1 at the crypt site [65,66]. Hedgehog and BMP signaling restrain proliferation and promote differentiation, in opposition to Wnt/β-catenin signaling [67].

Another major signaling pathway known to regulate proliferation and differentiation of intestinal stem and progenitor cells is the Notch signaling pathway. Unlike previous described pathways, Notch works by lateral inhibition between two adjacent cells [68]. Upon ligation of neighboring cells via the Notch ligands DII1, DII4 or Jagged1 on the Notch1 or 2 receptors, the receptor is cleaved, releasing its intracellular

domain (NICD). NICD translocates into the nucleus and promotes the transcription of target genes involved in proliferation and differentiation [69,70]. Inhibition of Notch signaling affects severely all proliferative cells in the crypt, including Lgr5^{+} ISC, which lead to lack of epithelial regeneration, dysregulation of epithelial homeostasis and cell fate determination [71].

1.1.2 Colorectal Cancer and the role of tumor initiating cells (TICs)

The tumorigenesis of CRC is a process in which cells accumulate several genetic alterations, affecting typical genes also known as tumor suppressors and oncogenes. CRC appear to arise as a result of a multistep event collecting genetic alterations, often in a preferred sequence specific manner, as first described by Vogelstein and coworkers 1988 [72]. The so-called adenoma to carcinoma sequence is based on the fact that most CRCs emerge from adenomas. In more than 20 decades of research it has been recognized that the progression from adenoma to carcinoma is an interplay of genomic and epigenomic instability [73–75]. This instability is based on one or a combination of three different mechanisms, namely chromosomal instability (CIN), CpG island methylator phenotype (CIMP), and microsatellite instability (MSI) [5]. In line with this, MSI was found as a frequent phenomenon in CRC [76,77]. Microsatellites are repetitive DNA sequences, consisting of tandem repeats, which are particular prone to errors during DNA replication due to an inefficient binding of the DNA polymerase [78,79]. Such errors, typically single base mismatches or short insertions or deletions, are normally identified and repaired by a DNA mismatch repair (MMR) system. Therefore, the appearance of MSI is defined as the mutational signature that results from an impaired MMR [80]. CRC tumors that evolve as a result of inactivation of the MMR system can be found in approximately 15 % of patients [81]. Mutations in the MMR system affect manly the proteins MLH1, MSH2, MSH6 and PMS2 these were found to be responsible for a genetic predisposition to CRC known as Lynch syndrome [82]. However, hypermethylation of MLH1 can be observed in most MSI CRC cases [83]. Hypermethylation are common epigenetic events in CRC and a mechanism of carcinogenesis described as CIMP [84,85]. Epigenetic signaling can be found in normal as well as in neoplastic tissues and is a tool to control gene transcription through chromatin condensation. In meaning that the state of chromatin determines the accessibility of DNA for gene transcription. Methylation of CpG islands correlates with chromatin condensation and therefore leads to a transcriptional inactivation of genes most prominently of those who have a tumor suppressor role [85,86]. Typical identified tumor suppressor genes found to be hypermethylated are *CDKN2A*, *MLH1*, *CDH1* and *VHL* [87–90]. Recently it could be demonstrated that genes involved in cancer progression are more likely to undergo hypermethylation[91]. Probably the most common genetic alteration in CRC is CIN followed by typical mutational landscape in tumor suppressor and oncogenes [5]. Intratumoral heterogeneity in cancer is most often a consequence of CIN and drives phenotypic adaption during tumor

evolution [92]. 70 % of CRCs are displaying the presence of an abnormal number of chromosomes, defined as aneuploidy [93]. CIN is defined as an unequal distribution of DNA to daughter cells that can involve either a gain or loss of whole chromosomes or structural aberrations [94]. Causes underlying aneuploidy include defects in the chromosome segregation machinery which was found to be the basis of an increased rate of mutations and are coupled to typical mutations in tumor suppressor genes and oncogenes in CRC [6,84]. Systematic investigations of genetic alterations in colorectal-tumor specimens representing various stages of neoplastic development, showed an initial loss of APC [95,96]. As described earlier in this work, APC is an important element in the implementation of WNT signaling and mutant APC disrupts complex formation and leads to elevated β-catenin levels and transcription of genes implicated in tumor growth and invasion [97]. Approximately 30 – 40 % of CRC cases harbor mutated *RAS* genes [95,96,100,101]. Activated RAS signaling is involved in manifold processes which is forwarded in different pathway traits through effector proteins like the Raf-MEK-ERK and phosphatidylinositol 3 kinase (PI3K) [98–100]. One critical downstream target of PI3K is Akt which is involved in multiple cell functions including cell growth, proliferation and survival [99]. In addition RAS is also linked to NF-κB signaling, which is known to be a critical factor in inflammation, immune response and cell survival [101]. Described mutations are followed by a frequently loss of tumor suppressor genes like SMAD4 and p53 [95,96]. P53 is certainly one of the best studied and most frequently altered genes in human cancers [102]. P53 is a cellular stress sensor, reacting on DNA damage, aberrant proliferative signals and oxidative stress. Upon activation, p53 exerts transcription of downstream targets which lead to cell cycle arrest, DNA repair, senescence or apoptosis [103]. Activated p53 is heavily modified on its N- and C-terminus, predominantly through phosphorylation of serin and threonine residues. Phosphorylation of p53 promotes its stabilization and modulates its affinity to distinct protein-protein interactions [103]. Most prominent antagonists of p53 are MDM2, E3-ubiquitin ligase and MDM4 which bind to p53 and prime it to degradation [104–106]. However, besides the role of wild type p53 as tumor suppressor, it could be shown, that mutated p53 can gain novel oncogenic functions, which promotes a more aggressive, metastatic cancer phenotype [107,108]. Although this model is an oversimplification of CRC tumorigenesis and the question whether CIN is a cause or a consequence of malignant process in CRC remains a topic of controversial discussions, it allows to align clinicopathological changes with genetic abnormalities.

However, it is widely accepted that described accumulations of genetic alterations mostly occur in a small subset of cells, so called tumor initiating cells (TICs), leading to an expansion of transformed cells, due to conferred, selective growth advantage. TICs are assumed to be a functionally homogenous stem-cell-like population which are able to give rise to more differentiated tumor cells and concurrently maintain the

potential for self-renewal [7,113]. The first evidence that CRC is a stem cell driven disease was reported by O´Brien et al. and Ricci-Vitiani and coworkers [8,9] more than 10 years ago. However, so far it has remained elusive whether a TIC originates from the ISC pool or from TA cells. Due to the high proliferative nature of TA cells they are more likely to accumulate DNA replication errors but based on the high turnover of TA cells, potential malignant cells are lost within a few days [109]. On the other hand, WNT activation experiments in ISCs shows that they are very potent in initiating adenomas [110]. In Xenograft models with human CRC cells, O´Brian et al. could show, that CD133$^+$ purified cells are able to enrich for cells with stem cell like features and TIC activity [8,9]. As CD133 as a TIC marker is highly debated [111,111], the search for other surface markers for TICs has been a field of intensive research [112]. However, identified putative TIC surface markers like EpCAM, CD44, CD166, ALDH and Lgr5 do not show a satisfactory restriction on TICs which would be required to isolate them in a high resolution [111,113,114]. Furthermore the expression of TIC markers as predictors of patients is controversial, expression of Lgr5 for instance was shown to be unrelated to patient prognosis [115]. Nevertheless, TICs in CRC are shown to play parent role in chemoresistance and may be responsible for tumor regeneration and relapse [116–119] and so represent attractive targets for advanced CRC therapy.

1.2 Transglutaminase 2 and its family members

The Transglutaminase (TGase) protein family, known for its transamidase activity, consists of eight Ca^{2+} dependent members, FXIII, TGM1 – 7 and a ninth member, which represents the only exception as a Ca^{2+} independent and catalytically inactive protein, called Band 4.2 [120]. Members of this superfamily are encoded by genes with high homology [120]. All enzymatic active TGases have an active site catalytic triad in common, consisting of a cysteine, histidine and aspartate residue, and catalyze post-translational modification of proteins Ca^{2+} dependently [121–125]. Although, all mammalian forms of TGases have perceptible structural homology and have several similar features, they differ in their tissue distribution and localization as well as in the mechanism of action and substrate specificity [126–128].

TGM2 is located at chromosome 20q11-12 and is organized in four domains which consist of an N-terminal β-sandwich, core domain (including the catalytic core) and C-terminal β-barrels 1 and 2. This organizational structure is highly conserved among TGases [129–131]. The N-terminal β-sandwich and the C-terminal β-barrels 1 and 2 assume a secondary β-sandwich structure, whereas the catalytic core domain presents α-helical structure [132].
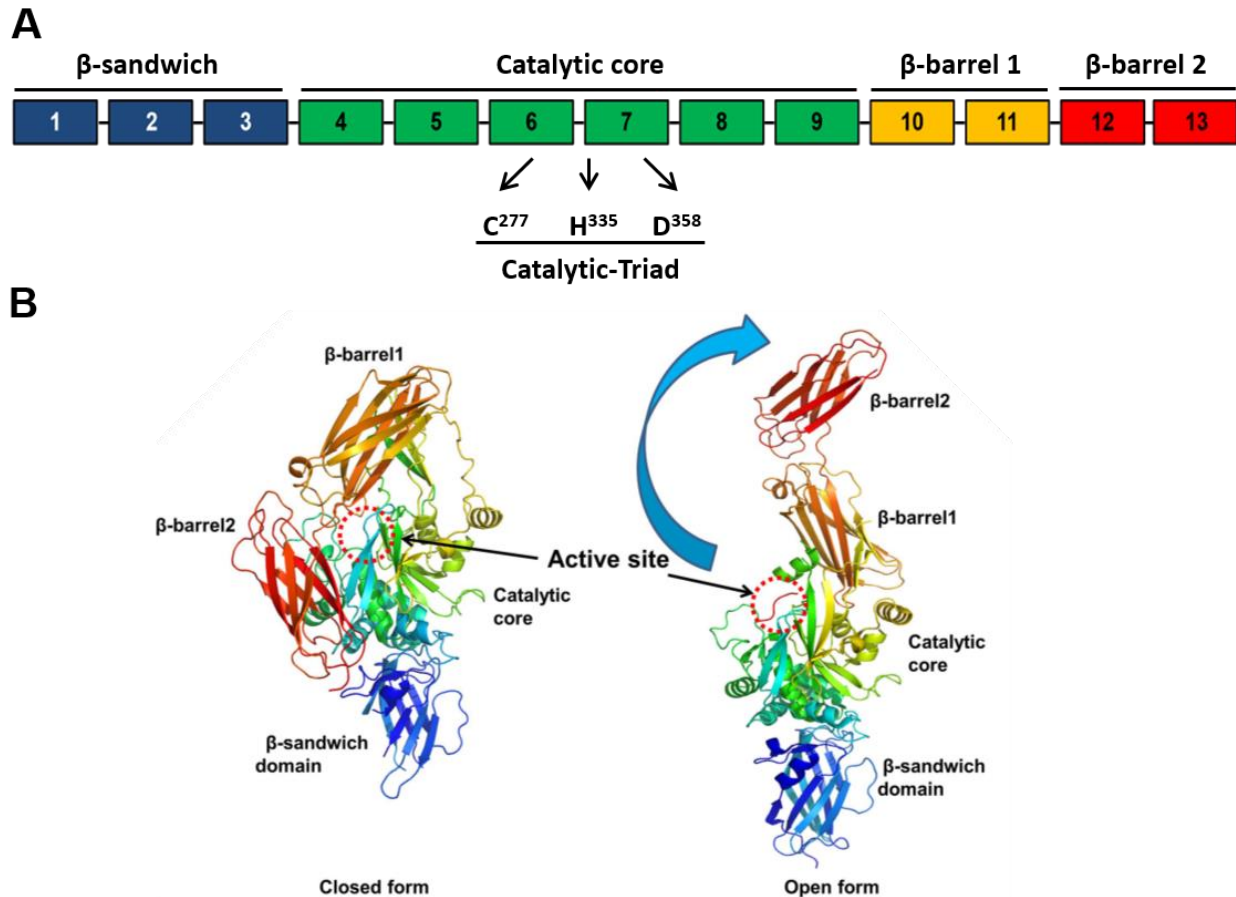
Figure 1 Structural domains and dynamic three-dimensional structures of TGM2

(**A**) The four distinct domains are indicated by colored boxes, the catalytic triad comprising C277, H335 and D358, is shown. (**B**) The structure of the compact, closed form (inactive form) and the expanded, opened form (active form) are shown. Adopted from Lee and Park et al. [1]

Domain 1, consisting of several β-strands, is crucial for the non-classical secretion of TGM2 on the EC surface [133,134]. Located in domain 2 is the active-site triad consisting of Cys^{277}, His^{335} and Asp^{358}, and the main Ca^{2+}-binding region [135,136] (Figure 1A). Domain 2 and 3 are interconnected through a regulatory loop which plays a pivotal role in TGase activity, since it acts as a joint which enables the domains to change their three-dimensional position of the protein. The C-terminal domains are important in regulating transamidase and GTPase/ATPase activity [135]. These four domains can undergo conformational changes upon Ca^{2+} or GTP binding. In presence of Ca^{2+} they adopt an extended enzyme structure that allows the access to the catalytic core, whereas GTP binding leads to a compact conformation [137,138] (Figure 1B).

1.2.1 Regulation of TGM2 expression and its alternative spliced isoforms

Hence, TGM2 fulfills many tasks it is inevitable to control its expression by a complex machinery of transcription factors and epigenetic and translational modifications. Several transcription factors for TGM2 could be identified. Predominantly stress stimuli like Hypoxia, ROS, inflammation or tissue injury leads to TGM2 expression. Among the most prominent factors are retinoic acid (RA) [139–141], cytokines like LPS, TNF-α, IL-6 as well as NF-κB and HIF1-α [142–149].

Furthermore, it was found that TGM2 can be regulated by epigenetic mechanisms. Investigations on the methylation status of the TGM2 promoter revealed a frequently methylated, therefore silenced TGM2 promoter, in normal cells. On the contrary, in neoplastic cells hypomethylation, which results in constitutive gene expression, was often seen [150].

Although full-length TGM2 is the best characterized isoform among the six consisting isoforms of TGM2, it is known that TGM2 variants are additionally important factors in TGM2 cell signaling and can fulfill completely different tasks. It is known that alternative splicing processes are a tool for enabling a single gene to have multiple functions [151]. Thus, it is a tightly regulated event seen in a cell type or developmental stage specific manner. Alternative spliced TGM2 variants are C-terminal truncated forms of TGM2. There are six described isoforms; full-length TGM2 isoform 1, the transcript encodes a polypeptide of 687 amino acids residues with an approximate molecular mass of ~75 kDa. The transcript of TGM2 isoform 2 codes for a polypeptide of 548 amino acid residues and with a molecular mass of ~62 kDa. Isoform 3 is the shortest TGM2 variant consisting of a polypeptide of 349 amino acids residues and an approximate molecular mass of ~38 kDa. The most recently discovered TGM2 splice variants are TGM2 isoform 4a and 4b, generated through an atypical alternative splicing event, resulting in proteins from similar mass to the full-length isoform 1, but with an alternative sequence on the C-terminus [152,153] (Figure 2). Overall, the loss of C-terminal residues affect their GTPase/ATPase as well as TGase activity, their ability to form complexes with other proteins and has an impact on its cellular localization [135,154,155].
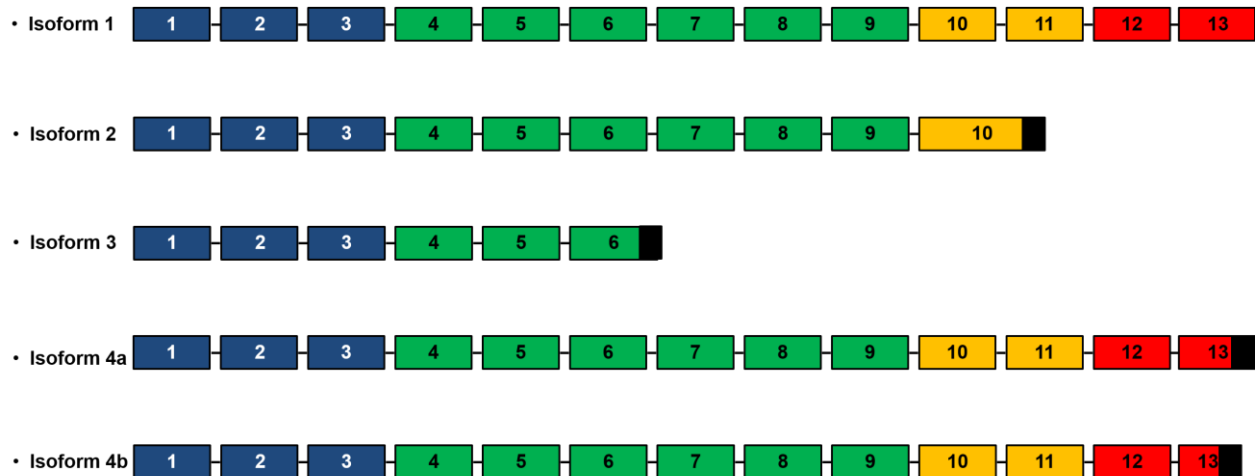
Figure 2 Alternative spliced isoforms of TGM2

Exons are numbered and colored boxes, a horizontal line indicates an intron. Blue exons build the β- sandwich domain, green boxes the core domain, yellow and red boxes form barrel 1 and 2 of TGM2. Black boxes represent alternative amino acids (AA) sequences due to change in the reading frames.

1.2.2 TGM2 and its enzymatic and non-enzymatic functions

TGM2 enzyme activity underlies a tight control mechanism to prevent cells from major disruption in cellular homeostasis due to deregulated enzyme activity. The Ca^{2+} activated transamidase reaction involves a movement of protein domains, which renders the enzymes catalytic core accessible for substrates [128,129]. Ca^{2+} activation can be antagonized by GTP binding. The nucleotide inhibits transamidase activity due to its binding and subsequently hydrolyzation to GDP, this reversible reaction convert TGM2 from a transamidase into a GTPase [132]. TGM2 was found to be regulated by lysophosphatidylcholine, which increases the sensitivity of TGM2 to Ca^{2+}, thus reduces the activation constant for Ca^{2+} to activate TGM2 [156]. Further, nitrosylation was shown to sensitizes TGM2 towards GTP inhibition and therefore decreases transamidase activity [157]. A number of studies showed that in absence of cellular stressors, TGM2 transamidase activity is inactive. This is due to the need for a relatively high concentration of Ca^{2+} in order to activate TGM2, which was determined as 90 – 560 µM for recombinant TGM2 [158]. Therefore, the low level of 100 nM free cytoplasmatic Ca^{2+} is not sufficient to activate cytoplasmatic TGM2 under normal physiological conditions. On the contrary, disposal cytoplasmatic GTP required for TGM2 inhibition exceeds the concentration needed to keep TGM2 in its GTP bound closed conformation [159]. However, extracellularly Ca^{2+} levels tend to reach a sufficient concentration to activate TGM2 and although the

enzyme switches to an open conformational state, it remains catalytically inactive, due to the formation of inhibitory disulfide bounds between the residues Cys^{370} and Cys^{371} [160,161], which is a result of the high oxidative state in the extracellular space. Nevertheless, TGM2 transamidation can be activated intracellularly due to Ca^{2+} influx as a consequence of extracellular stimuli, for instance. Furthermore, TGM2 can be sensitized to low Ca^{2+} concentrations possibly through interaction with cofactors [162,163]. This is particularly the case for extracellular TGM2, where binding to syndecan-4 increases Ca^{2+} sensitivity and transamidase activity [164].

The transamidation reaction, catalyzed by TGM2, is a multistep process which all enzymatic active TGases have in common. TGM2 cross-links proteins through an acyl-transfer reaction between the γ-carboxamide group of peptide-bound glutamine and the ε-amino group of peptide bound lysine, resulting in a ε-(γ-glutamyl) lysine isopeptide bond [165]. Post-translational protein modifications of TGases all involve an initial reaction in which a glutamine-containing protein act as an acyl-donor or -acceptor substrate and build - in the enzymes catalytic core - a covalently linked acylenzyme intermediate. This step is followed by binding of a second substrate, such as an amine (H_2NR) which is incorporated into the glutamine residue of the acceptor protein, or a protein which results in a protein-protein cross-linking (transamidation reaction) [127,166]. Further, the acylenzyme intermediate can by attacked by water (hydrolysis)[167] or an alcohol (esterification) [168]. Of note, a hydrolyzation reaction, catalyzed by TGases, results either in a protein deamination or in an isopeptide cleavage [169]. Among the numerous enzymatic reactions catalyzed by TGM2, protein-protein cross-linking is one of the best studied reaction of TGM2. Basically, this reaction can be subdivided according to the protein interaction partners. First, TGM2 can covalently incorporate proteins in addition to itself, to form high molecular weight complexes. Second, TGM2 builds isopeptide bounds intramolecularly, which influences protein conformation, stabilization and interaction. Third, intermolecular cross-linked isopeptides build by TGM2 lead to formation of dimers, oligomers and polymers, which are frequently involved in extracellular and intracellular signaling.

Besides the transamidase activity, TGM2 functions as an atypical GTPase and ATPase. Although the ability of TGM2 to bind and hydrolyze GTP was recognized early by Achyuthan and Greenberg in 1987 [170], the link between this function and its capability to act as a G protein was made several years later. Interestingly, this was discovered more by change, as Nakaoka and coworkers recognized that the GTP-binding protein Ghα, was identical to TGM2 [171]. It could be shown that binding of GTP initiates G protein like signaling, whereas GTP hydrolyzation terminates signal transduction and restores TGase activity [171]. The second subunit of TGM2/Ghα is Ghβ, which inhibits the GTPase as well as the TGase activity and keeps the enzyme in an inactive state. Dissociation of the β-subunit restores the G protein function [172].

It has been postulated that TGM2 can bind and hydrolyze ATP [173] and this reaction was found predominantly in the regulation of mineralization of the extracellular matrix (ECM) in osteoblasts [174]. Membrane Type 1 Matrix Metalloproteinase (MTI-MMP) is able to cleave TGM2 into short fragments [175], which promotes ATPase activity of TGM2. This in turn contributes to elevated inorganic phosphate (Pi) levels, which are essential for ECM mineralization [174].

Mishra and Murphy described together with colleagues a further enzymatic function of TGM2. They found an intrinsic kinase activity of TGM2 due to investigating the mechanism behind phosphorylation of insulin-like growth factor-binding protein 3 (IGFBP-3) in breast cancer cell membranes. Following investigations revealed several other targets for TGM2 kinase activity like p53, PKA and rb [176–178]. Ca^{2+} can inhibit the TGM2 kinase activity, in a concentration dependent fashion.

A number of studies revealed, that TGM2 could function enzymatically independent as a scaffold protein. Thus, TGM2 transmit signals through noncovalent protein interactions. First evidence for a TGM2 scaffold function was provided by Peng et al. who described a molecular mechanism of active nuclear transport of TGM2 due to scaffolding with the nuclear transport protein importin-α3 [179].

In summary, TGM2 signaling functions in an almost unimaginable variety depending on its localization, cell origin, enzyme activity, conformation, substrates and cofactors. In principle, TGM2 function and signaling can be subdivided in 3 major parts; a) cell-adhesion, migration and stabilization, b) trans-membrane-signaling and c) nuclear translocation and gene expression regulation. Although the protein cross-linking reaction of TGM2 is its best described and investigated catalytic reaction, in every TGM2 regulated cell signaling pathway, the additional functions of TGM2 can be found to fulfill important tasks.

1.2.3 TGM2 and its cancer promoting roles

In almost every cancer like colon, ovarian, breast or lung cancer, just to mention a few, the deregulation of proliferative pathways can be found leading to uncontrolled cell proliferation [180,181]. In general, activation of proliferation follows similar principles; growth factors bind and activate receptor tyrosine kinases (RTKs) on the cell membrane, the signal is transmitted either by small GTPases or the lipid kinase PI3K and conveyed from cytoplasmatic proteins to induce transcription of specific genes, to promote or inhibit cell growth, respectively [182]. TGM2 was found to be able to assist in diverse regulating steps in tumor growth and proliferation. In line with this it was reported, that TGM2 can assume intrinsic kinase activity. TGM2 was able to phosphorylate Insulin-like growth factor-binding protein 3 (IGFBP-3), which

renders the protein unable to bind and inhibit insulin-like growth factor I (IGF-I). Thus, TGM2 accelerate IGF-I signaling through inhibition of IGFBP-3 [183]. Further investigations on TGM2 kinase activity revealed p53 as additional substrate for TGM2 kinase activity. Phosphorylation of p53 by TGM2 inhibits binding of the p53 antagonist MDM2 and activates p53 signaling. In addition, TGM2 was found to phosphorylate retinoblastoma protein (rb), which is a known regulator of cell cycle progression and inhibitor of apoptosis (Mishra et al. 2007; Mishra und Murphy 2006). Furthermore, TGM2 was shown to interact directly with the GTPase-activating proteins (GAPs) Bcr and Abr [184]. GAPs regulate the GTPase activity of Rho family members including Rho, Rac and Cdc42, binding of GAPS leads to downregulation of the active GTP-bound form [185]. Interacting of TGM2 with Bcr blocks the binding to its substrate Rac, thus accelerates Rac mediated signaling [184]. TGM2 is able to signal as a TGM2/Ghα G protein in interplay with the G protein coupled receptor (GPCR) $\alpha_{1\beta}$- adrenergic receptor and transmit G protein signaling to the same extent as other G proteins [186] (Nakaoka et al. 1994). TGM2/Ghα mediates intracellular signaling via PLCδ$_1$, which hydrolyzes phosphoinositide and increases intracellular Ca^{2+} levels [187–189] and enhances proliferation [190]. In neonatal cardiomyocytes a correlation of norepinephrine-stimulated hypertrophy and enhanced TGM2 GTPase signaling is suggested due to elevated extracellular signal regulated kinase (ERK) signaling after altered TGM2/Ghα signaling [191].

Cancer evolution and inflammation are closely related mechanism due to sharing several signaling pathways. Inflammation is a typically response to infection or injury, but can also be induced by tissue stress and malfunctions [192]. Inflammation can be driven by an intrinsic or an extrinsic pathway, the former is triggered by genetic alterations, whereas the latter is exposed to inflammatory conditions like inflammatory bowel disease, which increases the risk of cancer [193,194]. Inflammation-related cancer development can be linked to failure of mechanism in the inflammatory machinery. Key factors in cancer-related inflammation are the transcription factors NF-κB, signal transducer and activator of transcription 3 (STAT3) and HIF1-α [193]. These inflammatory mediators generate an inflammatory microenvironment in tumors due to expression of chemokines and cytokines such as IL-1β, IL-6, IL-23, TNF-α and TGF-β which involves the recruitment and activation of various leukocytes. Recruited leukocytes and mast cells are, upon activation, the main resource of growth factors and cytokines due to a constant release of these inflammatory mediators [195].

In inflammatory cells, or cells under hypoxic stress and glucose deprivation, HIF1-α expression was found to transcriptionally regulate TGM2 expression and lead to an increased cell survival under conditions like inflammation [147–149]. Inflammatory signals, mediated through a cross-talk between the high affinity IgE receptor (FcεRI) and epidermal growth factor receptor (EGFR) were found to induce TGM2 expression via

a NF-κB dependent pathway [196]. TGM2 in turn accelerates NF-κB signaling, which usually underlies tight control mechanism and is mostly found to be inactive under normal conditions and inhibited by IκBα, which masks its nuclear localization signal (NLS) and so NF-κB is sequestered in the cytoplasm [197]. TGM2 was found to polymerize IκBα, polymerized IκBα itself will be degraded which leads to a non-canonical activation of NF-κB [198]. Nonenzymatic TGM2 was suggested to scaffold NF-κB and shuttle into the nucleus, where it binds to the histone deacetlyase-3 (HDAC3) promoter region. Furthermore, as a response to antigen-stimulated inflammation TGM2 binds to rac1 and promotes production of reactive oxygen species (ROS) [196].

Expression of TGM2 was shown to be induced by the cytokines LPS, TNF-α and IL-6. Predominantly, transcription of TGM2 by these factors can be observed as a consequence of inflammatory signals during hepatic fibrogenesis, for instance, it is believed to be involved in autophagy, ECM turnover and wound healing [142–144,146]. Fibrosis and wound healing are highly conserved and coordinated responses to tissue injury and trigger functional (proliferation) and phenotypic changes (epithelial to mesenchymal transition [EMT]). To promote these changes, architectural modifications in the ECM are required. TGM2 has long been known to interact with integrins like fibronectin (FN) and laminin. Integrins are crucially important due to mediating interaction between the cytoskeleton and extracellular matrix and activate intracellular signaling via the tyrosine kinase, focal adhesion kinase (FAK). TGM2 was found to either cross-link or non-covalently bind to interacting partners on the ECM and this is suggested to be decisive if TGM2 either mediates cell adhesion, migration or matrix assembly. Fibrinogen and FN can be incorporated and covalently cross-linked by TGM2 into homopolymers or heteropolymers. Formation of multimers by TGM2 was also seen for laminin and nidogen, thus leading to formation of very high molecular weight complexes to stabilize ECM and mediate cell adhesion and migration [199,200 201,202]. Signals from TGM2 mediated ligand-integrin interactions are propagated via the integrin cytoplasmic tails and are suggested to activate FAK, Akt and NF-κB, which are known inducers of EMT [203]. EMT is a process to reprogram epithelial cells into cells with mesenchymal characteristics which is a common feature of wound healing, tissue repair and inflammation [204]. Furthermore, β1 integrin associated TGM2 was found to direct interact with LRP1, a member of the LDL receptor superfamily which functions in lipoprotein metabolism, degradation of proteases and activation of lysosomal proteins [205,206].

Due to massive cell growth, tumors generally suffer from hypoxic stress and nutrient deprivation, therefore a metabolic adaption and increased angiogenesis can constantly be seen in tumors [207]. A hallmark in cancer cells is the new formation of blood vessels to ensure blood, oxygen and nutrient supply [181]. HIF1-α is a key driver of hypoxia induced angiogenesis and its activation results in transcription of

angiogenesis related genes like VEGF and PDGF. Under normal oxygen conditions HIF1-α signaling is steadily degraded, by the von Hippel-Lindau (VHL) tumor suppressor, for instance. TGM2 can deplete VHL through polymerization and therefore leads to activation of HIF1-α signaling [208]. In endothelial cells under hypoxic condition, TGM2 is secreted into the ECM and co-localizes with endostatin which affects migration and proliferation of fibroblasts as well as angiogenesis [209]. Extracellularly, integrin associated TGM2 was shown to interact with Platelet Derived Growth Factor Receptor (PDGFR). TGM2-mediated scaffolding of PDGFR and integrin enhances the transmission of extracellular signals, and mediates up-regulation of PDGFR linked downstream targets [210]. The Carboxyl-terminus of Hsp70-interacting protein (CHIP) was found as an ubiquitin E3 ligase, which leads to proteasomal degradation of TGM2. However, in renal cell carcinoma (RCC) CHIP can be found markedly decreased with a simultaneous altered TGM2 expression, which in turn leads to tumor growth and angiogenesis [211].

Regulation of angiogenesis goes hand in hand with cancer cell metabolic reprogramming. Transcription factors like HIF1-α and NF-κB promote angiogenesis and metabolic adaption to the tumor microenvironment. The relation of TGM2 to HIF1-α and NF-κB suggests a contribution of TGM2 in metabolic signaling. TGM2 is further described as a regulator of protein kinase A (PKA). PKA is a cAMP activated protein kinase, which plays a crucial role in glycogen metabolism. Based on a hypothesized role of TGM2 as a biomarker in prostate cancer cells, putative interaction partners were the subject of intensive research. Protein kinase, a protein anchor protein 13 (AKAP13) revealed to bind with high affinity to TGM2 [212]. Further it was suggested, that AKAP13 brings TGM2 and PKA to close proximity which facilitate PKA downstream signaling [212].

Besides the function of the ECM to give the cell structural support and its involvement in adhesion and movement, ECM signaling protects tumor cells from drug-induced apoptosis. ECM mediated chemoresistance is mediated by integrin signaling, due to activation of pro-survival pathways like Akt, PI3K and ERK1/2 [213]. As described previously in this work, TGM2 show pivotal functions in integrin mediated signaling in cancer and is proposed to alter survival pathways and drug resistance [214].

As TGM2 is a multifunctional enzyme and is able to exert a variety of functions, its activity is also associated to suppress and inhibit tumor growth. Among many other examples, TGM2 was described as a host defense against tumor development. Thus, TGM2 prevents the invasion of malignant metastatic melanoma cells via its interaction with GPR56[215], in mammary epithelial cells, TGM2 is suggested to mediate autophagy via a P53 dependent pathway and thus, constitutes an important barrier to prevent

oncogenic transformation[216]. These different results show the central importance to dissect the function of TGM2 in detail for every tumor entity individually.

1.3 Objectives of the study

Cancer is one of the most common disease worldwide, claiming 8,8 million deaths each year [2]. In the context of tumor diseases, CRC is one of the most prevalent cancer worldwide. Understanding the molecular interplay involved in the neoplastic transformation of intestinal cells, allows their specific targeting for an effective anti-cancer therapy. However, a detailed knowledge on CRC biology is required to therapeutically improve the survival outcome of patients with early and advanced CRC.

The aim of the present project was to identify and describe molecules that are decisively involved in the development of CRC and to find target and marker molecules with therapeutic potential, which can be selectively targeted or are able to precisely characterize TICs. TICs are more resistant to conventional anticancer therapy and provoke treatment escape and tumor relapse. To this extend the proteome profile of an aggressive TIC-enriched CRC subpopulation was investigated and revealed TGM2 as a promising target especially enriched in this subpopulation.

It was of great interest to deepen the understanding of molecular mechanisms underlying the role of TGM2 in CRC carcinogenesis and biology.

2. Material

2.1 Antibodies

Table 1 Antibodies for flow cytometry

Antigen	Clone	Conjugate	Company
CD133	W6B3C1	PE, APC	BD Pharmingen, San Diego, USA
EpCAM	9C4	Pacific Blue	BioLegend, San Diego, USA
Fixable viability dye		eFluor®780, eFluor®506	eBioscience, Frankfurt, Germany

Table 2 Antibodies for Western Blot/WES

Antigen	Source	Clone/Number	Company
Akt	Rabbit	C67E7	Cell Signaling, Danvers, USA
HIF-1α	Mouse	54	BD Bioscience, San Diego, USA
NF-κB	Rabbit	#3035	Cell Signaling, Danvers, USA
p53 ms	Mouse	1C12	Cell Signaling, Danvers, USA
p53 rb	Rabbit	#9282	Cell Signaling, Danvers, USA
p-p53(S15) ms	Mouse	16G8	Cell Signaling, Danvers, USA
p-p53(S15) rb	Rabbit	D4S1H	Cell Signaling, Danvers, USA
pAkt	Rabbit	D9E	Cell Signaling, Danvers, USA
pNF-κB	Rabbit	93H1	Cell Signaling, Danvers, USA
TGM2 ms	Mouse	CUB 7402	Abcam, Cambridge, USA
TGM2 rb	Rabbit	D11A6	Cell Signaling, Danvers, USA
α-Tubulin ms	Mouse	DM1A	Cell Signaling, Danvers, USA
α-Tubulin rb	Rabbit	11H10	Cell Signaling, Danvers, USA
β-Actin	Mouse	8H10D10	Cell Signaling, Danvers, USA

2.2 Bacterial strains

TOP10 chemically competent *Escherichia coli* (E.coli) from Invitrogen (Carlsbad, California, USA). Genotype: F- *mcr*A Δ(*mrr-hsd*RMS-*mcr*BC) φ80*lac*ZΔM15 Δ*lac*X74 *rec*A1 *ara*D139 Δ(*ara- leu)*7697 *gal*U *gal*K *rps*L (StrR) *end*A1 *nup*G.

2.3 Buffers and solutions

Table 3 Buffers and solutions

Buffer/solution	Ingredients/Source
Dissociation Enzyme Mix	Dispase 1u/ml, Dnase I 100U/ml, Collagenase 3 200u/ml 5mM CaCl$_2$
DMEM/F12	Gibco, Life Technologies, Darmstadt, Germany
DNA loading buffer (6x)	New England Biolabs, Ipswich, USA
Dulbecco's Modifies Eagle Medium (DMEM)	Gibco, Life Technologies, Darmstadt, Germany
Epidermal Growth Factor (EGF)	PromoCell, Heidelberg, Germany
FACS buffer	PBS, 2 % FCS, 0.05 % NaN$_3$, stored at 4°C
FACS fixation solution (2x)	2 % Paraformaldehyde in PBS, stored at 4°C
Fetal bovine serum (FBS)	PAA Laboratories, Pasching, Austria
Fibroblast Growth Factor (FGF)	PromoCell, Heidelberg, Germany
Hanks balanced salt solution (HBSS)	Sigma Aldrich, St. Louis USA
HEPES buffer 2x	Sigma Aldrich, St. Louis USA
LB medium	Roth, Karlsruhe, Germany
L-Glutamine	Gibco, Life Technologies, Darmstadt, Germany
M-PER Mammalian Protein Extraction Reagent	Thermo Fisher Scientific, Waltham, USA
N2 supplement	Gibco, Life Technologies, Darmstadt, Germany
P1 resuspension buffer (500 ml)	50 mM Tris HCL pH 8; 10 mM EDTA; 500 µl RNAse A; in 500 ml ddH$_2$O
P2 alkoline lysis buffer (500 ml)	200 mM NaOH, 1 % SDS in ddH$_2$O
P3 neutralisation buffer (500 ml)	300 ml patassium acetate; 57.5 ml acetate; 142.5 ddH$_2$O
Penicillin/Streptomycin	Gibco, Life Technologies, Darmstadt, Germany
Phosphate Buffered Saline (PBS)	PAA Laboratories, Pasching, Austria
PLA washing buffer PBS/Saponine 0.2 %	PLA washing buffer PBS/Saponine 0.2 %
PLA washing buffer PBS/Saponine 0.2 %/Tween 0.5 %	PLA washing buffer PBS/Saponine 0.2 %/Tween 0.5 %
PLA washing buffer PBS/Tween 0.5 %	PLA washing buffer PBS/Tween 0.5 %
Red blood cell lysing buffer	0.83 % NH$_4$Cl$_2$ in Aqua dest
Restriction buffer	New England Biolabs, Ipswich, USA

StemSpan; serum free expansion medium (SFEM)	Stem cell technologies, Vancouver, Canada
TAE buffer (10x)	Roth, Karlsruhe, Germany
Trypsin-EDTA solution (0.05 %)	Invitrogen, Carlsbad, USA

2.4 Cell culture media

McCoys 5A medium (Modified), complete:

Cells were maintained in McCoys 5A® supplemented with 10 % (v/v) Fetal bovine serum (FBS), 200 mM HEPES, 2mM L-glutamine, 50 U/ml Penicillin/Streptomycin

DMEM/F12 complete:

DEMEM/F12® is a 1:1 mixture of DEMEM® and Ham´s F-12® and supplemented with 10 % (v/v) Fetal bovine serum (FBS), 2 % (v/v) L-glutamine, 1 % (v/v) Penicillin/Streptomycin

Sphere medium

DMEM/F12®, supplemented with 20 ng/ml epidermal growth factor and fibroblast growth factor, 2 % N2 supplement, 20 mM HEPES, and 50 U/ml Penicillin/Streptomycin

2.5 Chemicals and reagents

Table 4 Chemicals and reagents

Chemicals	Company
Accutase	Sigma Aldrich, St.Louis, USA
Agarose	Roth, Karlsruhe, Germany
Ammonium Chloride	Sigma Aldrich, St.Louis, USA
Ampicilin (sodium salt)	Roth, Karlsruhe, Germany
Bovine serum albumin (BSA)	Sigma Aldrich, St.Louis, USA
Calcium Cloride ($CaCl_2$)	Merck, Darmstadt, Germany
Cobaltchloride ($CoCl_2$)	Sigma Aldrich, St.Louis, USA
Dimethyl sulfoxide (DMSO)	Sigma Aldrich, St.Louis, USA
Ethanol	Roth, Karlsruhe, Germany
Ethidium bromide	Roth, Karlsruhe, Germany
Ethylenediaminetetraacetic acid (EDTA)	Sigma Aldrich, St.Louis, USA
Gylcerin 88 % for cell culture	Gerbud, Heidelberg, Germany

Isopropanol	Roth, Karlsruhe, Germany
LB Broth	Roth, Karlsruhe, Germany
LDN27219	Sigma Aldrich, St.Louis, USA
Methanol	Roth, Karlsruhe, Germany
ProLong™ Diamond Antifade Mountant with DAPI	Thermo Fisher Scientific, Waltham, USA
Saponine	Sigma Aldrich, St.Louis, USA
Sodium Chloride (NaCl)	Roth, Karlsruhe, Germany
Thyrphostin 47	Sigma Aldrich, St.Louis, USA
Trizole	Qiagen, Venlo, Nederland
Trypan blue	Sigma Aldrich, St.Louis, USA
Tween 20	Sigma Aldrich, St.Louis, USA
Z-DEVD-FMK	R&D Systems, Abington, USA
z-VAD-FMK	R&D Systems, Abington, USA
β-mercaptoethanol	Gibco, Life Technologies, Darmstadt, Germany

2.6 Enzymes and ladders

Table 5 Enzymes and ladders

DNA ladder	Company
GeneRuler 100 bp	Thermo Fisher Scientific, Waltham, USA
GeneRuler 1 bp	Thermo Fisher Scientific, Waltham, USA

Enzyme	Company
AgeI	New England Biolabs GmBH, Germany
BamHI	New England Biolabs GmBH, Germany
EcoRI	New England Biolabs GmBH, Germany
SpeI	New England Biolabs GmBH, Germany
XbaI	New England Biolabs GmBH, Germany
XhoI	New England Biolabs GmBH, Germany
HotStar HiFidelity polymerase	QIAGEN, Hilden, Germany
Phusion High Fidelity DNA Polymerase	New England Biolabs GmBH, Germany
T4 DNA Ligase	New England Biolabs GmBH, Germany
Antarctic Phosphatase	New England Biolabs GmBH, Germany
DNaseI from bovine pancreas type IV	Sigma-Aldrich Chemie GmBH, Germany
RNase I from bovine pancrease	Sigma-Aldrich Chemie GmBH, Germany
Ribolock (RNase-Inhibitor)	Thermo Fisher Scientific, Waltham, USA
Collagenase 3	Worthington Biochemical Product, Lakewood, USA
Dispase	Worthington Biochemical Product, Lakewood, USA

Dnase I	Worthington Biochemical Product, Lakewood, USA

2.7 Kits

Table 6 Conventional Kits

Kits	Company
Apoptosis Detection Kit eFluor 450	BioLegend, San Diego, USA
Apoptosis Detection Kit FITC	BioLegend, San Diego, USA
Apoptosis Detection Kit Pacific Blue	BioLegend, San Diego, USA
Apoptosis Detection Kit PE	BioLegend, San Diego, USA
BD Fix Buffer I	BD bioscience, Franklin Lakes, USA
BD Perm Buffer III	BD bioscience, Franklin Lakes, USA
BD Pharm lyse^{TM} buffer	BD bioscience, Franklin Lakes, USA
Caspase 3 (active) FITC staining Kit	Abcam, Cambride, USA
Dulolink In situ PLA Probe Anti-Mouse MINUS	Sigma Aldrich, St. Louis, USA
Dulolink In situ PLA Probe Anti-Rabbit PLUS	Sigma Aldrich, St. Louis, USA
Duolink In situ Orange starter Kit Mouse/Rabbit	Sigma Aldrich, St. Louis, USA
HotStar HiFidelity Polymerase Kit	QIAGEN, Hilden, Germany
MTT proliferation assay	Sigma Aldrich, St. Louis, USA
NucleoBond Extra Endo free maxi kit	Macherey-Nagel, Düren, Germany
NucleoBond PC 100 Midi Kit	Macherey-Nagel, Düren, Germany
NucleoSpin Gel and PCR Clean-up	Macherey-Nagel, Düren, Germany
pGEM-T easy cloning vector kit	Promega, Madison, USA
Pierce Protease and Phosphatase Inhibitor Mini Tablets	Thermo Fisher Scientific, Waltham, USA
Proteom Profiler Human Apoptosis Array	R&D Systems, Abington, USA
QIAquick Gel Extraction kit	QIAGEN, Hilden, Germany
RNAeasy isolation kit	QIAGEN, Hilden, Germany
Separation and Detection Module	Protein Simple, San Jose, USA
Tissue Transglutaminase Microassay Kit	Zedira, Darmstadt, Germany
Tumor Cell Isolation Kit, human	Miltenyi Biotec, Bergisch Gladbach, Germany

2.8 Laboratory equipment and plastic ware

Table 7 Instruments

Instruments	Company
CellObserver 430 optical microscope	Carl Zeiss AG, Oberkochen, Germany
Centrifuge, Heraeus Megafuge 1. OR	Thermo Fisher Scientific, Waltham, USA
Centrifuge Rotana 460R	Hettich, Tuttlingen, Germany
Centrifuge, tabletop (Rotanta 200, 220R)	Hettich, Tuttlingen, Germany
Clean bench, HERAsafe KSP	Thermo Fisher Scientific, Waltham, USA
CO_2 Incubator, HERAcell 150i	Thermo Fisher Scientific, Waltham, USA
Digital PH caliper	Mettler Toledo, Greifensee, Schwitzerland
Dissection set	Heiland, Hamburg, Germany
DNA electrophoresis chamber	Bio-Rad, Hercules, USA
FACS AriaI and AriaIII cell sorter	BD, Franklin Lakes, USA
FACS CantoII	BD, Franklin Lakes, USA
Freezer -80°C Hereaeus	Thermo Fisher Scientific, Waltham, USA
Freezer -20°C and refrigerators	Liebherr, Bulle, Switzerland
HiSeq2000	Illumina, San Diego, USA
Incubator, Heraeus	Thermo Fisher Scientific, Waltham, USA
LightCycler 480 II quantitative PCR cycler	Roche Life Science, Rotkreuz, Switzerland
Nano-Drop 1000 sectrometer	Thermo Fisher Scientific, Waltham, USA
Thermal cycler MyCycler	Bio-Rad, Hercules, USA
Thermomixer	Biometra, Analytik Jena, Jena, Germany
Ultracentrifuge Optima L-90K	Beckman Coulter, Pasadena, USA
UV-Transilluminator GelDoc 2000	Bio-Rad, Hercules, USA
Vaccum pump	Integra Bioscience, Fernwald, Germany
Vortex Minishaker	Roth, Karlsruhe, Germany
Tecan Microplate Reader	Tecan, Männedorf, Switzerland
Trans-Blot Turbo System	Bio-Rad, Hercules, USA
Criterion Cell	Bio-Rad, Hercules, USA
WES	Protein Simple, San Jose, USA
Fusion Fx7	PEQLAB-Life Science, Germany
gentleMACS Dissociator	Miltenyi Biotec, Bergisch Gladbach, Germany

Table 8 Laboratory equipment

Instruments	Company
Aspirations pipettes (2 ml)	BD, Franklin Lakes, USA
Cell culture flasks (25, 75 and 175 cm2)	BD, Franklin Lakes, USA
Combitips plus (1, 5 and 10 ml)	Eppendorf, Hamburg, Germany
Conical polysterene tubes	Sasted, Nümbrecht, Germany
Counting chamber C-Chip, Neubauer improved	PegLab, Erlangen, Germany
Cryotubes (2ml)	Sigma Aldrich, St. Louis, USA
FACS tubes	Sasted, Nümbrecht, Germany
Falcon sterile centrifuge tubes (5, 15, and 50 ml)	Greiner Bio-One, Frickenhausen, Germany
Freezing box	NeoLab, Heidelberg, Germany
Insuline syringe (BD)	Franklin Lakes, USA
Microvette	Sasted, Nümbrecht, Germany
Non-tissue culture plates (6, 12 and 24 well)	BD, Franklin Lakes, USA
NUNC tissue culture plates seal tight (24 well)	Thermo Fischer Scientific, Waltham, USA
Pasteur pipetts (glas)	Roth, Karlsruhe, Germany
Petri dishes	Greiner Bio-One, Frickenhausen, Germany
Pipette tips (10, 100, 200 and 1000 µl)	Gilson, Limburg-Offheim, Germany
Protection gloves (Latex, Nitril)	Meditrade, Kiefersfelden, Germany
Reaction tubes (0.1, 0.2, 1.5 and 2 ml)	Eppendorf, Hamburg, Germany
Scalpels	Mediware Servopax, Wesel, Germany
Sterile cell strainer (40, 70, 100 µm)	BD, Franklin Lakes, USA
Sterile filters 0.22 µm	Merck, Millipore, Bilerica, USA
Sterile pipets (2, 5, 10, 25 ml)	Braun, Melsungen, Germany
Tissue culture dishes (3.5 and 10 cm)	Greiner Bio-One, Frickenhausen, Germany
Tissue culture plates (6, 12, 24, 96 well)	Sarstedt, Nümbrecht, Germany
Simport Double Cytosep	MSP, Atlanta, USA
StainTray Slide Staining System (humid chamber)	Simport, Quèbec, Kanada+E30:F33
Mini-Protean TGX Stain-Free Precast Gel	Bio-Rad, Hercules, USA

2.9 Mouse strains

NOD.CB17-Prkdc[scid]/J (non-obese diabetic/severe combined immunodeficiency [NOD/SCID]) mice (Jackson Laboratory, USA). All mice were used at 10-14 weeks of age if not stated otherwise. All mice were bred and maintained under specific pathogen-free conditions. Experiments were performed in accordance with German animal welfare legislation and were approved by the relevant authorities (Regierungspräsidium Darmstadt).

2.10 Oligonucleotides

Table 9 Primer for shRNA cloning

Description	Sequence (5' to 3')
TGM2 shRNA1 for	CCGGTATCACCCACACCTACAAATACTCGAGTATTTGTAGGTGTGGGTGATATTTTTG
TGM2 shRNA1 rev	AATTCAAAAATATCACCCACACCTACAAATACTCGAGTATTTGTAGGTGTGGGTGATA
TGM2 shRNA2 for	CCGGTTGTGCTGGGCCACTTCATTTCTCGAGAAATGAAGTGGCCCAGCACAATTTTTG
TGM2 shRNA2 rev	AATTCAAAAATTGTGCTGGGCCACTTCATTTCTCGAGAAATGAAGTGGCCCAGCACAA
TGM2 shRNA3 for	CCGGACAGCAACCTTCTCATCGAGTCTCGAGACTCGATGAGAAGGTTGCTGTTTTTTG
TGM2 shRNA3 rev	AATTCAAAAAACAGCAACCTTCTCATCGAGTCTCGAGACTCGATGAGAAGGTTGCTGT
TGM2 shRNA4 for	CCGGTGAGAAATACCGTGACTGCCTCTCGAGAGGCAGTCACGGTATTTCTCATTTTTG
TGM2 shRNA4 rev	AATTCAAAAATGAGAAATACCGTGACTGCCTCTCGAGAGGCAGTCACGGTATTTCTCA
TGM2 shRNA5 for	CCGGCCACCCACCATATTGTTTGATCTCGAGATCAAACAATATGGTGGGTGGTTTTTG
TGM2 shRNA5 rev	AATTCAAAAACCACCCACCATATTGTTTGATCTCGAGATCAAACAATATGGTGGGTGG
HIF1-α shRNA 1 for	CCGGCCGCTGGAGACACAATCATATCTCGAGATATGATTGTGTCTCCAGCGGTTTTTG
HIF1-α shRNA 1 rew	AATTCAAAAACCGCTGGAGACACAATCATATCTCGAGATATGATTGTGTCTCCAGCGG
HIF1-α shRNA 2 for	CCGGGCCGCTCAATTTATGAATATTCTCGAGAATATTCATAAATTGAGCGGCTTTTTG
HIF1-α shRNA 2 rew	AATTCAAAAAGCCGCTCAATTTATGAATATTCTCGAGAATATTCATAAATTGAGCGGC
HIF1-α shRNA 3 for	CCGGTGCTCTTTGTGGTTGGATCTACTCGAGTAGATCCAACCACAAAGAGCATTTTTG
HIF1-α shRNA 3 rew	AATTCAAAAATGCTCTTTGTGGTTGGATCTACTCGAGTAGATCCAACCACAAAGAGCA
HIF1-α shRNA 4 for	CCGGTATGCACTTTGTCGCTATTAACTCGAGTTAATAGCGACAAAGTGCATATTTTTG
HIF1-α shRNA 4 rew	AATTCAAAAATATGCACTTTGTCGCTATTAACTCGAGTTAATAGCGACAAAGTGCATA

Table 10 CRISPR guide RNAs

Description	Sequence (5' to 3')
TGM2 CR Exon 1 s	CACCGtgatactcaccctcggcca
TGM2 CR Exon 1 as	AAACtggccgagggtgagtatcaC
TGM2 CR Exon 5 s	CACCGctctgacacagtttgaaga
TGM2 CR Exon 5 as	AAACtcttcaaactgtgtcagagC

2.11 Plasmids

Table 11 Generated and used plasmids

Plasmide name	Description	Reference
pMD2.G.VSV-G+E9:G17	Expression plasmid for VSV-G (env); pseudotyping of lentiviral particles; CMV promoter	[217]
pMDLg.HIVGag-Pol.pRRE	Expression plasmid for structural genes (gag/pol) of HIV-1; lentiviral particle assembly; CMV promoter	[218]
pRSV.HIV-REV	Expression plasmid for lentiviral reverse transcriptase (rev) of HIV-1; RSV promoter	[219]
pRRL.PPT.SFFV.IRES.eGFP.WPRE	Lentiviral vector with a 5' packaging signal coding for a fusion protein of hImportin and the fluorescent protein eGFP; lentiviral gene transfer; SFFV promoter	[220]
pRRL.PPT.SFFV.MCS.IRES.VENUSnucmem.WPRE	Lentiviral vector with a 5' packaging signal coding for a fusion protein of hImportin and the fluorescent protein VENUS; lentiviral gene transfer; SFFV promoter	Cloned from pRRL.PPT.SFFV.IRES.eGFP.WPRE
pRRL.PPT.SFFV.MCS.IRES.tdTOMATOnucmem.WPRE	Lentiviral vector with a 5' packaging signal coding for a fusion protein of hImportin and the fluorescent protein tdTOMATO; lentiviral gene transfer; SFFV promoter	Cloned from pRRL.PPT.SFFV.IRES.eGFP.WPRE
pRRL.PPT.SFFV.MCS.candidate CDS.IRES.VENUSnucmem.WPRE	Lentiviral vector with a 5' packaging signal coding for the candidate CDS and a fusion protein of hImportin and the fluorescent protein VENUS; lentiviral gene transfer; SFFV promoter	Cloned from pRRL.PPT.SFFV.IRES.VENUSnucmem.WPRE
pRRL.PPT.SFFV.MCS.candidate CDS.IRES.tdTOMATOnucmem.WPRE	Lentiviral vector with a 5' packaging signal coding for the candidate CDS and a fusion protein of hImportin and the fluorescent protein tdTOMATO; lentiviral gene transfer; SFFV promoter	Cloned from pRRL.PPT.SFFV.IRES.tdTOMATOnucmem.WPRE
pLenti Crispr v2	Lentiviral vector with a fluorecent protein BFP	[221]

CDS = coding sequence; CMV = cytomegalovirus; HIV-1 = human immunodeficiency virus type-1;

SFFV = spleen focus-forming virus; VSV = vesicular stomatitis virus; VSV-G = glycoprotein G of VSV

2.12 Software

Table 12 Software

Software	Company
GraphPad Prism 6 and 7	GraphPad
MS Office 2013	Microsoft GmbH, Germany
Clone manager	Sci-Ed Software
BD FACS DIVA	BD Bioscience
Image J	National Institute of Health
GSEA	Broad Institute
DAVID	Laboratory of Immunopathogenesis and Bioinformatics
Compass	Protein simple

3. Methods

3.1 Molecular and biochemical methods

3.1.1 Polymerase chain reaction (PCR)

PCR for specific amplification of DNA double strands were performed in 50 µL reaction volume using Phusion® High-Fidelity DNA Polymerase or in 20 µl reaction volume using HotStar HiFidelity polymerse (Qiagen).

3.1.2 PCR purification

Purification of PCR products from the reaction was performed using the NucleoSpin® Gel and PCR Clean-up Kit following the manufacturer's protocol. DNA was eluted using Milli-Q H_2O or the elution buffer provided in the kit. DNA was stored at -20°C.

3.1.3 Restriction enzyme digest

Restriction digests of DNA were performed in 20-60 µl reactions for ~3h at 37°C with enzyme concentrations and buffer conditions as recommended by the manufacturer.

3.1.4 DNA preparation (Mini-prep)

Alkaline lysis was used to isolate plasmid-DNA from chemical competent *E. coli* bacteria. The overnight culture of 2 ml bacteria suspension was harvested by centrifugation (1800 x g, 10 min, 4°C), resuspended in 250 µl P1 buffer followed by adding 250 µl buffer P2 for alkaline lysis and incubation for 5 min at RT. Lysis was stopped with 250 µl of neutralization buffer P3 incubating on ice for 5 min, followed by centrifugation for 15 min at 18200 x g at 4°C to get rid of cell debris, protein and genomic DNA. Supernatant was mixed with 700 µl of isopropanol and centrifuged again for 20 min at 18200 x g at 4°C to precipitate the plasmid-DNA. Plasmid DNA was washed once with 500 µl 70 % ethanol for 5 min with 18200 x g at 4°C. DNA pellet was dried at RT for 15-20 min, before 30 µl endotoxin-free water was added to re-suspend the

plasmid DNA. Concentration and quality of the purified plasmid DNA was analyzed with a spectrophotometer (Nanodrop 1000, Thermo Fischer Scientific).

3.1.5 Agarose gel electrophoresis

- **Analytical electrophoresis**

Analytical Agarose gel electrophoresis was performed usually using 0.7-1.5 % Agarose (depending on the size of the DNA fragment) supplemented with Ethidiumbromide (EtBr). Samples were prepared using 6x sample buffer and were run for 30 min at a constant voltage of 100 V in 1x TAE buffer. DNA was visualized by an UV-transilluminator and documented using a CCD camera.

- **Preparative electrophoresis**

Preparative electrophoresis was performed using 0.7-1.5 % Agarose (depending on the size of the DNA fragment) supplemented with EtBr. Samples were prepared using 6x sample buffer and were run for 30 min at a constant voltage of 100 V in 1x TAE buffer. DNA was visualized by an UV-transilluminator and documented using a CCD camera. Relevant gel pieces were excised from the gel and stored in a 1.5 ml reaction tube.

3.1.6 Ligation

Ligations were performed in 10-20 µL reactions using 50-150 ng vector DNA, insert DNA in a molar ratio of 1:1, 1:3 or 1:6 and 1 U T4 DNA Ligase in the buffer recommended by the manufacturer. Ligations were performed at RT for 1 h or at 16°C over-night.

3.1.7 Transformation

Chemically competent *E.coli* bacteria from Invitrogen (Carlsbad, California, USA) in 100 µl stocks were thawed on ice and mixed with 5-50 ng DNA in 2-10 µl. After 30 min incubation on ice DNA uptake was mediated by heat shock for 45 sec at 42°C followed by 2 min chill on ice. Cells were supplemented with 450 µl sterile SOC or LB medium (without antibiotics) and incubated shaking at 37°C for 1 h. 100 µl (20 %) of bacteria suspension was plated on LB-Agar plates supplemented with ampicillin and incubated overnight at 37°C. 400 µl (80 %) of bacterial suspension was pelleted (18260 x g, 1 min), 300 µl of medium was withdrawn. The residual volume was plated on LB-Agar plates supplemented with ampicillin and incubated overnight at 37°C as well. Single bacteria colonies grown on ampicillin were picked and expanded in 4 ml LB-medium containing 100 µg/ml ampicillin and cultivated at 37°C and continuous shaking at 250 rpm. 2 ml bacteria suspension was harvested for analytical plasmid DNA preparation. The remaining culture was stored at 4°C as starting culture for larger scale plasmid DNA preparation in 250 ml LB medium (100 µg/ml ampicillin).

3.1.8 Plasmid preparation (Maxi prep)

Plasmid DNA was purified from 250 ml bacteria culture using the EndoFree Plasmid Maxi Kit following the respective manufacturer's recommendations. Plasmid DNA was eluted using DNA storage buffer and stored at -20°C.

3.1.9 Determination of DNA concentration

DNA concentration was determined spectrometically using the NanoDrop 1000 UV-/Vis Spectrophotometer.

3.1.10 Sequencing

Sequencing was performed by Sequence Laboratories GATC, with plasmid and primer concentrations as suggested by the company.

3.1.11 Viral vector generation

A third generation self-inactivating HIV -1 based lentiviral vector system (lentiviral particles) was used for gene transfer into standard culture cell lines. At first, the open reading frame (ORF) of a fluorescent reporter protein (either VENUS hImportin subunit α1 (AA2-67) or tdTOMATO-hImportin subunit α1 (AA2-67)) was inserted into the third generation self-inactivating lentiviral vector pRRL.PPT.SFFV.IRES.eGFP.wPRE by replacing the ORF of green fluorescent protein (Schambach et al. 2006a). Therefore, the ORF of all three fluorescent reporter proteins as well as the lenitviral backbone were cut with Pml and BsrGI out of their plasmid backbones and cleaned by DNA gel extraction. The purified linear DNA was ligated building the new VENUS-hImportin or tdTOMATO-hImportin containing lentiviral vectors and validated by sequencing. In a second cloning step, an in silico self-constructed multiple cloning site (MCS) containing 10 restriction enzyme recognition sites was inserted after the SFFV promoter for multiple cloning techniques:

5'-GATCCTCGAGGCCGGCCGCGCGCGCCGGCGACTAGTCCGGATTTAAATCTAGACGCGTA-3'
3'-GAGCTCCGGCCGGCGCGCGCGGCCGCTGATCAGGCCTAAATTTAGATCTGCGCATGGCC-5'
BamHI FseI MauBI MreI XhoI SpeI SwaI XbaI MluI AgeI

- **Generation of shRNA constructs**

The forward and reverse primer of TGM2 shRNAs (each 10 µl of 100 µM) plus 2.2 µl NEB buffer 2 were incubated at 95°C for 10 min in a water bath and slowly cooled down against the RT, allowing optimal annealing of the two oligomers. The pLKO lentiviral expression vectors were linearized using BamHI and AgeI and purified as described above. The annealed oligomers were ligated with their overlapping 5' ends with the linearized lentiviral expression vector and transformed into chemically competent TOP10 bacteria building new lentiviral expression vectors. (Vector maps in the appendix)

- **Generation of TGM2 constructs**

TGM2 isoforms and point mutated TGM2 constructs were produced and cloned into our lentiviral expression vectors by BioCat, Heidelberg, Germany (Vector maps in the appendix).

- **Generation of CRISPR constructs**

CRISPR sgRNAs were produced and cloned into a lentiviral vector expression system by Frank Schnütgen (Vector maps in the appendix).

3.1.17 Western Blot

- **Western Blot procedure in general**

Cells were lysed on ice in M-PER Mammalian extraction Reagent and substituted with Pierce Protease and Phosphatase Inhibitor Mini Tablets (Thermo Fisher, USA) according to the manufacturer's protocol. Protein concentration was determined using Bio-Rad protein assay Kit II (Bio-Rad, Hercules, USA).

25µg – 50µg of protein was applied to SDS-PAGE and transferred to a PVDF membrane using the Trans-Blot Turbo-Transfer System (Bio-Rad). Primary antibodies were incubated overnight at 4°C. The bound primary antibodies were detected by the use of horseradish peroxidase (HRP)-conjugated secondary antibodies and the ECL Prime detection system (GE Healthcare). The band density of each band was quantified using ImageJ-software.

- **Validation of TGM2 knockout or knockdown efficiency**

Cells were lentivirally transduced with an MOI5 (multiplicity of infection 100), either with control or shTGM2-1, shTGM2-2 or Crispr a or b and cultured for 3 days. An aliquot of the cells was used to determine the transduction efficiency via flow cytometry. For further investigations, only cells with a transduction efficiency of ≥ 80 % were used. The knockdown effect was verified using Western Blot analysis.

- **Validation of protein expression under hypoxic conditions**

Cells were maintained under hypoxic condition using a hypoxic chamber or Cobalt(II)-chloride (50 µM or 100 µM) for 24h, 48h, and 72h. Every further step was accomplished on 4°C.

3.1.18 Protein expression studies with Wes^{TM} System

Cells were lysed on ice in M-PER Mammalian extraction Reagent and substituted with Pierce Protease and Phosphatase Inhibitor Mini Tablets (Thermo Fisher, USA) according to the manufacturer's protocol. Protein concentration was determined using Bio-Rad protein assay Kit II (Bio-Rad, Hercules, USA). Used protein concentration ranged from 0.05 µg (TGM2) to 4 µg (phosphoproteins). If multiplexing of several antibodies within one capillary was not feasible, i.e. due to cross-reaction of used antibodies, same sample

was used twice in the same run once for detection of protein of interest and once do determine the loading concentration. Further sample processing and applying on the capillary was performed according to the manufacturer's protocol. Default run settings were used, except determining protein expression of phospho-antibodies, hence primary antibody time was set on 90 min. The common primary antibody dilution was 1:50 except for phospho-antibodies, here a dilution of 1:25 was accomplished. Protein concentration was validated using High-Dynamic-Range (HDR) multi-image analysis for every tested sample. Alpha Tubulin was used as a loading control.

3.1.19 Proteome Profiler Human Apoptosis Array Kit

SW480 cells were transduced with either shSCRMBL as a control or with shTGM2-1 and shTGM2-2. Three days after transduction, cells were lysed on ice in M-PER Mammalian extraction Reagent and substituted with Pierce Protease and Phosphatase Inhibitor Mini Tablets (Thermo Fisher, USA) according to the manufacturer's protocol. The Proteome Profiler Human Apoptosis Array Kit (R&D Systems, United Kingdom) procedure was performed as described in the manufacturer's instructions. Statistical analysis was performed using ImageJ software.

3.1.20 RNA Sequencing

100,000 SW480 cells were transduced for three days with either shSCRMBL as a control or shTGM2-1 or shTGM2-2. Transduction efficiency was validated by FACS. RNA isolation was performed using RNAeasy isolation kit (Quiagen) according to the manufacturer's instructions. The quality and concentration of libraries were determined by an Agilent 2100 Bioanalyzer and RiboGreen fluorescence on Qubit (Invitrogen). Library preparation was performed at the DKFZ Core Facilities Genomics and Proteomics Unit (Heidelberg, Germany). The library was prepared using Illuminas's TruSeq Stranded Total RNA Library Prep kit and sequenced on an Illumina HiSeq 4000 (San Diego, CA, USA) system using a 100-bp paired-end approach. The resulting FASTQ files were aligned to the hg19 draft of the human genome and counts per gene were estimated using STAR (v.2.5.3).

Read count normalization, differential expression calculation and multidimensional scaling was performed using the DESeq2 package in R (v.3.4.1). Pathway analysis was performed using the gene set enrichment analysis (GSEA) software (v.3.0) on the hallmark gene sets (H) dataset [222]. Only pathways with an FDR-corrected q-value below 25 % were considered significant. Top 10 hits were shown.

3.1.21 Proximity ligation assay

Slides and filters were placed into the Simport Double Cytosep (MSP, USA) according to the manufacturer's instructions. 50,000 SW480 cells were used for every sample chamber. Cells were centrifuged at 500 g for 5 min and low acceleration. After centrifugation, cells were encircled with a liquid blocker pen and after 2 – 3 min, fixed with 20 µl 4 % Paraformaldehyde for 20 min at 4°C. For every spot a reaction volume of at least 15 µl was used. After fixation, the slides were washed twice with PBS for 5 min in a staining jar, on a shaker with gentle orbital shaking. After washing the outline of the circle, it should be dried gently and blocked and permeabilized using Duolink blocking solution (Sigma Aldrich, USA) for 1h 20min at 4°C in the humidity chamber. Slides were washed with PBS/0.2 % Saponine for 5 min under agitation at room temperature (RT) and primary antibodies were added. The two primary antibodies were raised in different species. For 2 spots 0.5 µl primary mouse and 0.5 µl primary rabbit antibody were diluted in 49 µl Duolink antibody dilution reagent (Sigma Aldrich, USA). On every spot 15 µl of antibody mix was added and incubated at 4°C overnight in a humidity chamber. The slides were washed in a staining jar for 5 min at RT as described before.in the following order; PBS/0.5 %Tween20, PBS/0.2 % Saponine/0.5% Tween20, PBS/0.5 % Tween20. The Duolink PLA probes (Sigma Aldrich, USA) were diluted 1:5 according manufacturer's instructions and incubated for 60 min at 37 °C in a humidity chamber. Before ligation slides were washed in the order as described before. Ligation was performed after the manufacturer's instructions and 15 µl ligase mix was added at each spot. After ligation slides were washed in a staining jar for 5 min at RT in the following order; PBS/0.2 % Saponine/0.5 % Tween20, PBS/0.5 % Tween20, PBS. The amplification mix was prepared according to the manufacturer's instructions and 15 µl amplification solution was added on each spot for 100 min. at 37°C in a humidity chamber. The cells were washed in the following order; PBS/0.2 % Saponine/0.5 % Tween20, PBS/0.5 % Tween20, PBS. Spots were mounted with mounting medium, which contains DAPI. Finally, the slides were analyzed using a fluorescence microscope at 40X (CellObserver 430 optical microscope, Karl Zeiss).

3.1.22 Tissue Transglutaminase Microassay

To evaluate the transamidase activity of different CRC cell lines, or lentiviral manipulated cells, the cells were treated as previously described. All lentiviral manipulated cells were treated for 3 days and the transduction efficiency was monitored by FACS. Cells were lysed on ice in M-PER Mammalian extraction Reagent (Thermo Fisher) and the tissue transglutaminase microassay (Zedira, Germany) was performed according to the manufacturer's instructions. Briefly, protein samples were incubated in the presence of

calcium, DTT and biotin-pepT26 in the wells of the delivered microtiter plate. Each well has been covalently coupled to spermine. In the presence of active TGM2, spermine is incorporated into the y-carboxamide of the glutaminyl residue of biotin-pepT26. Enzymatic reaction is determined by its interaction with streptavidin labelled peroxidase. A substrate solution for peroxidase was added and colour developed. Colour intensitiy was measured on the Infinite 200 microplate reader (Tecan, Germany).

3.2 Cell Culture methods

3.2.1 Cultivation of adherent cell lines

The CRC cell lines SW480 and HCT116 were cultivated in McCoy's 5a medium, supplemented with 10 % fetal bovine serum (FBS), 200 mM HEPES, 2 mM L-glutamine, 50 units/ml Penicillin/Streptomycin in 37 °C humidified atmosphere with 5 % CO_2. All CRC cell lines were purchased from CLS Cell Lines Service GmbH, Eppelheim, Germany. The cell lines HEK293T (human embryonic kidney) and NIH3T3 (murine embryonic fibroblasts) were cultivated in DMEM medium supplemented with 10 % fetal bovine serum (FBS), 20mM HEPES and 3.5mM L-glutamine in a standard cell culture incubator with 5.5 % CO_2 and 95 % humidity at 37°C. Every 2 – 3 days, when the cells were confluent to 70 –80 %, passaging was performed using Trypsin-EDTA to detach the cells from the culture flask. All manipulations of the cells were performed using S1 and S2 assigned sterile clean bench according to the declared safety working conditions.

3.2.2 Time-Lapse imaging and subsequent single cell tracking

For time-lapse imaging of SW480 TGM2 knockdown cells, the cells were transduced with either shSCRMBL as a control or with shTGM2-1 or shTGM2-2 two days before imaging and 20,000 transduced SW480 cells were seeded per position in 24-well culture plates (NUNCbrand, Greiner Bio-One). For time-lapse imaging of HCT116 $p53^{-/-}$ and HCT $p53^{wt}$, 20,000 cells were seeded per position and after sedimentation, virus particles were added with a MOI of 5 in 500 µl culture medium.

Seeded cell were incubated for at least 3 hours in the cell culture incubator, the plates were gas-tight sealed with adhesive tape and placed inside a CellObserver 430 (Zeiss) microscope. Cells can be imaged for several days under stable temperature conditions. Phase contrast images were acquired every 2-3 min using a 10x phase contrast objective (Zeiss), and an AxioCamHRm camera (at 1388x1040 pixel resolution) with a self-written VBA module remote controlling Zeiss AxioVision 4.8 software. Fluorescence was

detected every 1 hour with HXP illumination (Osram) and the filter sets for GFP (AH7-Z38), YFP (F46-003) and APC (HC628/40, ET66LP XR, ET700/75, AHF Analysentechnik AG). Tracking of individual cells and their progeny was performed manually with the help of a self-written program (Timm´s Tracking Tool; TTT) developed by Timm Schroeder which can determine and record multiple parameters of individual cells at each time point (Rieger et al. 2009). Single cells were observed and tracked supervised by marking the cell by a scientist. Cell fates such as cell division, cell death, and loss of fluorescent reporter expression observed while tracking were attributed in the TTT interface and saved into the pedigree. The generation time of an individual cell was defined as the time span between two cell divisions. Dead cells were depicted by their shrunk, non-refracting appearance coupled with immobility. Transgene-expression was determined by nuclear membrane tdTOMATO or GFP fluorescence.

3.2.4 Patient material

Human CRC and adjacent normal mucosa tissue were obtained after surgical resection and characterization by a pathologist. Tissue collection was approved by the Ethics Committee of the University Hospital Frankfurt, and after written consent had been received from all patients involved in the study.

Solid tissues were minced in $5mm^2$ or, if possible, smaller pieces. Minced tissue was transferred into 50 ml falcon tubes (Grainer Bio One, Germany) and extensively washed with PBS (PAA Laboratories) containing 50 U/ml Penicillin/Streptomycin. The washing step was performed till the supernatant did not show any cloudiness anymore, to this end fresh PBS/Penicillin/Streptomycin solution was added. After sedimentation of suspended particles, supernatant was discarded carefully. In the next step the tissue was dissociated with 200 U/ml Collagenase type III, 1 (?) U/ml Dispase, and 100 U/ml DNase I (all Worthingtorn, USA) in HBSS containing 5 mM $CaCl_2$ for 30 - 60 min at 37°C. Every 15 min the cell suspension was subjected to MACS tissue dissociator for 40 s. After enzymatic dissociation, next steps were performed on ice. To obtain single cell suspension samples were filtered through sterile 100, 70 and 40 µm nylon meshes (BD, Heidelberg, Germany). Between every filtration step, cells were centrifuged for 5 min at 500 g and resuspended in serum-free DMEM/F12 (Gibco, Germany) containing 20 mM HEPES, and 50 U/ml Penicillin/Streptomycin. Contaminating red blood cells were removed by osmotic lysis with Red Blood cell lysing buffer for 10 min at 37°C. Depending on the scientific question, cells were further processed.

3.2.4 Purification of epithelial cells from patient derived tissue

After preparation of a single-cell suspension from patient derived tissue, cells were magnetically labeled using human Tumor Cell Isolation Kit (Miltenyi Biotec). Briefly, the single cell suspension was incubated with 20 µl the "Non-Tumor Cell Depletion Cocktail A" and "Non-Tumor Cell Depletion Cocktail B" and incubated for 15 min at 4°C. Then the magnetic separation was proceeded. LS Columns (Miltenyi Biotec) were placed in the magnetic field of a MACS® separator. The flow-through containing unlabeled cells, enriched for human tumor cells, was collected.

3.2.3 Sphere formation assay

Freshly isolated, patient-derived single CRC and mucosa cells were suspended in serum-free DMEM/F12 (Gibco, Germany) supplemented with 20 ng/ml epidermal growth factor and fibroblast growth factor, 2 % N2 supplement (Life Technologies, Germany), 20 mM HEPES, and 50 U/ml Penicillin/Streptomycin at a density of 50,000 cells (tumor) and 100,000 cells (normal) per well in ultra-low-attachment 24-well plates (Corning, Germany), as described by Kreso and O'Brien [223]. Tyrphostin 47 and LDN27219 (Sigma Aldrich, Germany) were dissolved in dimethyl sulfoxide (DMSO) according to the manufacturer's instructions. Cells were treated with 10 µM for LDN27219 and 10 µM and 100 µM for Tyrphostin 47 or vehicle control. Plates were scored microscopically for tumorsphere formation after 7 and 14 days.

Cells derived from CRC cell lines were seeded at a density of 5000 cells in ultra-low-attachment 24-well plates (Corning, Germany) and after sedimentation cells were transduced with shSCRMBL, shTGM2-1 or shTGM2-2 by adding virus particles with a MOI of 5 in 500 µl culture medium. TGM2 knockout or control spheres derived from transduced cells were assessed microscopically after 7 and 14 days.

3.2.5 In vivo drug pretreatment

All animal experiments were approved by the local authorities and mice were used at 6 – 8 weeks of age. Tyrphostin 47 and LDN27219 (Sigma Aldrich, Germany) were dissolved in dimethyl sulfoxide (DMSO) and stored at -20°C. 50,000 SW480 cells per well were seeded in culture medium containing either a concentration of 10 µM of LDN27219 or 100 µM of Tyrphostin 47 in 24-well plates (BD, Germany). After 3 days of in vitro treatment, 50,000 living cells were subcutaneously injected into the flank of NOD.CB17-Prkdcscid/J (non-obese diabetic/severe combined immunodeficiency [NOD/SCID]) mice (Jackson Laboratory, USA). The tumor growth was monitored twice a week. When tumors reached a diameter of 1 cm, mice were sacrificed and tumor weight and size was determined.

3.2.6 In vivo drug treatment

50,000 living SW480 cells were subcutaneously injected into the flank of NOD.CB17-Prkdcscid/J (non-obese diabetic/severe combined immunodeficiency [NOD/SCID]) mice (Jackson Laboratory, USA). When tumor size reached 0.2 – 0.3 cm in diameter Tyrphostin 47 (2.2 mg/kg) and LDN27219 (25 mg/kg) was administered orally (LDN27219) or intraperitoneal (Tyrphostin 47), three times a week and compared with a vehicle control group. Tumor growth was measured every third day using a caliper, and mice were sacrificed when tumor size reached a diameter of 1 cm.

3.2.7 In vivo monitoring of TGM2 knockout cells

SW480 cells were transduced with shTGM2-1, shTGM2-2 or shSCRMBL. After 3 days of in vitro expansion 50,000 living SW480 cells were subcutaneously injected into the flank of NOD.CB17-Prkdcscid/J (non-obese diabetic/severe combined immunodeficiency [NOD/SCID]) mice (Jackson Laboratory, USA). Tumor growth was measured every third day using a calipercaliber, and mice were sacrificed when tumor size reached a diameter of 1 cm.

3.2.8 Annexin V/7AAD staining for apoptotic cells

SW480 cells were transduced with shTGM2-1, shTGM2-2 or shSCRMBL control for 3 days. Annexin V/7AAD (BioLegend) was performed according to the manufacturer's instruction. Briefly, apoptotic cells can be distinguished from living cells by 7-AAD and Annexin V labeling. For this purpose, cells were resuspended

in Annexin V binding buffer, stained with Annexin V and 7-AAD and incubated for 15 min at RT. Finally, the cells were analyzed by FACS (LSR Fortessa, BD).

3.2.9 In vitro cell proliferation assays

- **MTT proliferation assay**

1,500 CRC cells (SW480 or HCT116 cells) per well, were seeded in 96-well plates (Sarstedt, Germany) and upon sedimentation cells were transduced with either TGM2 shRNAs or TGM2 constructs (TGM2-Iso1, TGM2-Iso2, TGM2^{C277C}, TGM2^{R580A} and TGM2$^{C277S+R580A}$) by adding virus particles with a MOI of 5. After 3 and 7 days MTT (Sigma Aldrich, Germany) proliferation assay was performed according to the manufacturer's instructions. To ensure a constant transduction efficiency of >80 %, for every measured time point an aliquot of cells was used to determine the transduction efficiency via flow cytometry.

- **Rescue experiment**

SW480 cells were transduced with TGM2 overexpressing constructs (TGM2-Iso1, TGM2-Iso2, TGM2^{C277C}, TGM2^{R580A} and TGM2$^{C277S+R580A}$) for 3 days. After 3 days of transduction 20,000 cells per well were seeded in 96-well plates (Sarstedt, Germany). When cells are adhered (>4h after seeding) cells were transduced with Crispr a and b or non-target control (NTC), virus particles were added with a MOI of 2.5 for each Crispr, in 100 µl culture medium. After 3, 7 and 14 days, cells were dislodged with 50 µl Accutase^{TM} for 10 min at 37°C and resuspended in 150 µl icecold PBS (PAA Laboratories). Two aliquots of the cells were used to determine the transduction efficiency via flow cytometry and to determine the cell count using C-chip counting chamber. Subsequently, cells were reseeded in 96-well plates in 100 µl culture medium.

3.2.10 Active caspase 3 apoptosis assay

50,000 SW480 cells per well, were seeded in 24-well plates (Sarstedt, Germany) and upon sedimentation cells were transduced with TGM2 shRNAs by adding virus particles with a MOI of 5. After three days active caspase 3 cells were measured by FACS using caspase 3 (active) FITC staining kit (Abcam, USA) according to the manufacturer's instructions. Briefly, SW480 cells were lentivirally transduced with either shSCRMBL, shTGM2-1 or shTMG2-2. 48h or 72h after transduction, cells were harvested and incubated with the

caspase 3 inhibitor DEVD-FMK conjugated to FITC serving as the fluorescent in situ marker. The inhibitor is internalized and binds to activated capsase-3 in living cells. A costaining with Annnexin V and 7-AAD was performed. The cells were analyzed on a FACSCanto II.

For the rescue experiment with the caspase 3 inhibitor, TGM2 knockdown cells were grown in culture medium containing the caspase 3 inhibitor z-VAD-FMK at a concentration of 100 μM or the vehicle control. After three days active caspase 3 cells were measured by FACS using caspase 3 (active) FITC staining kit (Abcam, USA) according to the manufacturer's instructions.

3.2.11 Stable Isotope Labelling by Amino Acids in Cell Culture (SILAC) and Mass Spectrometry (MS)

SW480 cells were grown in two different SILAC McCoy's culture media (10 % dialyzed FBS and 1 % penstrep) (PAA Laboratories GmbH, Pasching, Austria; Thermo Fisher Scientific, Waltham, MA). The "light" SILAC medium was supplemented with unlabelled L-lysine and L-arginine, while the "heavy" SILAC medium was supplemented with arginine and lysine containing heavy isotopes of carbon and nitrogen ($_{13}C_6$-lysine and $_{13}C_6$ $_{15}N_4$-arginine). After 5 cell passages, cells were harvested and stained with CD133 antibody. Subsequently, FACS sorting was performed. CD133^{high} expressing cells were gained from cells grown in "heavy" SILAC medium and CD133$^+$ cells (bulk) from cells grown in "light" SILAC medium (and vice versa as a control). For both subpopulations the same number of cells were sorted to ensure an equivalent amount of protein. After sorting, cells were washed with PBS and lyzed as described by Oellerich et al. [224]. Lysates were incubated with 200 ml Strep-Tactin Superflow matrix for 1h at 41°C. For each approach, 500 ml desthiobiotin buffer (Iba Bio Tagnology) was used to elute purified proteins at RT. Eluates were pooled in equimolar amounts, concentrated in ultrafiltration spin columns (Sartorius, Göttingen) and subsequently the samples were separated by one-dimensional SDS-PAGE (Invitrogen, Carlsbad, CA, USA) followed by Coomassie blue staining. Each gel lane was cut into 23 gel slices. All slices were reduced with 10mM DTT for 55 min at 56°C, alkylated with 55mM IAA for 20 min at 26°C and in-gel digested with trypsin (Promega, Madison, WI) according to the protocol described by Shevchenko et al. [225]. MS measurements were carried out using a nanoflow LC system (Agilent, Boeblingen, Germany) coupled to a nanoelectrospray LTQ-Orbitrap XL hybrid mass spectrometer (Thermo Fisher Scientific, Waltham, MA) as previously described by Oellerich et al. [224]. Raw data were analysed with MaxQuant software (Version 1.0.12.31) in combination with Mascot search engine for peptide and protein identifications (Version 2.2.04, Matrix Science).

3.3 Digital analysis methods and statistics

3.3.1 Statistics

Statistical analysis was performed with GraphPadPrism software (version 6.0 and 7.0, STATCON). Statistical significance was determined by a t-test (two-tailed, unpaired, equal variances) if not mentioned differently (see figure legends). The significance level for all tests was set to $\alpha = 5$ %. *, p-value < 0.05; **, p-value < 0.01; ***, p-value < 0.001.

3.3.2 DAVID analysis

The list of significantly (p<0.05) and differentially regulated proteins in proteomic data (1.5-fold) was submitted as a list with official gene symbols for DAVID analysis and aligned to human genetic background. Go terms are subdivided in "Cellular Compartment", "Molecular Function" and "Biological Function". Only the highest enriched cluster within a subgroup is displayed. The classification stringency was set on "high".

4. Results

4.1 Identification of TGM2 as a novel druggable target in colon cancer

To identify molecules that are involved in the development of CRC or are potential targets for CRC treatment, a screening based on the expression of CD133 in SW480 cells was established. CD133 is a five-transmembrane glycoprotein and was first described in hematopoietic stem and progenitor cells [226] and is highly expressed in colon cancer initiating cells (CC-ICs) [8,9]. These studies highlight the importance of CD133 as a marker in CRC for an aggressive cell subpopulation within the CRC cell conglomerate and encouraged us to perform further investigations.

4.1.1 Protein expression profiling revealed high TGM2 expression in a colorectal cancer cell subpopulation enriched for tumor initiating cells

Malkomes et al. were able to identify different cell subpopulations based on their CD133 expression in SW480 CRC cells. CD133^{high} expressing cells showed a significantly higher proliferative potential, are more aggressive and induce an earlier tumor formation and growth in vivo compared to CD133^{-} and CD133^{+} SW480 cells [10]. These results indicate that this aggressive CD133^{high} expressing cell subpopulation is enriched for TICs. To identify molecular differences between the CD133^{high} subpopulation and CD133^{+} cancer cells, stable isotope labeling by amino acids (SILAC) in cell culture in combination with mass spectrometry was performed [225] (Figure 3A). The aim was to identify differences in protein expression in order to discover potential new targets for a specific and directed anticancer therapy. For this purpose, 5 individual runs were performed, 781 regulated, and overlapping proteins could be detected by comparing CD133^{high} and SW480 CD133^{+} cells (Figure 3B).

By using a threshold of 1.5-fold (p<0.05) regulation, this differential expression analysis revealed 133 upregulated and 45 downregulated proteins (Figure 3C). In order to obtain an overview of proteins which are potentially involved in an aggressive tumor formation and tumor growth, all significantly upregulated proteins were analyzed according to their appearance in DAVID functional annotation cluster (Figure 3D). DAVID is a platform which offers the possibility to measure relationships among the annotation terms of genes and highlights important annotation groups by enrichment scores. It is possible to study functionally related genes and their relationship in a network. Therefore, the identified proteins were assigned to their genes and analyzed by DAVID.

D

GO Term   P- Value [-log10]
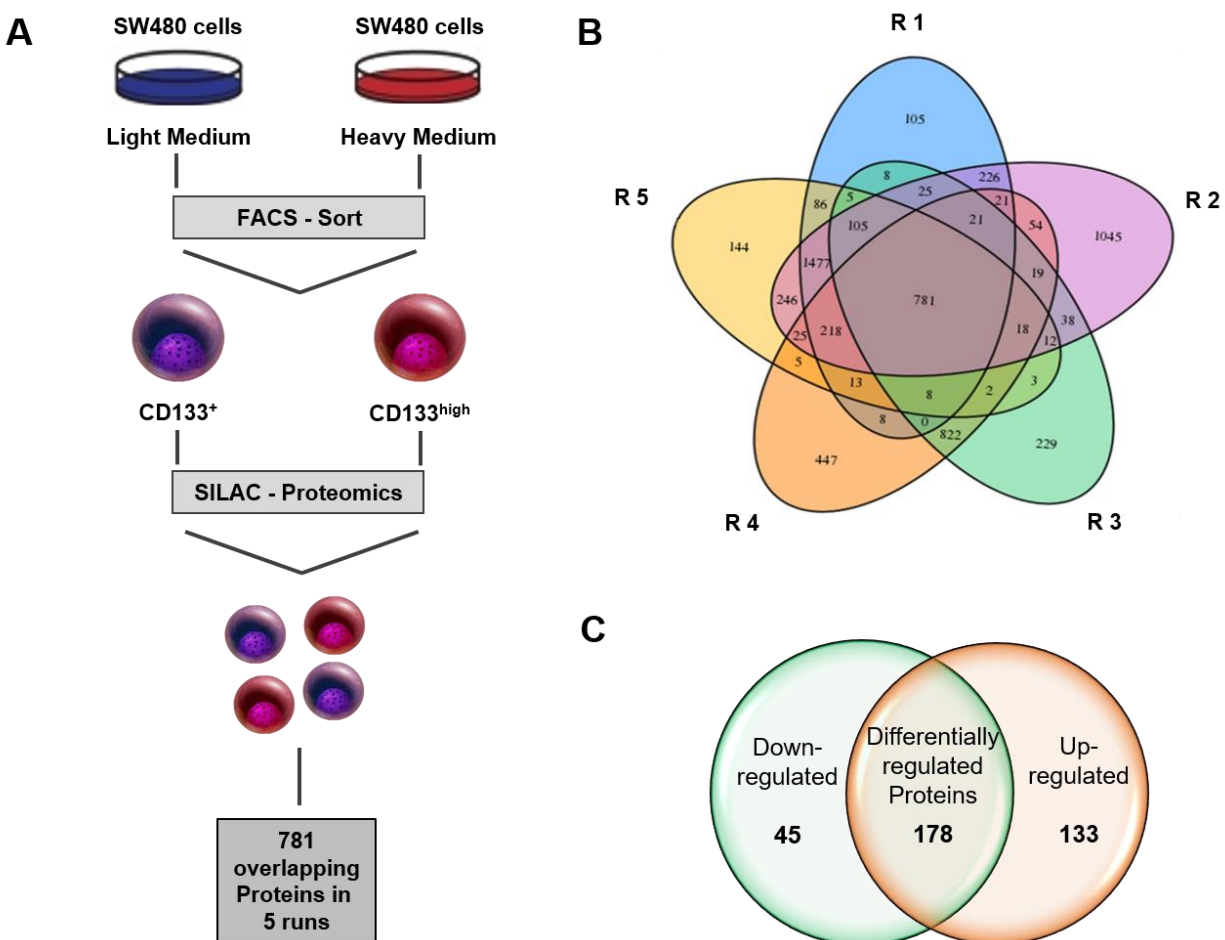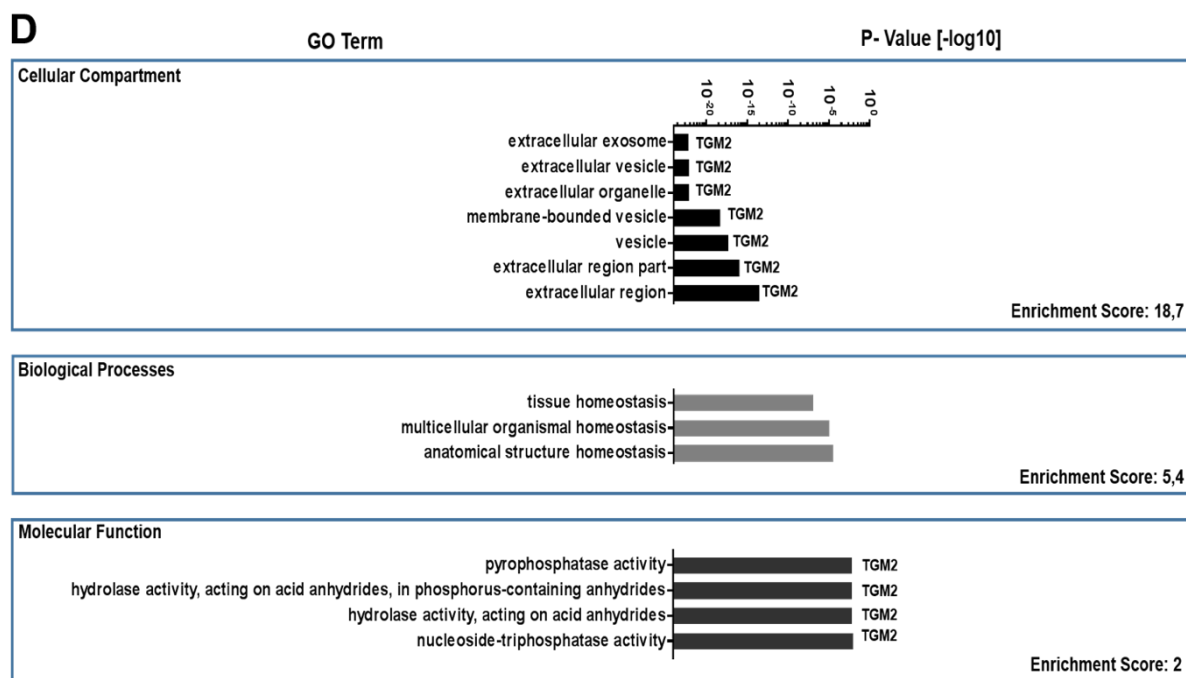
Figure 3 Screening for drug-gable targets within an aggressive CRC cell subpopulation

(**A**) Schematic overview of SILAC-based experimental setup for the identification of differentially regulated proteins in a TIC enriched, (CD133^{high} subpopulation) of SW480 CRC cells. SW480 cells were grown in medium containing light (blue) or heavy labelled amino acids (red). Next, harvested and FACS-sorted SW480^{+} and SW480 CD133^{high} (TIC enriched) were lysed and protein lysates from the two cell populations were then quantified with mass spectrometry (MS).
(**B**) VENN-Diagram of detected proteins within 5 individual runs, 781 expressed and overlapping proteins could be found. R=Round
(**C**) Remaining 179 differentially regulated proteins by using a cutoff of 1.5-fold enrichment and a p-value of 0.05. 137 proteins were upregulated and 42 downregulated.
(**D**) DAVID functional annotation clustering analysis of significantly ($p<0.05$, 1.5-fold) upregulated proteins. Significantly regulated proteins were submitted as a list with official gene symbols and aligned to human genetic background. GO terms are subdivided in "Cellular Compartment", "Molecular Function" and "Biological Function". Only the highest enriched cluster within a subgroup is displayed. The classification stringency was set on "high". TGM2 appears frequently in the highest DAVID annotated clusters.

Gene ontology (GO) terms are subdivided in "Cellular Compartment", "Molecular Function" and "Biological Function". Clusters with the highest enrichment score within these subgroups are highlighted here (Figure 3D). This cluster analysis allowed potential target molecules to be identified based on their abundance within the highest enriched cluster. Further, a literature screening was performed to unravel their impact in cancer and to examine whether small molecules are available. One interesting candidate of detected target molecules was transglutaminase 2 (TGM2), which appeared frequently in the highest DAVID annotated clusters (Figure 3D).

4.1.2 TGM2 is overexpressed in primary human colon cancer (CRC)

TGM2 is a multifunctional enzyme with pleiotropic functions and is discussed to play a role in different diseases like breast cancer or neurodegenerative disorders [227–230]. So far, little is known about the role of TGM2 in CRC and it has been the subject of controversial discussions. Since proteomic analysis revealed TGM2 as a prominent protein in the aggressive CD133^{high} subpopulation, the focus of this work was the investigation of TGM2 function in CRC. For this purpose, the TGM2 protein expression level was determined by comparing patient-derived tumor tissue with the corresponding normal tissue.

It was critical in this work to evaluate the expression level of TGM2 exclusively in epithelial cells and to avoid potential masking effects of cells derived from the surrounding stroma. For this purpose, a method to isolate epithelial cells from tumor and normal tissue, containing heterogeneous cell populations including lymphocytes, fibroblasts, and endothelial cells was established. Upon producing a single cell suspension of normal and corresponding tumor tissue, the cells were enriched for epithelial cells by magnetic activated cell sorting (MACS) based on their expression of EpCam, which is an epithelial adhesion molecule and exclusively expressed in epithelial cells [231]. Purified tumor cells were subsequently lysed and the TGM2 protein expression was validated. For protein detection the WES[TM] system was introduced, which allows the detection of low protein expression levels by a size-based protein separation technology (Figure 4A). With this approach, it was feasible to investigate TGM2 expression exclusively in cells of epithelial origin and gives the opportunity to precisely quantify and compare the expression level in matched patient samples. Monitoring the TGM2 protein expression level in eight matched patient specimen, revealed an average of more than three times higher TGM2 expression in tumor tissue in comparison to normal tissue after normalizing the TGM2 expression to loading control (Figure 4B, C). A higher TGM2 expression could be shown for every tested patient (Figure 4D).
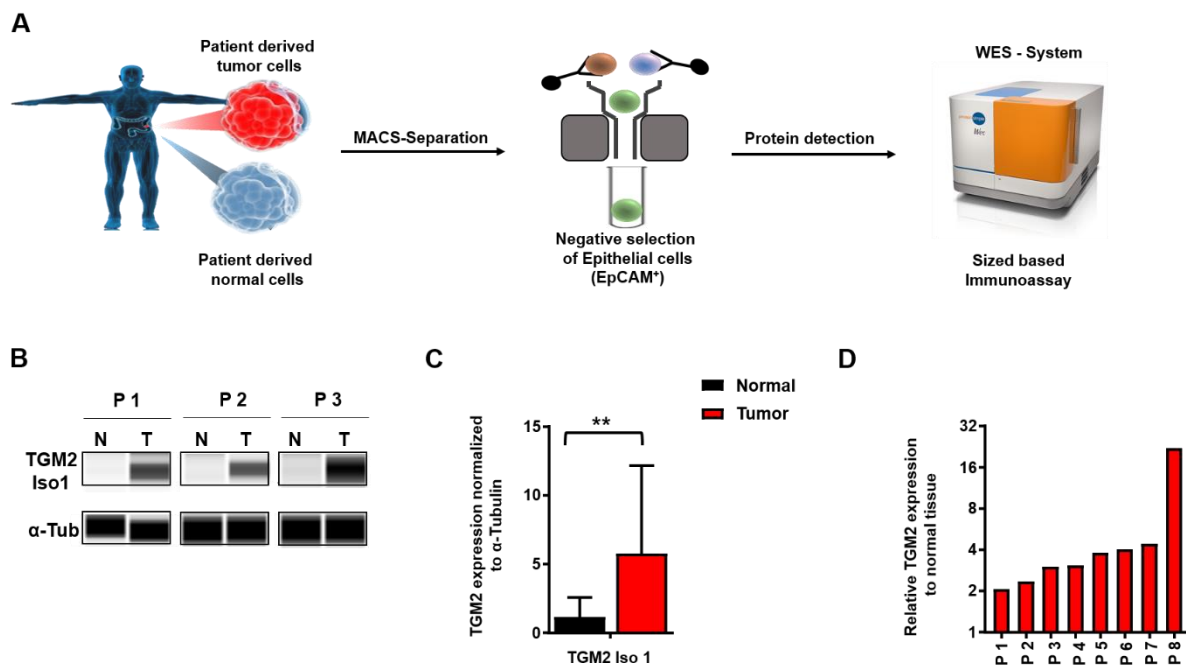
Figure 4 TGM2 expression is upregulated in patient derived tumor tissue

(**A**) Scheme of the experimental outline. Patient derived tumor and normal tissue were isolated and enriched for epithelial cells (EpCAM[+]-cells). After cell lysis TGM2 expression was detected via sized based Immunoassay using the WES-System.

(**B**) Exemplary WES-Runs of TGM2 expression in patient material showing normal tissue versus the corresponding tumor tissue. (Antibodies: TGM2 ms, CUB 7402, Abcam; α-Tubulin rb 11H10, Cell Signaling)

(**C**) Quantitative analysis of TGM2 protein expression comparing patient derived normal and corresponding tumor tissue. Protein expression was normalized to α-Tubulin loading control. The data is represented as mean +/- SD, N=8, statistical significance was determined using Wilcoxon test ** p<0.008.

(**D**) The graph displays the relative TGM2 expression in tumor tissue according to the corresponding normal tissue in ascending order. Each patient is represented by a bar. P1-8 = Patient No. 1 -8

4.1.3 TGM2 transamidase activity is elevated in CRC

The expression data in primary tumor tissue suggested a function of TGM2 in CRC biology, but whether this could be linked to an elevated TGM2-enzyme activity remained elusive. It is not certain whether an elevated TGM2 protein expression in tumor tissue, as shown here, translates into a higher enzyme activity. Although there is accumulating evidence, that miss-regulated TGM2 and its transamidation activity is involved in pathological processes [232], it is still an open question whether TGM2 enzymatic activity plays a role in CRC. Therefore, primary tumor and normal epithelial cells were purified as described previously and TGM2 activity was measured using a colorimetric, TGM2 specific, transamidase in vitro assay (Figure 5A). The assay measures the quantity of enzymatically incorporated, biotinylated T26 peptide into the amine substrate, which is covalently coupled to the wells of the microtiter plate. A significant induction of TGM2 transamidation activity could be found in cancer tissue compared to matched normal tissue samples

(Figure 5B). In every tested patient, the cross-linking activity was increased and appears to reflect the high protein expression pattern in tumor tissue (Figure 5C).

These results indicated that high TGM2 expression is directly proportional to high transamidase activity and let assume pivotal functions in CRC disease genesis and progression.
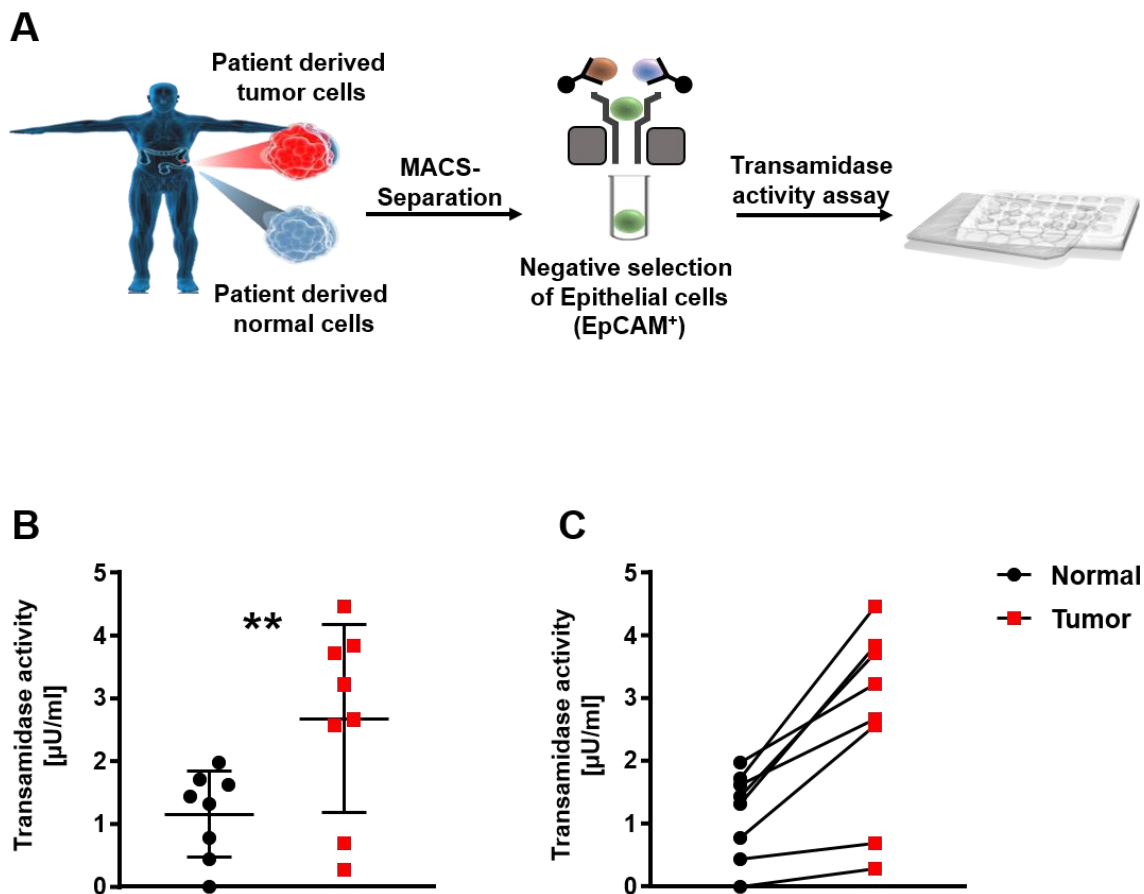
Figure 5 TGM2 expression is upregulated in patient derived tumor tissue

(**A**) Scheme of the experimental outline. Patient derived tumor and normal tissue were isolated and enriched for epithelial cells (EpCAM+-cells). After cell lysis TGM2 transamidation activity was detected via a specific in vitro TGM2 transamidase activity assay.

(**B**) Quantitative analysis of TGM2 transamidation activity comparing patient derived normal and corresponding tumor tissue. Each dot represents one patient. N=8, statistical significance was determined using Wilcoxon test ** p<0.001.

(**C**) The graph displays TGM2 transamidase activity in tumor tissue according to the corresponding normal tissue. Connecting lines show increased transamidase activity in every tested patient.

4.2 TGM2 is essential for colon cancer cell survival

To further examine and enlighten the role of TGM2 in CRC, functional studies were performed using lentiviral vectors to generate loss-of-function phenotypes by TGM2 knockdown (shRNAs) and knockout (CRISPR/Cas9).

4.2.1 Growth ability of CRC cells is highly affected upon loss of TGM2

Genetic engineering techniques allows the investigation of the role of a specific gene in biological processes. To assess the potential role of TGM2 in CRC, genetic knockdown and knockout experiments were performed. In detail, a RNA interference system was used by generating lentiviral silencing constructs, coupled with a fluorescence reporter protein (tdTOMATO) which allows a stable knockdown of TGM2 via shRNAs. In addition, a CRISPR/Cas9 system was established to mediate a genetical knockout of TGM2. The CRISPR/Cas9 system uses a nuclease, CRISPR-associated protein 9 (Cas9), that complexes with small guide RNAs (sgRNAs) to cleave DNA in a sequence-specific manner. To improve the specificity of Cas9-mediated genome editing and to facilitate homozygous gene knockout, two sgRNAs were designed and cells were transduced with both sgRNAs. Again, the CRISPR/Cas9 knockout was mediated by a lentiviral construct coexpressing a blue fluorescent protein (BFP) to determine positive transduced cells by flowcytometry (Figure 6A).

Upon TGM2 silencing by RNAi in CRC cell lines (SW480, HCT116) through lentiviral transduction, the protein expression level was analyzed and revealed strong reduction (70% and 64% vs control) of TGM2 in SW480 (Figure 6A, B). Furthermore, the cells were counted after 3 and 7 days of in vitro culture to analyze their proliferative behavior. TGM2 knockdown cells showed a significantly decreased cell count in the observation period of 7 days compared to the scramble control transduced cells (Figure 6C, D). The scrambled shRNA is a negative control, which has a randomized nucleotide sequence and does not target a known gene. These findings demonstrate that loss of TGM2 strongly contributes to growth disadvantages in CRC cells.
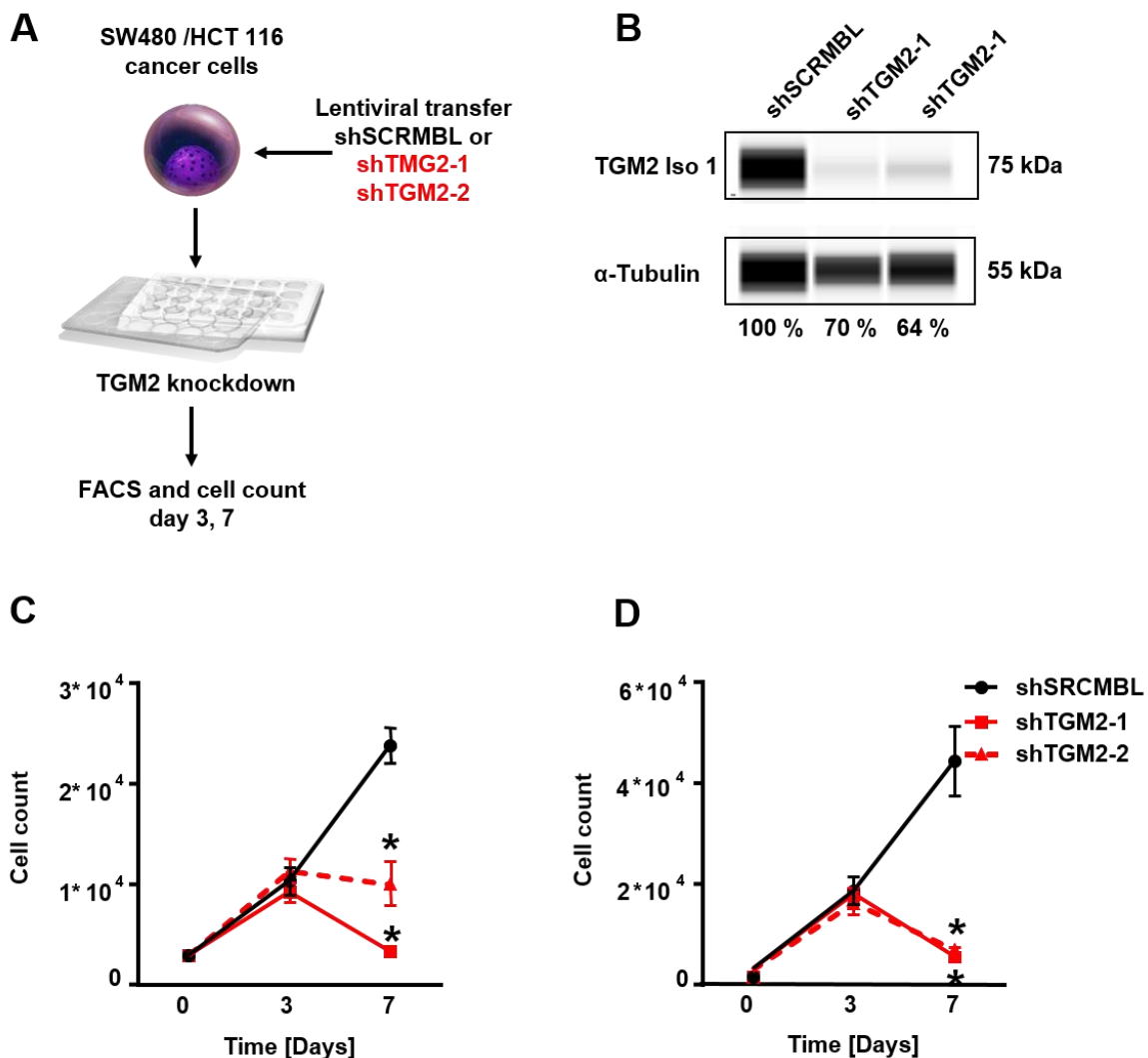
Figure 6 Reduction of TGM2 results in a decreased cancer cell growth in vitro

(**A**) Experimental setup of in vitro expansion of TGM2 knockdown cells. SW480 or HCT 116 cell were transduced with TGM2 shRNAs (shTGM2-1, shTGM2-2) or control (shSCRMBL) and seeded into 24 well plates. The cells were analyzed for their transduction by FACS and counted at the indicated time points.

(**B**) Knockdown efficiency of TGM2 shRNAs was validated after 3 days of transduction using WES analysis. Quantitatively evaluation of knockdown-efficiency showed a knockdown-efficiency of 70 % for shTGM2-1 and 64 % for shTGM2-2. N=3 (Antibodies: TGM2 ms, CUB 7402, Abcam; α-Tubulin rb 11H10, Cell Signaling)

(**C**, **D**) The FACS analyses and cell counts allowed the calculation of the expansion of transduced cells over-time for SW480 cells (**C**) and HCT 116 cells (**D**). Mean +/- SD, N=3. Statistical significance was determined using Mann-Whitney test * p<0.05

Although RNAi-mediated studies are widely used for investigating gene function, they have several disadvantages, such as the variability and incompleteness of knockdowns and the potential of off-target effects [233]. Therefore, a CRISPR/Cas9 system was introduced as a second system to investigate the biological effects of loss of TGM2 in CRC. First the efficacy of DNA cleavage and subsequent gene knockout of CRISPR a and b was screened by protein expression (Figure 6C).

In order to test whether genetic knockout of TGM2 has the same effect as TGM2 knockdown with shRNAs, SW480 cells were transduced with lentiviral particles of sgRNA-1 and sgRNA-2 and monitored for the indicated time points (Figure 7B).
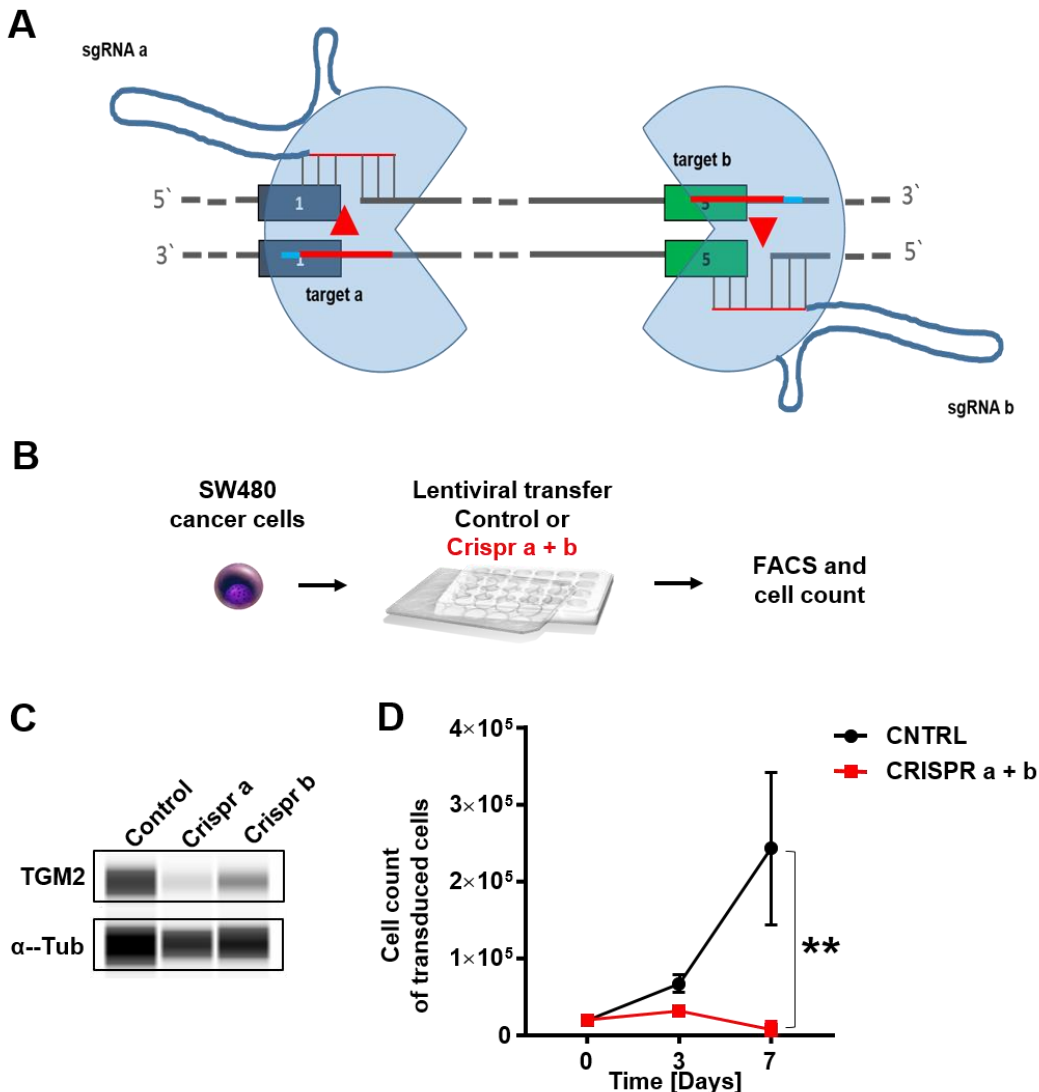
Figure 7 Gene editing with CRISPR/Cas9 induces growth disadvantages in SW480 cells

(**A**) Schematic illustration of inducing of DNA double-stranded breaks using a pair of single-guide RNAs (sgRNAs) guiding the endonuclease Cas9 to a specific gene sequence. SgRNA 1 targets a specific intron-exon site on exon 1 and sgRNA 2 an intron-exon region on exon 5. Targeting intron-exon regions leads to a knockout of endogenous TGM2 whereas ectopic expressed TGM2 stays unaffected.
(**B**) Experimental scheme of the in vitro expansion analysis. SW480 cells were transduced with the indicated lentivirus. After 3 and 7 days in culture, the cells were counted and analyzed via FACS concerning their transduction efficiency.
(**C**) Exemplary WES run of TGM2 expression in SW480 cells after lentiviral transduction with Crispr a, b or control vector. (Antibodies: TGM2 ms, CUB 7402, Abcam; α-Tubulin rb 11H10, Cell Signaling)
(**D**) In vitro expansion kinetic of SW480 TGM2 knockout cells after transduction with both Crispr a and b. The data is represented as mean +/- SD, n=3. Statistical significance was determined using Mann-Whitney test. ** p<0.01

Indeed, the observation within 7 days revealed a stagnation in the expansion ability during the first 3 days, and after 7 days a significant reduction of the cell number in TGM2-knockout cells, in comparison to the non-target control. The effect of TGM2 knockout is comparable to TGM2 knockdown (Figure 7D). In order to further investigate the impact of TGM2 depletion additional functional experiments were implemented.

4.2.2 TGM2 affects the tumorigenicity of TICs in vitro and in vivo

The ability of TICs to give rise to progressively growing tumors is defined as their tumorigenicity. To assess the influence of TGM2 on the tumorigenicity of TICs in CRC, cells after TGM2 knockdown were subjected to a sphere formation assay. Sphere-forming assays are widely used as a surrogate test to identify TICs, based on their reported capacity to self-renew and differentiate in serum-free culture conditions in vitro, in contrast to differentiated tumor cells, which are dying due to anoikis in serum-free culture conditions [234]. TICs are supposed to be able to maintain long-term clonal growth in functional repopulation assays [235].

CRC cells were transduced with TGM2-shRNAs and SCRMBL-shRNA, as a control, and cultivated in a serum-free medium, to exhibit the contribution of TGM2 to TIC tumorigenicity (Figure 8A). Transduced SW480 and HCT116 cells were observed over 14 days and a significant reduction of tumorspheres could be shown already 7 days after cells were transduced with TGM2-shRNAs, in comparison to control transduced cells (Figure 8C, D). The analysis by microscope showed not only a reduced number of detectable spheres, but also a reduced diameter (Figure 8B). This data clearly shows that the loss of TGM2 severely affects CRC cell growth and their tumorigenicity.
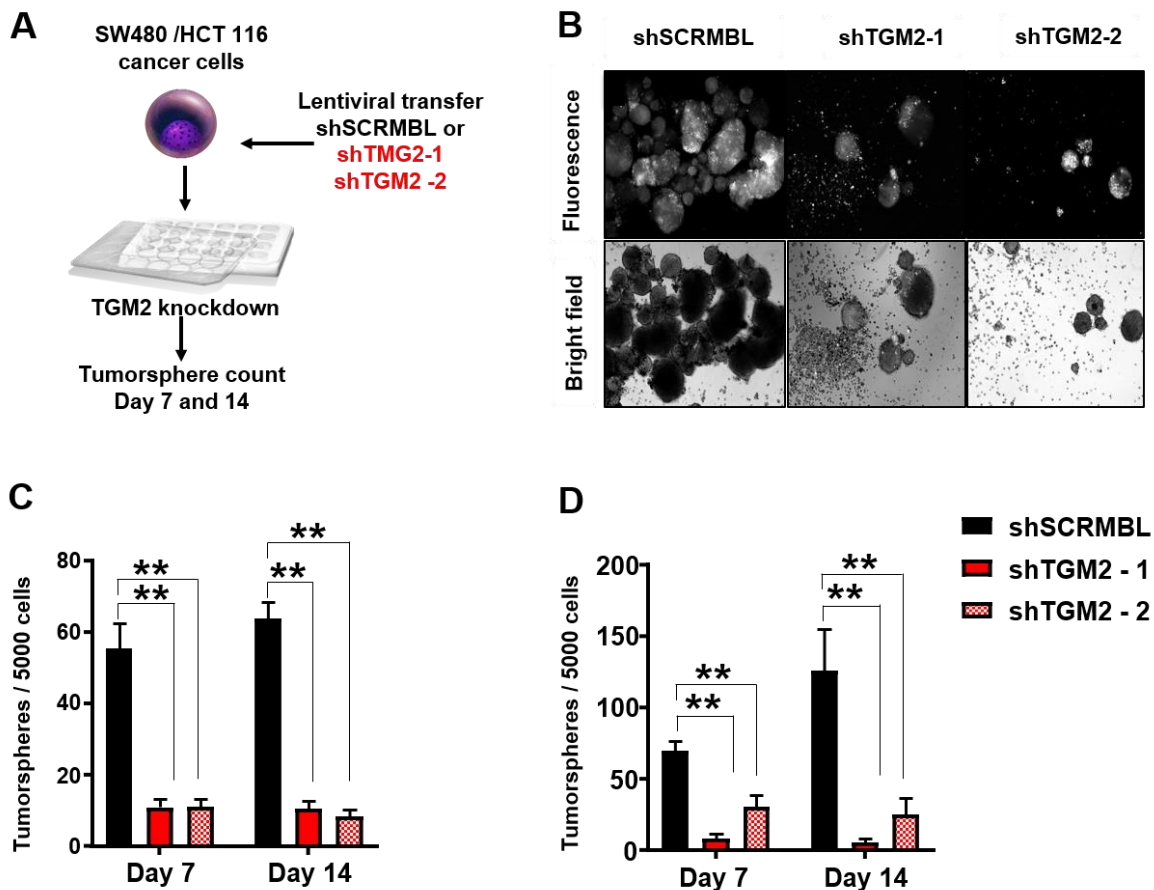
Figure 8 TGM2 knockdown leads to decreased tumorigenicity in CRC cells

(**A**) Scheme of the experimental setup of the tumorsphere forming assay of 5000 SW480 or HCT116 cells after TGM2 knockdown using shTGM2-1 and shTGM2-2 or shSCRMBL. Spheres were counted at indicated time points
(**B**) Exemplary phase contrast and fluorescent microscopy images of tumor spheres of SW480 cells at day 14, showing a decreased tumorsphere formation capacity.
(**C**) Tumorsphere formation assay using 5000 SW480 or (**D**) HCT116 cells transduced with control or TGM2 shRNAs. The number of tumorspheres is shown at indicated time points. Data are represented as mean + SD, N=3, statistical significance was determined using Mann-Whitney test ** p<0.01

However, sphere-forming assays as a read out of stem cell activity are only a surrogate measure of cells to exhibit stem cell traits [236]. Taken this into account, the tumorigenicity of CRC cells after TGM2 knockdown was analyzed in an in vivo transplantation setting. Hence, SW480 cells were transduced and expanded for 3 days, 50,000 living cells were subcutaneously injected into NOD/SCID mice and tumor growth was monitored every week (Figure 9A). Cells, which were transduced with shSCRMBL as a control, showed a fast tumor initiation and growth whereas TGM2-knockdown cells showed a significant reduction of tumor initiating ability (Figure 9B). In the TGM2-knockdown cohort the first outgrowth of tumors could be detected 3 weeks later compared to control transduced animals. The remaining tumor growth after TGM2-

knowdown may be explained by the presence of initially untransduced cells as contaminants. Similar to the tumorsphere experiments, CRC cells were no longer able to induce tumor growth when TGM2 expression level has been significantly reduced. Taken together these results implicate that suppression of TGM2 decreases the oncogenic potential of TICs and tumor growth in CRC (Figure 9B, C).
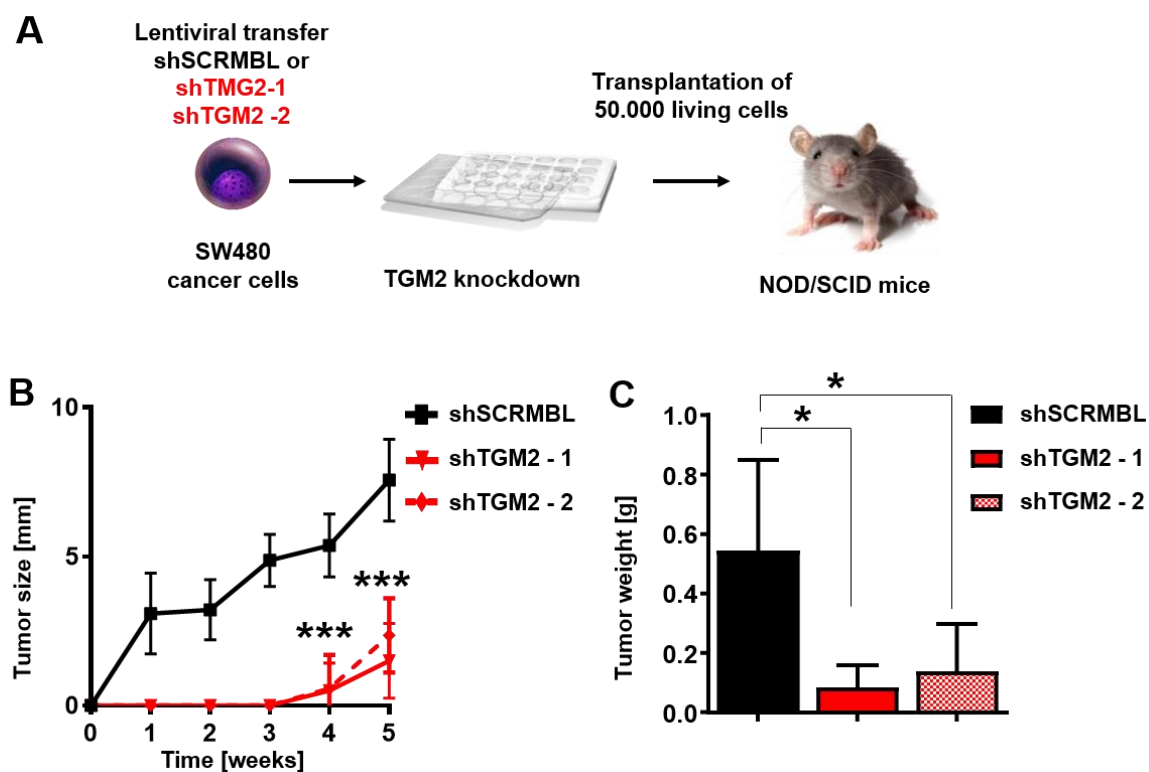
Figure 9 TGM2 knockdown leads to a significantly reduced tumor initiation capacity and growth

(**A**) Experimental scheme of the transplantation setup of lentiviral manipulated SW480. Cells were transduced with TGM2 shRNAs or scramble control and expanded for 3 days. After injection of 50,000 living cells subcutaneously into NOD/SCID mice tumor growth was monitored once a week.
(**B**) Tumor engraftment were monitored over time and measured with a caliper. The data is represented as mean +/- SD, N=8 mice/group, statistical significance was determined using Mann-Whitney test, *** p<0.001
(**C**) After sacrificing the mice, the tumor weight was compiled. The data is represented as mean + SD, N=8 mice/group, statistical significance was determined using Mann-Whitney test * p<0.05

4.2.3 Selective TGM2 inhibition reduces colorectal tumor initiation and colorectal cancer growth in vivo

To take functional analyses one step further, it was essential to translate and confirm these findings in preclinical and therapeutic models. Therefore, two potent and specific TGM2 inhibitors, Tyrphostin 47 and LDN-27219 [237,238] were used to assess the potential of TGM2 targeting, to reduce tumor growth and TIC acitivity in vivo. LDN27219 is a reversible, slow binding inhibitor that appears not to bind at the enzyme`s active site but rather at the enzyme`s GTP site, or at least at a site that regulates binding of GTP [238]. Tyrphostin 47 binds tightly to TGM2 and targets activated TGM2 and the free thiol groups that are required for an active enzyme [237]. To evaluate these inhibitors as candidates for targeted CRC therapy, tumor xenograft models were used to monitor the consequence of TGM2 inhibition on CRC tumorigenicity and tumor growth. In a first set of experiments, the in vitro effect of these inhibitors on CRC TIC cells was tested. Therefore, SW480 cells were pretreated either with LDN27219, Tyrphostin 47 or DMSO as control for 72h, then 50,000 viable cells were injected subcutaneously into NOD/SCID mice (Figure 10A). After the first tumors achieved an average diameter of 1 cm, the mice were sacrificed and tumor weight and size were determined. In both conditions, the inhibition of TGM2 resulted in a significant reduction of tumor volume and growth (Figure 10B). These results are comparable to previous knockdown and knockout experiments and showed that inhibition of TGM2 using two different small molecule compounds significantly decreased the TIC activity and tumorigenicity in preclinical CRC models. These results support the notion of TGM2 as a vulnerable target for CRC therapy.
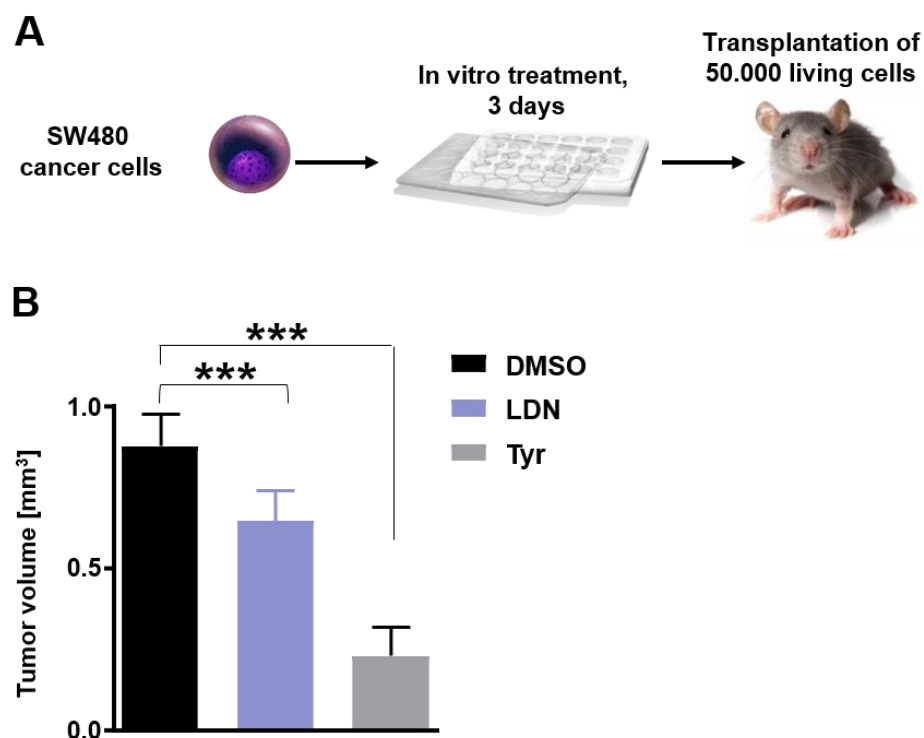
Figure 10 TGM2 inhibition reduces tumor initiation and growth in xenograft mouse models

(**A**) Experimental set up of pretreatment experiment and measured tumor sizes. SW480 cells were treated with TGM2 inhibitors for 3 days, then 50,000 living SW480 cells were transplanted subcutaneously into NOD/SCID mice and tumor growth was monitored over time.

(**B**) After first tumor reached a size of ~ 1 cm in diameter, mice were sacrificed and tumor volume was measured. Treated tumors both with LDN27219 (LDN) at a concentration of 10 µM and with Tyrphostin 47 (Tyr) to a concentration of 100 µM, showed a significant decrease of tumor volume in comparison to DMSO control. The data is represented as mean +/- SD, N=8, * p<0.05

Next we used a therapeutic mouse model with established xenograft tumors before the in vivo treatment started in order to understand the efficacy of cancer therapeutics, closely recapitulating the situation in patients [239]. To investigate therapy response of established CRC tumors, NOD/SCID mice with established tumors were treated with LDN27219 (25 mg/kg), Tyrphostin 47 (2.2 mg/kg) or vehicle control to further investigate the anticancer effect of TGM2 inhibition (Figure 11A). Tyrphostin 47 was injected intraperitoneally 3 times a week whereas LDN27219 was applied orally in the same temporal sequence. The tumor growth was monitored until first tumors reached an approximate diameter of 1 cm. Tyrphostin 47 did not show any significant inhibitory effect (Figure 11C) on tumor growth in contrast to LDN27219 which resulted in an almost complete stagnation of tumor development. Mice treated with LDN27219 showed only small tumors that were equal in size as before the start of treatment (Figure 11B). The failure of Tyrphostin 47 may be explained by an inefficient bioavailability or unfavorable pharmacokinetics. During

inhibitor treatment mice did not show at any given timepoint signs of poor welfare or weightloss indicating a favourable toxicity profile. Treatment effects of LDN27219 on tumor development showed that inhibition of TGM2 may be a promising approach in CRC therapy. Newly designed TGM2 inhibitors, that have been already tested in first clinical trials showed promising results and should be included in future experiments [240,241].
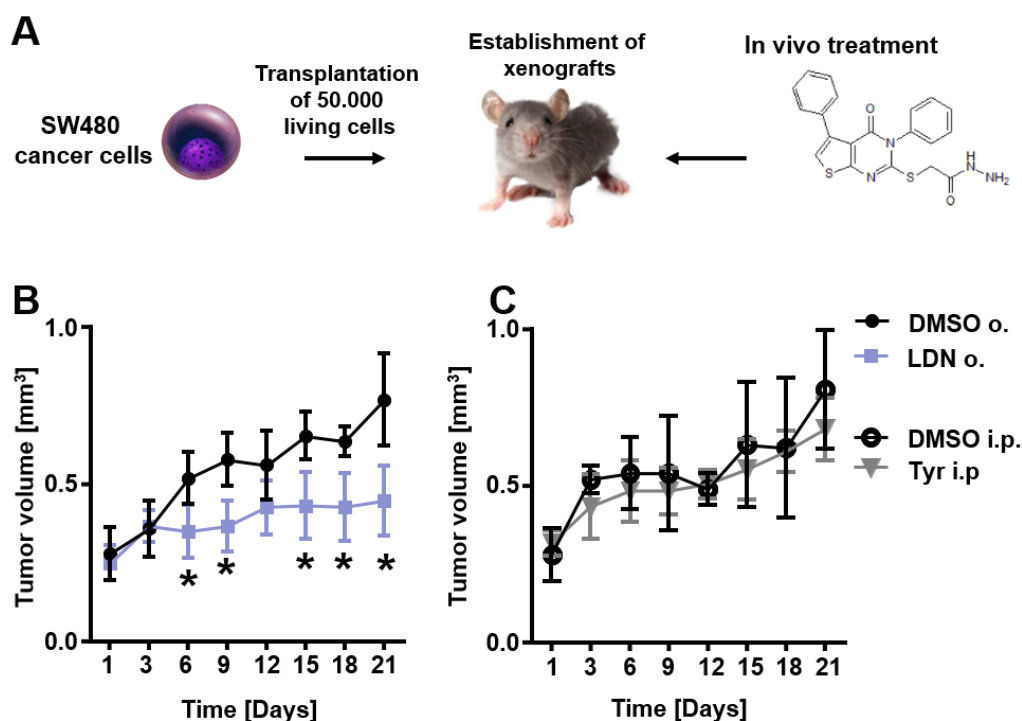
Figure 11 Tumor treatment with TGM2 inhibitors reduced tumor growth in xenograft mouse models

(**A**) Experimental set up of treatment experiment of established tumors. 50,000 living SW480 cells were transplanted subcutaneously into NOD/SCID mice. After tumors reached a size of ~ 2.5 mm mice were treated with TGM2 inhibitors. LDN27219 was applied orally, Tyrphostin 47 intraperitoneally. As an example of an inhibitor the chemical structural formula of LDN27219 is depicted. Tumor growth was monitored over time.
(**B**) Established tumors orally treated with LDN27219 (LDN o.) is shown. The data is represented as mean +/- SD, N=8, statistical significance was determined using Mann-Whitney test * $p<0.05$
(**C**) Established tumors treated intraperitoneally with Tyrphostin 47 (Tyr i.p.) is shown in comparison to DMSO vehicle control. The data is represented as mean +/- SD, N=8, statistical significance was determined using Mann-Whitney test

4.2.4 Chemical inhibition of TGM2 leads to a decreased expansion of patient derived spheroids

In order to translate the effect of TGM2 inhibition seen with CRC cell lines to primary CRC cells in patients, a patient derived long-term spheroid culture of freshly isolated CRC cells was established. After producing a single cell suspension, 50,000 patient-derived tumor epithelial cells were seeded into an ultra-low attachment 24 well plate and treated with LDN27219, Tyrphostin 47 or vehicle control (Figure 12A). In this work, patient derived CRC spheroids, designated as colonospheres, were used to evaluate the chemosensitivity of CRC cells towards TGM2 inhibitors. The ability to induce colonospheres was monitored over a period of 3 weeks after treatment with TGM2 inhibitors or vehicle control. Primary CRC cells treated with Tyrphostin 47 showed a significantly reduced capacity to form colonospheres in a dose-dependent manner (Figure 12E). Using LDN27219 a significant reduction in number and diameter of formed colonospheres could be achieved by applying a concentration of 10 µM (Figure 12D). To date, the effects of both selected inhibitors were not verified in human CRC. The chemical inhibition of TGM2 which in turn lead to a decreased colonosphere formation indicates a pivotal role of TGM2 in CRC progression and activity of CRC initiating cells.
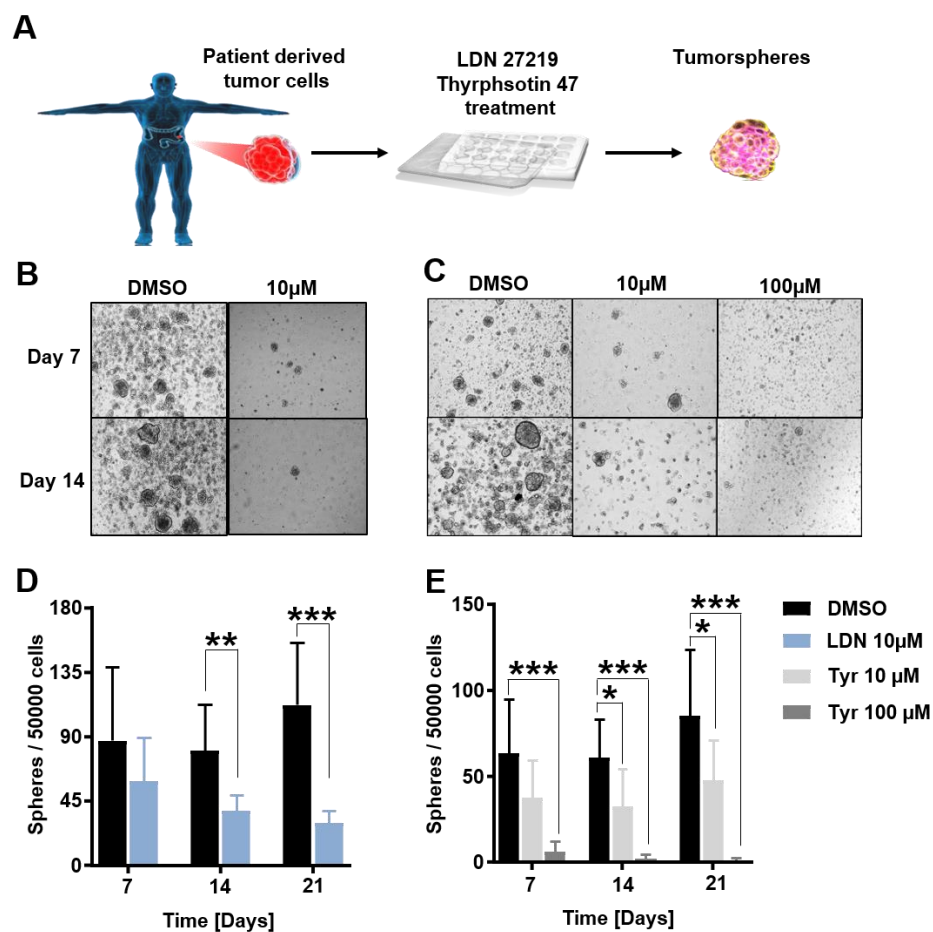
Figure 12 Targeting TGM2 inhibits cell proliferation and tumorigenicity in primary, patient derived CRC cells.

(**A**) Experimental scheme of the chemosensitivity assay. Patient derived tumor cells were isolated and treated with TGM2 inhibitors. The ability to form colonospheres was monitored over a time period of 21 days.
(**B** and **C**) Exemplary phase contrast microscopy images of colonospheres on day 14, showing a decreased sphere formation capacity of cells treated with LDN27219(**B**) and Tyrphostin 47 (**C**).
(**D and E**) Quantification of colonospheres per 5000 primary tumor cells treated with LDN27219 (LDN)(D) and Tyrphostin 47 (Tyr) (E). The number of spheres is shown at indicated time points. The data is represented as mean + SD, N=3 LDN, N=4 Tyr, statistical significance was determined using Mann-Whitney test ** p<0.01, *** p<0.001

4.3 The full length TGM2 isoform 1 is essential for CRC cell survival

Downregulation of endogenous TGM2 with shRNA or small molecule inhibitors, as wells as complete knockout of TGM2 mediated by CRISPR/Cas9, severely affected tumor growth and tumorigenicity in CRC. Thus, the question arises whether ectopic expression of TGM2 would raise cell proliferation and tumorigenicity. In addition, it has been reported that the expression and activation of different TGM2 isoforms, which are able to function, as a GTPase and/or a transamidase (TGase), are differentially regulated in several different human cancers [155,242,243]. To elucidate whether a specific transcript of TGM2

might play a predominant role in CRC, and to investigate which biological function of TGM2 is involved in CRC development and progression, lentiviral TGM2 overexpressing constructs were generated, that covered transcriptional variants and enzymatic mutants.

4.3.1 Modulating transamidase activity gains insights into TGM2 function in CRC

First, to investigate the impact of TGM2 overexpression, SW480 and HCT 116 cells were transduced with TGM2 overexpressing constructs. For this purpose, the coding sequence (CDS) of TGM2 isoform 1 (TGM2-Iso 1) and isoform 2 (TGM2-Iso 2) were cloned into lentiviral overexpression constructs coupled to a fluorescent marker protein (VENUS) (Figure 13A, B). TGM2 executes various biological functions and most of them rely on its ability to modify proteins, due to a Ca^{2+}-dependent posttranslational transamidation activity. In addition, it can also bind and hydrolyze GTP, Ca^{2+}-independently [170,244]. Binding of GTP inhibits the crosslinking activity but allows TGM2 to function in signal transduction [171]. To generate TGM2 constructs lacking either the transamidase activity (TGM2^{C277S})[122] or GTP-binding activity (TGM2^{R580A})[137] or both (TGM2$^{C277S+R580A}$), point mutations were inserted in the CDS and lentiviral overexpression construct were produced as described above (Figure 13A, B). This allowed us to assign biological functions of TGM2 to the individual enzymatic functions as well as to decipher the role of TGM2 isoforms in CRC. To verify the overexpression and transamidation ability of the generated constructs, SW480 cells were transduced with either an empty vector control or the different generated constructs. 72h after transduction cells were lysed and the transamidation ability as well as TGM2 protein expression were assessed (Figure 13 C - F). In comparison to the empty vector control, TGM2^{R580A} mutant showed an elevated crosslinking activity due to an insensitivity to the GTP regulation owing to the destroyed GTP-binding site. In contrast, the TGM2^{C277S} and TGM2$^{C277S + R580A}$ mutants did not exhibit any transamidase activity, based on the deletion of cysteine in the catalytic triad of TGM2, which makes the enzyme catalytically inactive for the cross-linking reaction[122]. TGM2$^{C277S + R580A}$ mutant is expected to be completely catalytically inactive as it can neither catalyze a transamidase reaction nor function as a GTPase (Figure 13F)[137]. Since TGM2 is known to also function independent of its enzymatic activity, this construct served to test the possibility that TGM2 could act as a catalytically inactive molecule in CRC. Importantly, TGM2-Iso 2 showed no elevated transamidase activity although it has a lower GTP-binding affinity as already described before [135,242]. As expected, overexpression of TGM2-Iso 1 resulted in a high transamidase activity compared to control (Figure 13E). A basic level of detectable enzymatic conversion in transaminase inactive constructs was due to remaining endogenous wild type TGM2 activity (Figure 13E, F). The elevated protein expression level was determined

by WES and showed a strong TGM2 expression in every tested overexpression construct in comparison to the control-transduced cells, indicating the functionality of generated constructs (Figure 13C, D).
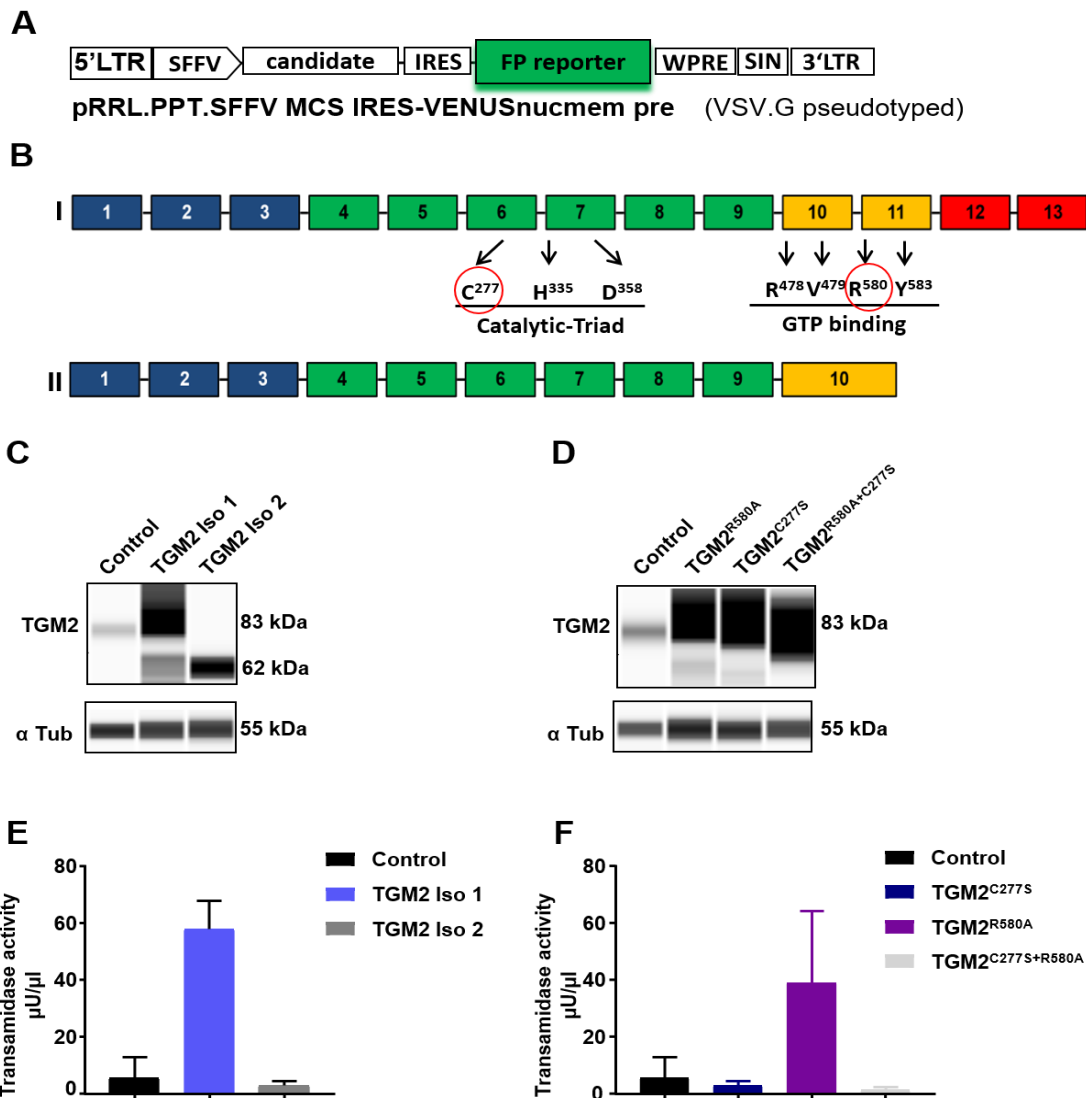
Figure 13 Generation of TGM2 cDNA, coding for TGM2 Isoform 1, TGM2 Isoform 2 or mutated TGM2 constructs

(**A**) Schematic overview of a third generation self-inactivating lentiviral vector provided by Axel Schambach. After the SFFV promoter TGM2 cDNA constructs of TGM2 isoform 1 (BI), TGM2 isoform 2 (BII) or mutated TGM2 (BI) were inserted.

(**B**) Schematic representation of human TGM2 mRNA coding for TGM2 Isoform 1 (I) or TGM2 Isoform 2 (II). Insertion of a point mutation and thereby replacing Cys-277 with Ser (C277S) leads to a transamidase inactive enzyme. The mutation of Arg580 to Ala (R580A) completely abolished GTP binding activity. A C277S and R580A mutated construct is completely enzymatic inactive. Colored boxes indicate exona, and horizontal lines indicate introns. Blue exons build the β- sandwich domain, green boxes the core domain, yellow and red boxes form barrel 1 and 2 of TGM2.

(**C-D**) Exemplary WES run showing TGM2 expression of SW480 cells after lentivirally manipulation with TGM2 overexpressing constructs. (Antibodies: TGM2 ms, CUB 7402, Abcam; α-Tubulin rb 11H10, Cell Signaling)

(**E**) Transamidase activity assay with cell lysates of SW480 overexpressing TGM2 isoform 1 (TGM2 Iso 1), TGM2 isoform 2 (TGM2 Iso 2) or control vector after 3 days.

(**F**) Transamidase activity assay with cell lysates of SW480 cells overexpressing a transamidase inactive construct (TGM2^{C277S}), a GTPase inactive and transamidase active mutant (TGM2^{R580A}), a transamidase and GTPase inactive mutant (TGM2$^{C277S+R580A}$) or control vector.

(**E-F**)The data are represented as mean +SD, statistical significance was determined using Mann-Whitney test. * p<0.05 ** p<0.01, ns = not significant. N = 3

4.3.2 Overexpression of TGM2 does not lead to CRC growth advantages

For further investigations, SW480 or HCT 116 cells were transduced with the overexpressing constructs containing the sequences of either TGM2-Iso 1 or TGM2-Iso 2 to simulate an enhanced expression of a specific isoform. The following experiment was performed to seek the expansion ability over a period of 7 days of TGM2-overexpressing cells. It should be determined whether TGM2 is able to function as an oncogene and thus its overexpression leads to growth or survival advantages. The transduced SW480 or HCT 116 cells, ectopically expressing TGM2 isoforms, expanded similar to the control cells in vitro and no growth advantage or disadvantage by overexpressing TGM2 isoforms in CRC cells could be detected (Figure 14B, C). It is conceivable that endogenous TGM2 is sufficient for CRC cell growth and further increase does not elevate its function. Another possible explanation for the unaffected cell growth could be due to regulatory mechanisms which tightly control TGM2 expression, activity and degradation within the cell. So it was reported that the C-terminus is important for protein stability which could result in a fast TGM2-Iso 2 [245] turnover. Also the activation of intracellular TGM2 requires stringent control mechanisms to prevent uncontrolled cross-linking of proteins with critical functions [153].

The same experimental setup was performed to examine the effects of overexpressed, point-mutated constructs. In this case, a significant reduction of cell expansion could be detected when cells were manipulated with $TGM2^{C277S + R580A}$, a slight reduction of expansion ability was also detectable when overexpressing $TGM2^{R580A}$. Only $TGM2^{C277S}$ did not show any disadvantages in growth compared to control (Figure 14E, F). These results suggest that neither ectopically overexpression of TGM2 Iso1 nor TGM2 Iso2 do have an impact on cell growth. In contrast, $TGM2^{C277S + R580A}$ a catalytically "dead" mutant seems to have dominant negative characteristics.

Since these findings showed almost no effect on CRC cells growth upon overexpressing several TGM2 constructs and selective elimination of transamidation activity leads to growth disadvantages, it is more likely that TGM2 rather acts as a pro-survival factor than an oncogene. To further stress this hypothesis, a set of rescue experiments were performed.
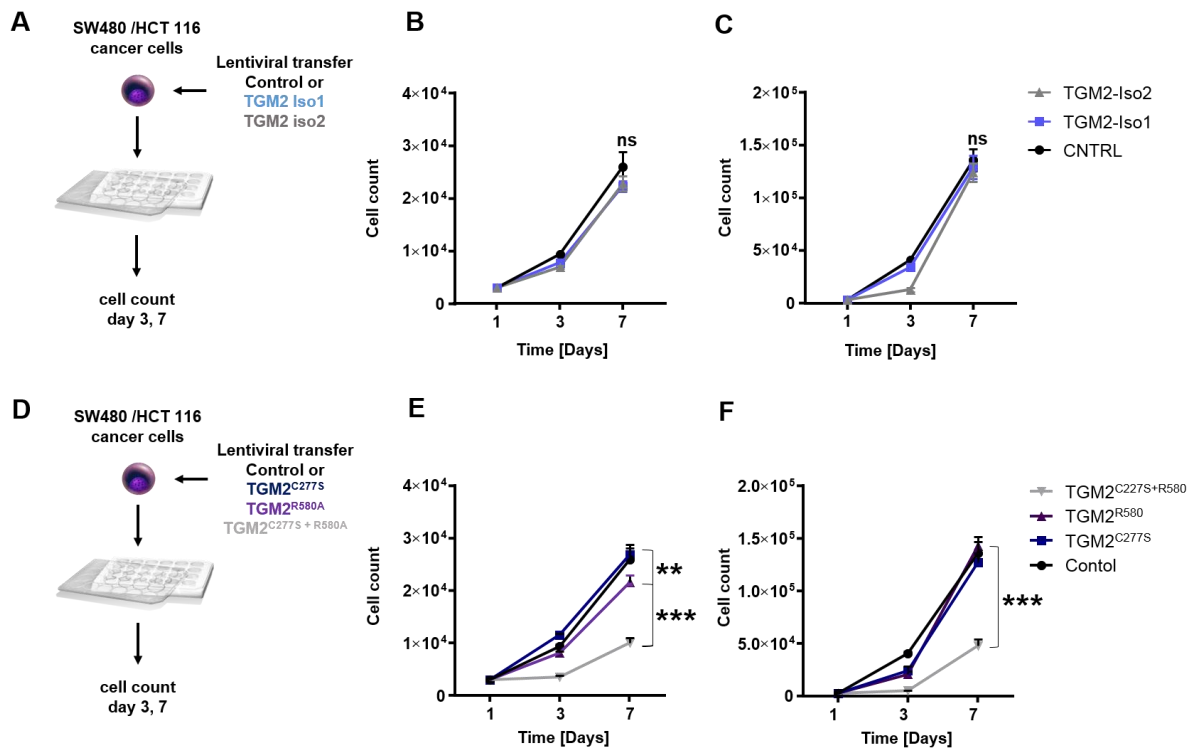
Figure 14 Overexpression of TGM2 Isoforms and increase of enzymatic functions does not lead to growth advantages

(**A**) Experimental scheme of the transduction setup and the in vitro expansion analysis. SW480 and HCT116 cells overexpressing TGM2 Isoforms or vector control were counted after 3 and 7 days

(**B**) SW480 cells overexpressing either TGM2 isoform 1, 2 or vector control.

(**C**) HCT116 cells overexpressing either TGM2 isoform 1, 2 or vector control.

(**D**) Experimental scheme of the transduction setup and the in vitro expansion analysis of SW480 and HCT116 cells overexpressing mutated TGM2 constructs which are transamidase inactive (TGM2^{C277S}), GTPase inactive (TGM2^{R580A}) or transamidase and GTPase inactive (TGM2$^{C227S+R580A}$). Cells were counted after 3 and 7 days.

(**E**) SW480 cells overexpressing either TGM2^{C227S}, TGM2^{R580A}, TGM$^{C227S+R580A}$, or vector control

(**F**) HCT116 cells overexpressing either TGM2^{C227S}, TGM2^{R580A}, TGM$^{C227S+R580A}$, or vector control.

(**B**-**C**, **E**-**F**) The data are represented as mean +SD, statistical significance was determined using Mann-Whitney test. ** $p<0.01$ *** $p<0.001$, ns = not significant. N = 3

4.3.3 TGM2 isoform 1 rescues TGM2 knockout cells through its transamidase activity

To deepen the understanding for the role of TGM2 and its splice variants and enzymatic function in CRC biology, a rescue experiment, using ectopic expression of TGM2-Iso 1, TGM2-Iso 2 or TGM2 mutants, was performed. Importantly, in this experimental approach, endogenous TGM2 was eliminated by CRISPR/Cas9. Therefore, sgRNAs were generated to recognize a specific intron-exon region of the TGM2 gene. Thus, it is guaranteed that only the endogenous gene will be switched off, but not the overexpressing construct, which does not contain any intron sequences. SgRNA-1 is complementary to an exon-intron

region located to exon 1, sgRNA-2 is complementary to an exon-intron region located to exon 5 (Figure 7A).

To examine which TGM2 isoform plays a crucial role in CRC, stable transduced SW480 cell lines, either overexpressing a control vector, TGM1-Iso 1 or TGM2-Iso 2 were generated and expanded for 3 days. Next, overexpressing cell lines were double transduced with lentiviruses containing sgRNA-1 and sgRNA-2. The proliferative behavior was assessed and cells were counted on day 3, 7 and 14 (Figure 15A, C). The transduction was monitored via FACS at the same time-points, which allowed calculating the expansion of the transduced cells. While cells, which were expressing TGM2-Iso 2 nearly disappeared over the course of 14 days, TGM2-Iso 1 expressing cells expanded in culture, thereby rescuing SW480 TGM2-knockout cells from cell death (Figure 15B). These results showed that only TGM2-Iso 1 was able to rescue TGM2-knockout cells. In contrast, cells only expressing TGM2-Iso 2 could not prevent cells from cell death. This is most likely caused by the inability to execute the cross-linking transamidase reaction emphasizing a subordinate role of TGM2-Iso 2 in CRC. In contrast, these results suggests a crucial for TGM2-Iso 1 in CRC sell survival.

To consolidate the findings that the pro-survival function of TGM2 is linked to the transamidase function, point-mutated constructs were expressed in SW480 cell lines. Again, to ensure that TGM2 functions are not taken over by the endogenous expressed TGM2, TGM2 gene was again deleted by using a CRISPR/Cas9 system, identical to previous experimental setting. Thus, only the exogenously expressed TGM2 mutants were present in the cell (Figure 15A, C). The proliferative behavior after overexpression of point-mutated TGM2 constructs were assessed on day 3, 7 and 14 and transduction efficiency was monitored by FACS to calculate the expansion of transduced cells. TGM2 mutants TGM2$^{C277S+R580A}$ and TGM2^{C277S} were not able to rescue the TGM2-knockout phenotype whereas TGM2^{R580A} showed a better expansion and proliferation ability over time (Figure 15D). It can be assumed, that the pro-survival activity of TGM2^{R580A} can be attributed to its transamidating ability, since cells transduced with the transamidase lacking mutants TGM2$^{C277S+R580A}$ or TGM2^{C277S} did not show any rescue effect.
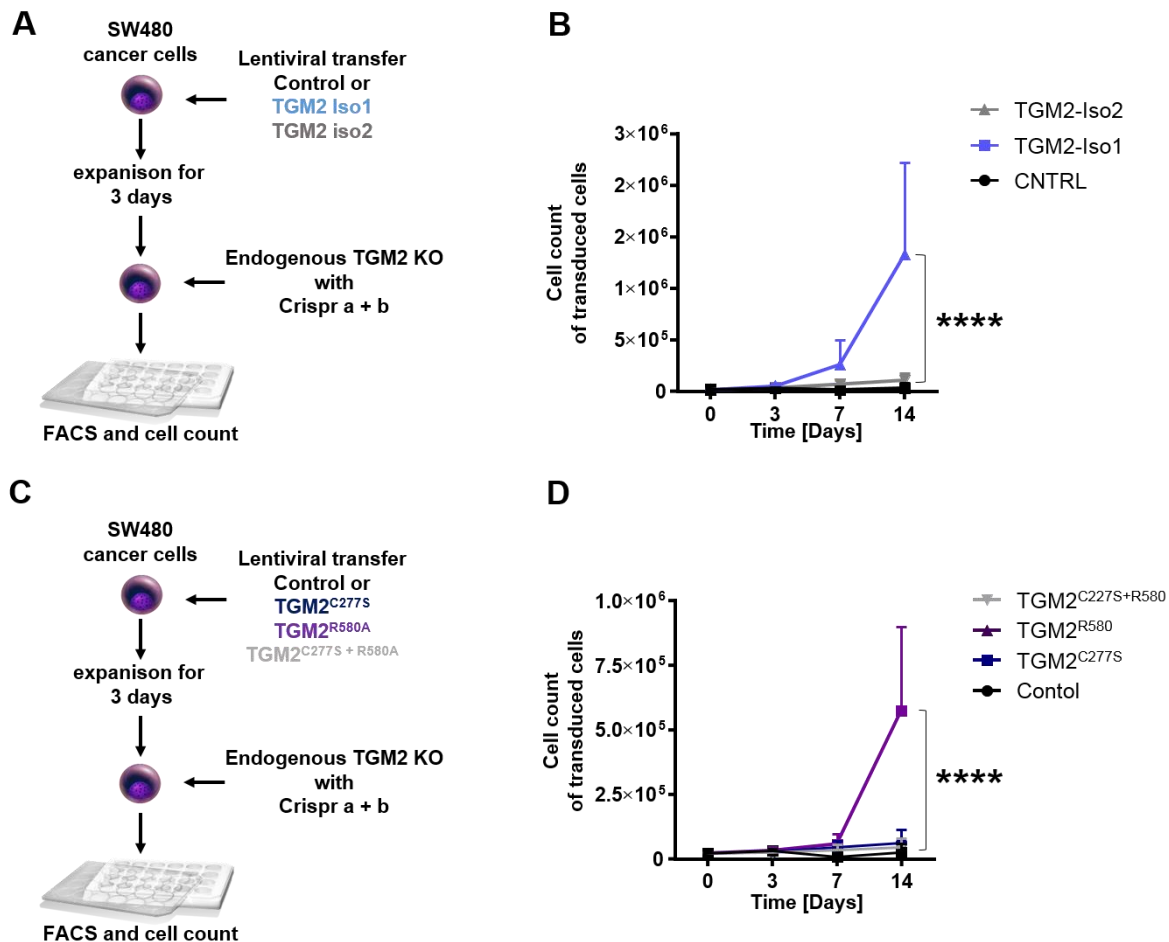
Figure 15 The transamidase activity of TGM2 Isoform 1 is essential for CRC survival

(**A**) and (**C**) Experimental set up to generate a knockout-rescue system to evaluate the role of TGM2 Isoforms and importance of the different enzymatic function of TGM2 in SW480 cells. SW480 cells were lentiviral transduced with TGM2 Iso 1, TGM2 Iso 2 or control vector (**A**) or transduced with mutated TGM2 constructs C227S, R580A, C277S + R580A or control (**C**) and expanded for 3 days. Subsequently, cells were double transduced with Crispr a and b or control to genetically knockout endogenous TGM2. Resulting genetically manipulated cells expressing only ectopic TGM2.
(**B**) Gene knockout and followed gene rescue experiments to confirm the specific role of TGM2 Iso 1 and TGM2 Iso 2 or evaluate important enzymatic functions (**D**) of TGM2 in SW480 cells. Transduction efficiency was evaluated by FACS and expansion kinetic monitored over 14 days. The data is represented as mean +SD, n=3. Statistical significance was determined using Mann-Whitney test ****p<0.0001.

4.4 TGM2 prevents colon cancer cells from apoptosis by its ability to interact with p53

To enlighten the molecular mechanism of TGM2 action in CRC, we sought to find the reason for the growth disadvantage of CRC upon loss of TGM2 activity. The reduced expansion ability of TGM2 knockdown or knockout cells can be explained by two different scenarios. Either TGM2 knockdown results in growth arrest or inhibits the survival of CRC cells. Therefore, the proliferative behavior as well as the occurrence of cell death events upon TGM2 knockdown were assessed.

4.4.1 Depletion of TGM2 leads to the induction of apoptosis

First, it was investigated whether TGM2 depletion induces apoptosis of SW480 cells. Apoptotic cells can be distinguished from living cells by 7-AAD and Annexin V labeling. During early apoptosis phosphatidylserine translocates to the external leaflet where it can be detected with fluorochrome labeled Annexin V. Late apoptotic cells can be distinguish by 7-AAD and Annexin V labeling, due to the ability of 7-AAD to penetrate leaky plasma membranes and intercalate into the DNA [246] (Figure 16B). Suppression of TGM2 in SW480 cells led to a ~3-fold increase of apoptotic cells, when compared to the control transduced cells (Figure 16C). As previous experiments showed that overexpression of TGM2 did not increase proliferation of CRC cells, the latter experiment supports the role for TGM2 as a potential gatekeeper against cell death in CRC SW480 cells. To further consolidate this phenotype and to investigate the effects of TGM2 suppression at single cell resolution, time-lapse imaging and subsequent single cell tracking of CRC cells were performed. Continuous single cell tracking is a potent technique which allows the identification of changes in cellular behavior, cell fate, generation time, location, cell-cell contact, marker expression, migration of each individual cell at each time point [247]. Dying cells can easily be identified in video-microscopy by their shrunk size, the loss of their shape and finally by the loss of their reporter fluorescence. The technique allows the observation of single cells and to follow them for several cell generations (Figure 16D). The phase contrast pictures were acquired every two to three minutes to keep the identity of every individual cell. The single cell tracking was performed using the self-written TTT software [248,248]. Single cells were tracked by scientists and cell fates such as cell division and death observed while tracking were added into a pedigree for every single cell (Figure 16D). The statistical analysis revealed an earlier occurrence of apoptotic events in TGM2 depleted cells. Almost all cells, which were transduced with TGM2 shRNAs died in the same cell generation (G0) and were not able to divide and give rise to daughter cells. On the other hand, control-transduced cells showed a significant lower induction of apoptosis and were able to divide (Figure 16E).
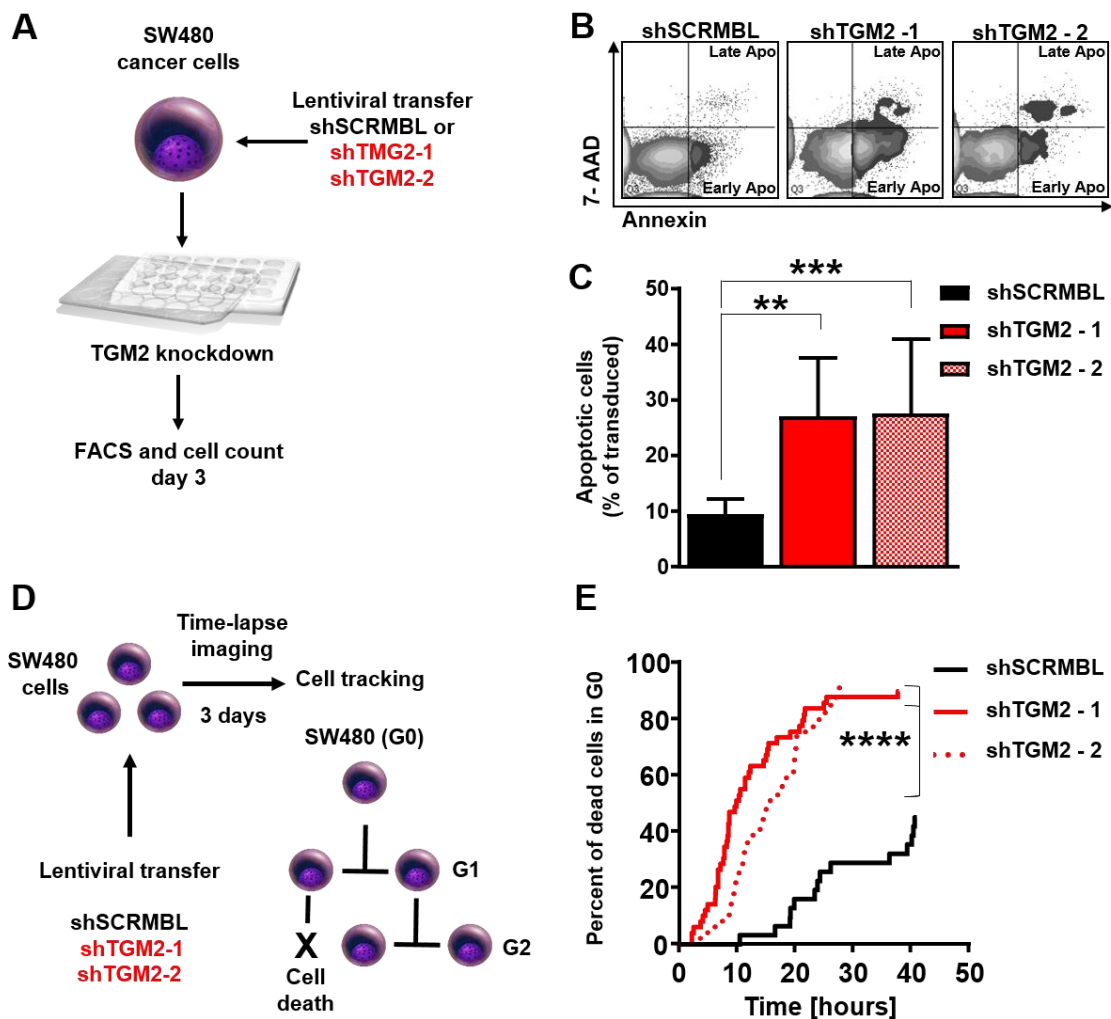
Figure 16 TGM2 knockdown induces cell death in SW480 cells

(**A**) Experimental setup to measure induction of apoptosis after TGM2 silencing in SW480 cells with TGM2 shRNAs for 3 days.

(**B**) Representative FACS plots displaying the induction of apoptosis after TGM2 silencing. Annexin und 7-AAD positive cells are delineated as late apoptotic cells (Late Apo) and Annexin positive cells are indicated as early apoptotic (Early Apo) cells.

(**C**) Percentage of apoptotic cells after TGM2 knockdown 3 days after transduction. The data is represented as mean + SD, N=3. Statistical significance was determined using Mann-Whitney test. ** p<0.01, *** p<0.001

(**D**) Experimental setup of time-lapse imaging analysis and schematic overview of a pedigree including a cell death event in generation 1.

(**E**) Time-lapse imaging and subsequent single cell tracking of SW480 cells after TGM2 silencing together with control. Cumulative cell death events in % of transduced cells over-time. Statistical significance was determined using Log-rank (Mantel-Cox) test. **** p<0.0001

4.4.2. Elucidating the molecular network of TGM2 in colon cancer cells by RNA-sequencing.

To identify key biological pathways associated with TGM2 and to understand the regulatory mechanisms underlying loss of TGM2, the transcriptional consequences of TGM2 knockdown were investigated by RNA-Seq. in SW480 cells. Gene expression profiling by RNA-Seq. is widely applied in cancer research to identify differentially regulated pathways in tumor cells [222]. It provides a powerful tool to decipher global and quantitative gene expression patterns.

For this purpose, SW480 cells were transduced with either lentiviruses encoding shTGM2 - 1 or scramble control. After 3 days of cell expansion, the cells were collected and RNA isolation and sequencing were performed. A total of 32,911 gene transcripts were detectable, using a cut off p = 0.05 and a fold change of 2, 1,452 downregulated and 996 upregulated genes could be found (Figure 17C). To investigate biological processes, which correlate with the RNA-Seq. data, a gene set enrichment analysis (GSEA) was performed. GSEA determines whether a defined set of genes correlates with a particular phenotype within the microarray data. Therefore, significantly up- and downregulated genes were analyzed (Figure 17C). The subsequent functional analysis was performed to identify differentially expressed genes (DEGs) and regulatory pathways. For this purpose, GSEA was performed against Hallmark gene-set signatures. The GSEA analysis provided a link between TGM2 and regulation of genes of critical importance in cancer development and progression for example PI3K-, AKT-, MTOR-, P53-, KRAS-signaling, inflammatory response etc. (Figure 17C, B).
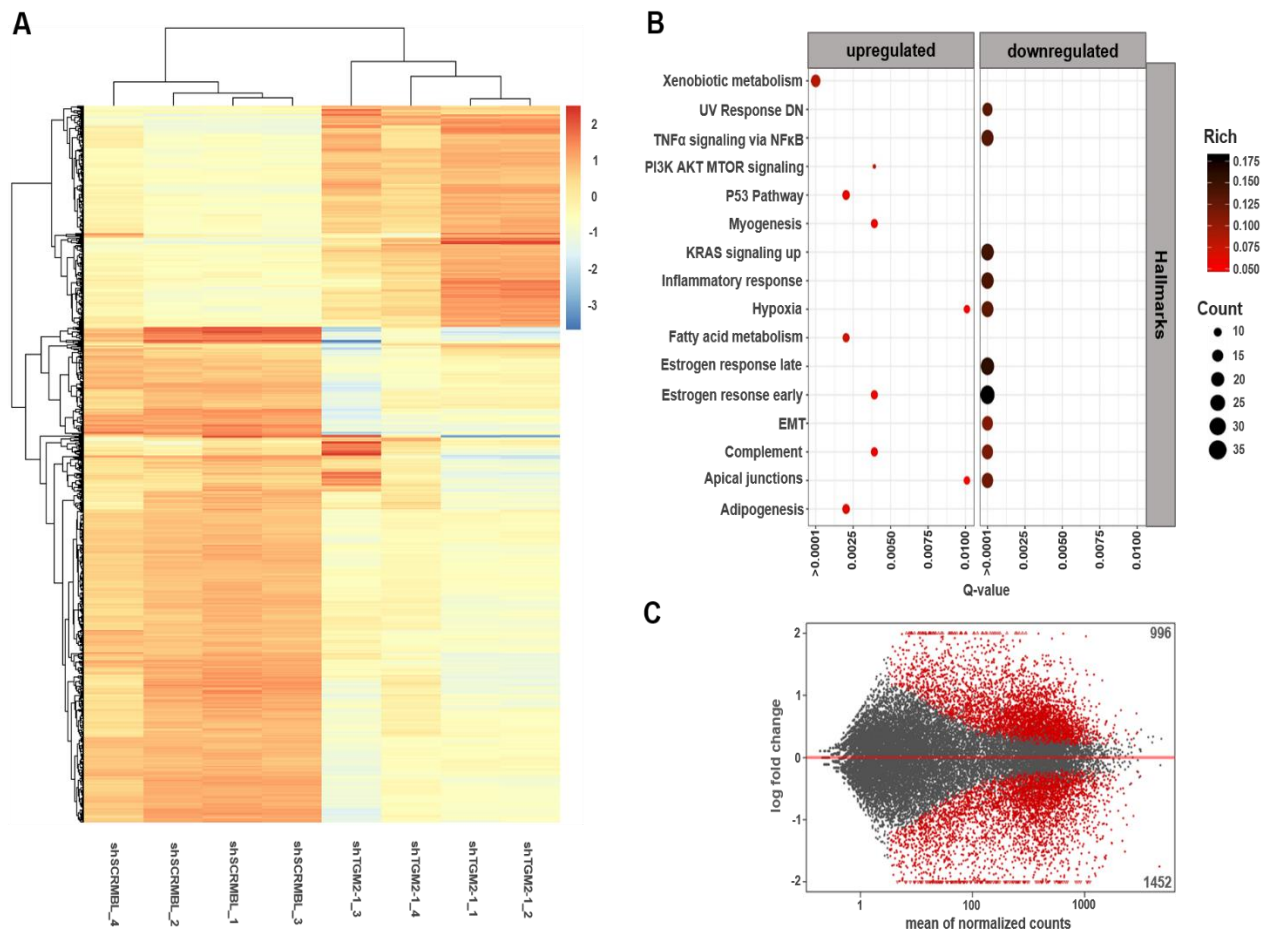
Figure 17 Gene expression profiling and functional analysis reveals that TGM2 is involved in cancer hallmark traits

(**A**) Global changes of DEGs (Differentially expressed genes) Hierarchical clustering of DEGs was generated after shTGM2-1 treatment**.** The expression levels of the 1000 most regulated genes were visualized and the scale form least abundant to highest range is delignated as Z-score. Their phylogenetic relationships were shown on the left tree. The top tree indicates the cluster relationship of the samples.

(**B**) Scatter plot of enriched Hallmark statistics. Rich factor is the ratio of the differentially expressed gene number to the total gene number in a certain Hallmark. Q-Value is corrected P-value ranging from 0-1. The color and the size of the dots represent the Rich factor and the number of DEGs mapped to the indicated pathways, respectively. Top 10 enriched Hallmarks of significantly and differentially (Fold2, p=0.05) regulated genes are shown in the figure.

(**C**) Dot plot of the differential gene expression analysis between control and shTGM2 - 1. Gray dots are genes not significantly regulated and red dots significantly changed genes (p value < 0.05), respectively. The log2 mean of the transcript count is on the X axis and the log2 fold change is on the y axis. 996 genes are upregulated, significant (p value < 0.05) and differentially (Fold2) regulated and 1452 genes are downregulated, significant (p value < 0.05) and differentially (Fold2) regulated in comparison shSCRMBL.

4.4.3 TGM2 does not influence NFkB, AKT or HIF1-α signaling in CRC cells

Since depletion of TGM2 induces massive cell death, it can be hypothesized that TGM2 plays an important role in tumor cell survival. To identify key biological pathways associated with TGM2 and to understand the regulatory mechanisms underlying the induction of cell death in absence of TGM2, common aberrant regulated pathways in cancer, based on RNA-Seq. data, were investigated. Based on the results of RNA-Seq. data, a possible involvement of TGM2 in NF-kB, Akt or HIF signaling can be assumed. This is further underlined by the fact, that TGM2 has already been implicated in these signaling pathways in different cancer types [228,249].

Because current findings in this work suggested that NF-κB as well as Akt were attractive candidates contributing to a signaling cascade involved in TGM2 action, the activation status of these proteins were determined upon TGM2 silencing. Therefore, lentiviral manipulated TGM2-knockdown SW480 cells were lysed 72h after transduction and protein expression was determined in comparison to scramble control. As readout for the expression and activation status of Akt or NF-κB, anti-pan-AKT, anti-pan-NF-κB as well as anti-phospho-AKT and anti-phospho-NF-κB antibodies were used. NF-κB is a protein complex consisting of large precursor proteins, p150 and p100, which undergo processing to generate the mature NF-κB subunits, p50 and p52. Both participate in target gene transactivation by forming heterodimers with RelA (p65), RelB or c-Rel [250]. Several subunits of NF-κB are designated in Figure 18B.

However, the results shown in Figure 18B demonstrated that loss of TGM2 did not compromise the activation neither of Akt nor NF-κB by phosphorylation, compared to vector control upon TGM2 knockdown. As each of these molecules showed no dependence on TGM2 signaling, it can be hypothesized that TGM2 does not mediate its pro-survival function via these two pathways in CRC cells (Figure 18B, C).
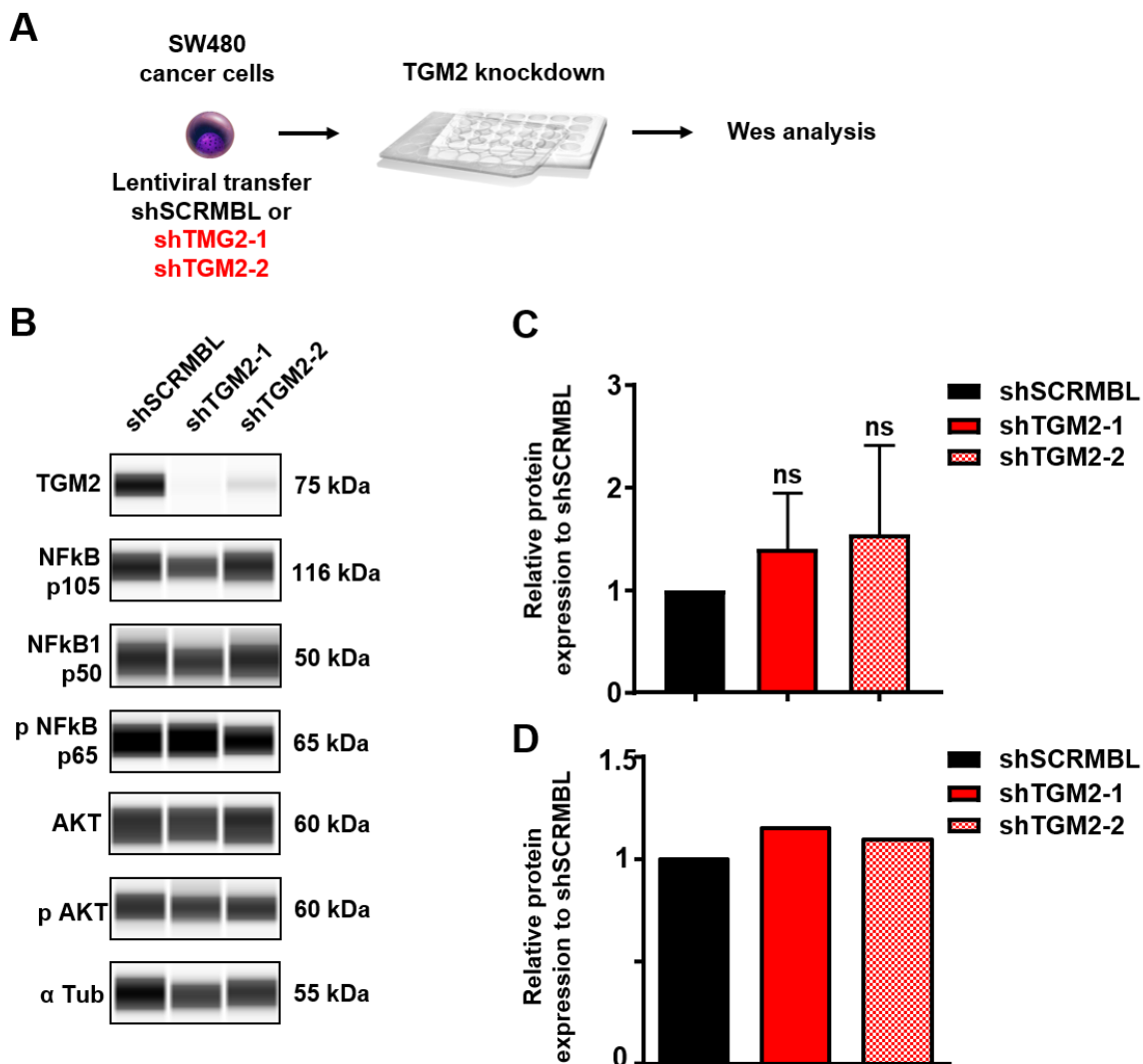
Figure 18 TGM2 is not involved in NFkB or AKT signaling in CRC

(**A**) Experimental scheme of transduced SW480 TGM2 knockdown cells. After 3 days of TGM2 silencing WES analyses were performed.

(**B**) Representative WES-runs displaying protein expression of NFκB p105 precursor protein, NFκB p50 subunit, activated phospho NFκB p65 (p NFκB p65), endogenous AKT and activated phospho AKT (p AKT) upon TGM2 knockdown, α-Tubulin expression serves as a loading control.

(**C**) Quantitative expression analyses of activated phospho NFκB p65 (p NFκB p65) in SW480 TGM2 knockout cells 3 days after transduction. The data is represented as mean + SD, N=3. Statistical significance was determined using Mann-Whitney test. ns = not significant. (Antibodies: TGM2 ms, CUB 7402, Abcam; α-Tubulin rb 11H10, Cell Signaling; AKT rb C67E7, Cell Signaling; p-AKT rb D9E, Cell Signaling; NF-κB rb #3035 Cell Signaling; pNF-κB rb 93H1 Cell Signaling)

(**D**) Quantitative expression analysis of activated phospho AKT (p AKT) in SW480 TGM2 knockout cells 3 days after transduction. N=1

Next, it should be determined whether TGM2 regulates HIF1-α signaling in CRC. It is known that most of the solid tumors suffer under oxidative stress caused by massive and uncontrolled cell replication events [182]. To escape this obstacle, cancer cells tend to switch from an aerobic to an anaerobic metabolism [251]. HIF1-α plays an important role in this metabolic switch. There is evidence that TGM2 is upregulated upon hypoxic stress and further leads to HIF1-α expression [252].
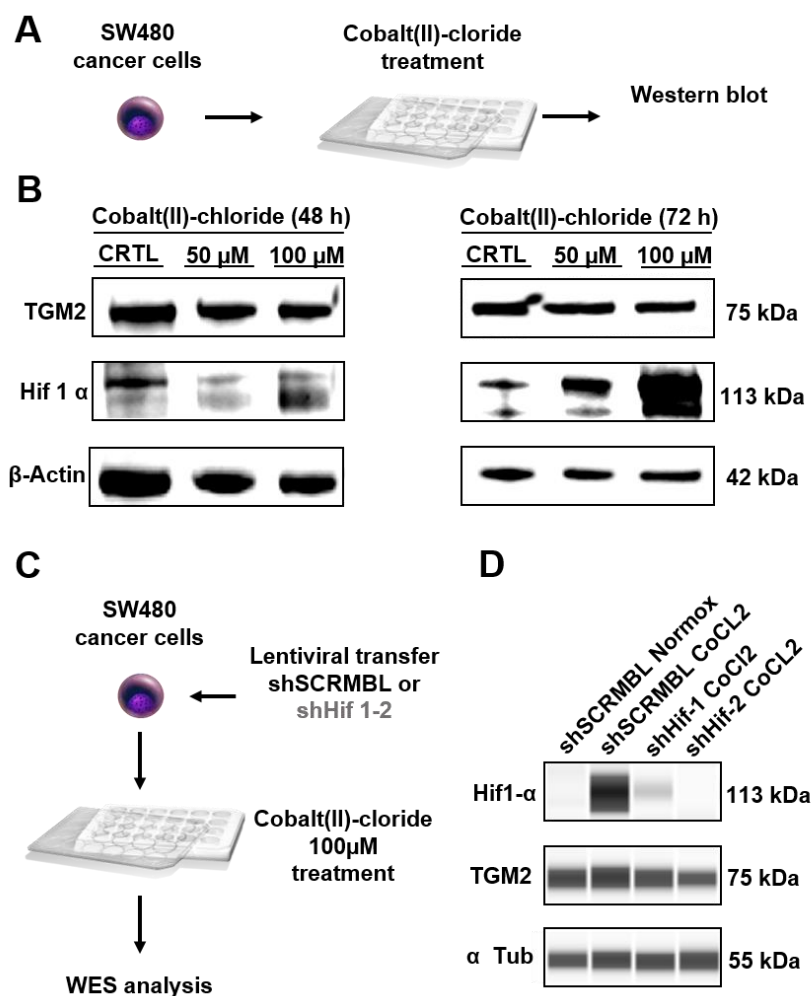
Figure 19 Hypoxic condition and HIF-1α does not influence TGM2 signaling

(**A**) SW480 cells were treated with different Cobalt(II)-chloride (CoCl₂) or vehicle control concentrations to mimic hypoxic condition in vitro. After 48 and 72 hours cells were lysed and western blot analyses were performed.
(**B**) Representative Western plots displaying the induction of HIF-1α expression under hypoxic condition after 48 and 72 hours. β-Actin represents the loading control. (Antibodies: TGM2 ms, CUB 7402, Abcam; HIF-1α ms 54, BD Bioscience)
(**C**) Schematic setup of SW80 cells treated with HIF-1α shRNAs. SW480 cells were transduced and treated with 100 µM Cobalt(II)-chloride (CoCl₂) for 72h. After cell lysation WES analyses were performed.
(**D**) Representative WES-run of SW480 cells after HIF-1α silencing and 100 µM Cobalt(II)-chloride (CoCl₂) treatment for 72h. HIF-1α and TGM2 expression were detected and compared to shSCRAMBL under hypoxia (shSCRMBL CoCl₂) and normoxia (shSCRMBL Normox). (Antibodies: TGM2 ms, CUB 7402, Abcam; α-Tubulin rb 11H10, Cell Signaling)

It has been reported by Jang et al., that hypoxia can induce TGM2 expression through an HIF-1α dependent pathway in glioblastoma, cervix carcinoma and neuroblastoma cells [148]. With Cobalt(II)-chloride (CoCl$_2$), a chemical inducer of HIF-1α, it is possible to mimic hypoxic conditions in cell culture. The TGM2 expression level was assessed after CoCl$_2$ treatment in SW480 cells. Western blot analysis showed that TGM2 expression did not increase after treatment with different CoCl$_2$ concentrations in contrast to HIF-1α, which expression was elevated after 72h of hypoxia (Figure 19B, D). To confirm whether TGM2 expression in SW480 cells is mediated by HIF-1α, the TGM2 protein level was examined in hypoxia after downregulation of HIF-1α using HIF-1α-shRNAs. No significant changes in the expression level of TGM2 could be detected neither in comparison to normoxic or hypoxic conditions, nor after HIF-1α depletion with HIF-1α –shRNAs under hypoxic conditions (Figure 19D). These results indicate no coherence of hypoxia-induced HIF-1α and TGM2 expression or a direct dependence of both molecules on each other in CRC.

4.4.4 TGM2 blocks p53-induced apoptosis

As no direct link between TGM2 and Akt, NF-κB and HIF-1α signaling was found in CRC, a screen of an array of proteins involved in apoptosis and cell death (R&D Systems Proteome Profiler Apoptosis Array) was implemented, to identify the mechanism behind the induction of cell death upon TGM2 depletion. Therefore, the proteome profile of apoptotic cells was monitored after TGM2-knockdown in SW480 cells compared to scramble control (Figure 20A). The results of the array demonstrated trends towards an increased expression of pro-apoptotic proteins (procaspase 3, phosphorylated p53, pRAD 17) and anti-apoptotic proteins (HIF-1α, HSP 27, HSP32, HSP 70) with at least a 2-fold increase in expression in TGM2 knockdown cells compared to control (Figure 20B, C).
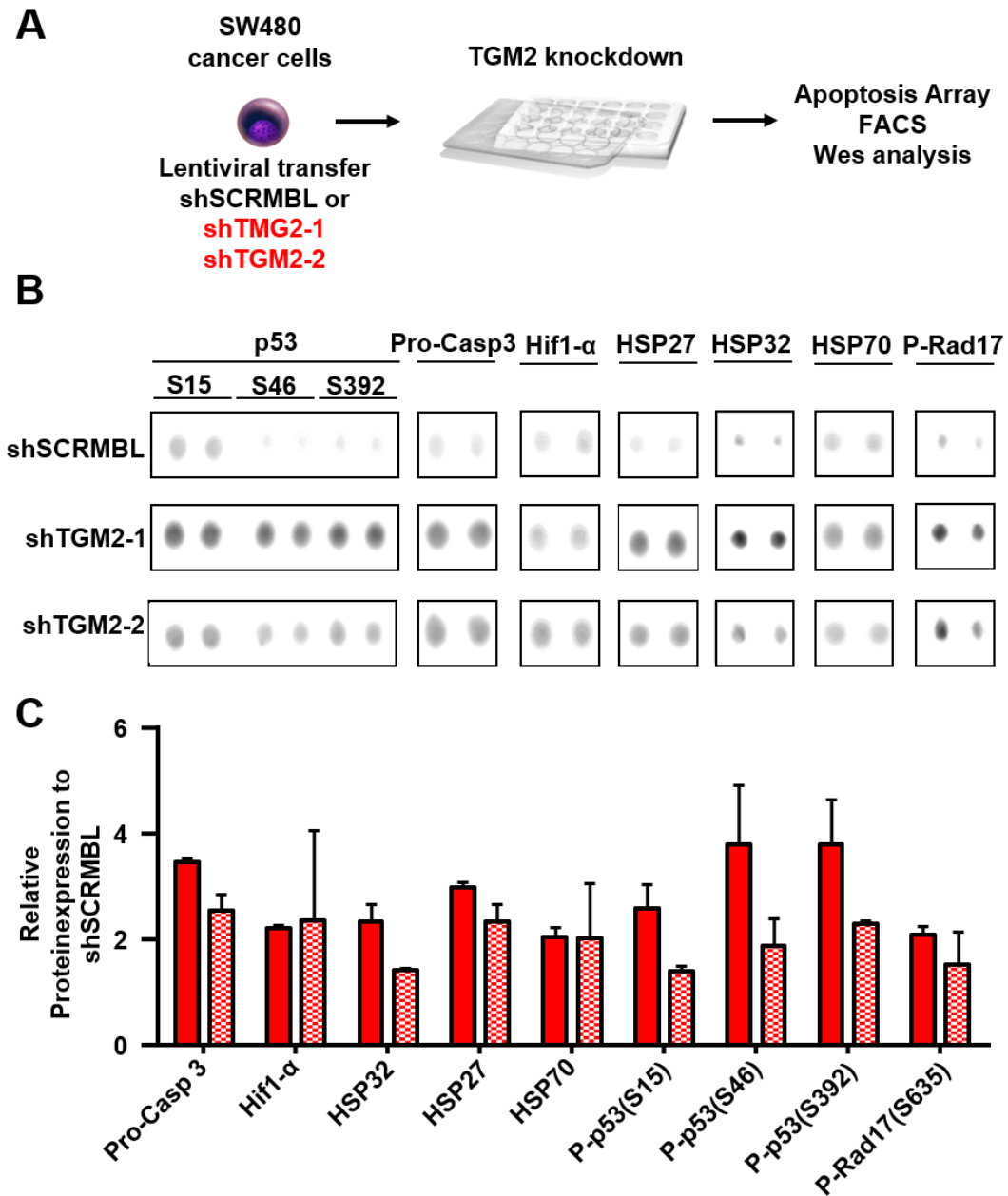
Figure 20 Protein expression analysis revealed caspase 3 and p53 as potential TGM2 interacting partners

(**A**) Experimental scheme of the transduction setup of lentiviral manipulated SW480

(**B**) Representative Proteome Profiler Array™-Human Apoptosis Array analysis of SW480 cells manipulated for 3 days with shTGM2-1, shTGM2-2 or control, proteins with 2fold enrichment, at least in one tested TGM2 shRNA, are shown. Casp = Caspase, p = Phspho

(**C**) Densitometry analysis of antibody arrays, relative protein expression of 2fold-enriched proteins, at least in one of tested shRNAS, are shown. N=2 individual experiments, P = Phospho

Apoptosis is executed by caspases, a family of cysteine proteases. Once activated, upstream initiator caspases like Caspase 8 and 9, cleave and activate downstream executioner caspases, such as caspase 3, caspase 6 and caspase 7 [253]. The apoptosis array revealed procaspase 3 as one of the significantly higher expressed proteins in comparison to scramble control. In order to confirm that apoptosis possibly occurs through caspase 3 activation after loss of TGM2 in CRC cells, cleaved caspase 3 expression was probed by flow cytometry upon TGM2 silencing (Figure 21A, B). The results showed that caspase 3 activation is increased more than 3-fold by TGM2-sh1 and TGM2-sh2 at 72 hours after TGM2-knockdown compared to scrambled control. It was therefore of high interest to study the coherence of TGM2 silencing and induction of apoptosis mediated by caspase 3.
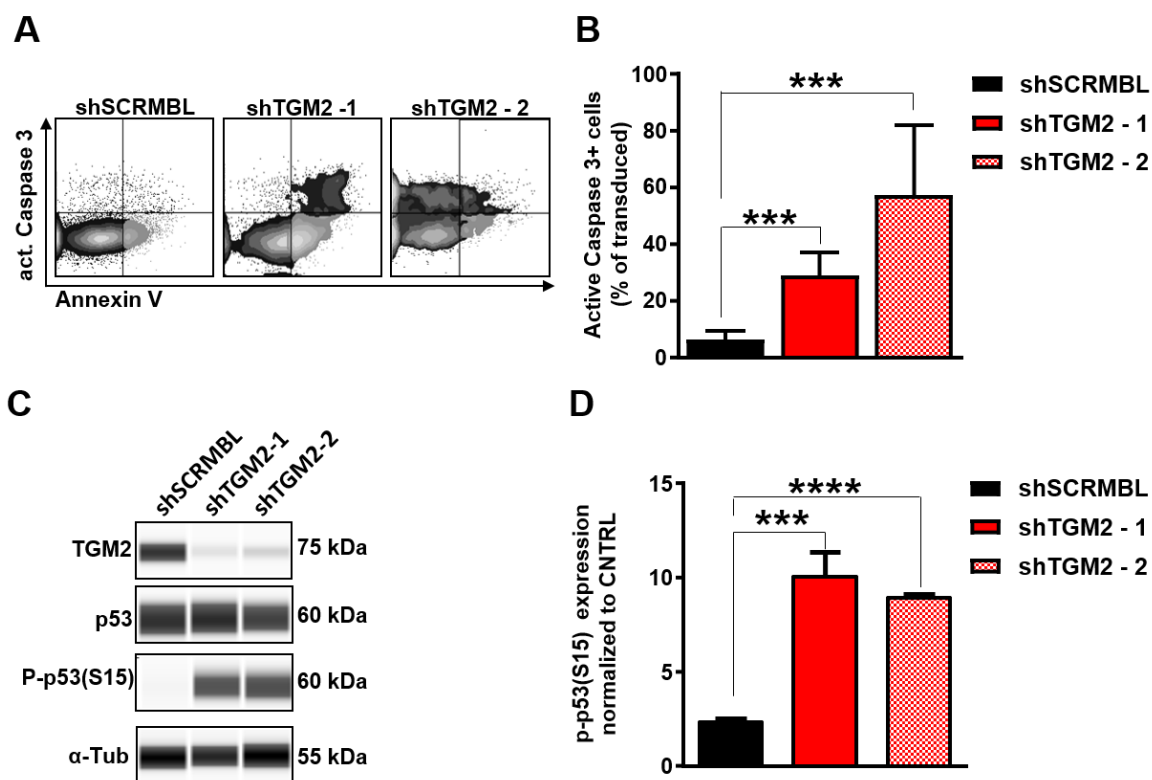
Figure 21 TGM2 knockdown induces activation of p53 and caspase 3

(**A**) Representative FACS plots displaying the induction of apoptosis after TGM2 silencing
(**B**) Percentage of active caspase 3 positive cells after TGM2 knockdown 3 days after transduction. The data is represented as mean + SD, N=3. Statistical significance was determined using Mann-Whitney test. *** $p<0.001$
(**C**) Representative WES-runs displaying protein expression of TGM2, endogenous p53 and activated p-p53(S15) upon TGM2 knockdown, α-Tubulin (α-Tub) expression served as a loading control
(**D**) Quantitative expression analyses of activated phospho p-53(S15) in SW480 TGM2 knockout cells after 3 days of transduction. The data is represented as mean + SD, N=3. Statistical significance was determined using Mann-Whitney test. *** $p<0.001$

To further assess potential interaction partners of TGM2, the next step was to interrogate the p53 signaling pathway, which was upregulated upon TGM2 silencing revealed by RNA-Seq. data and apoptosis array. To confirm the hypothesis that TGM2 signaling is probably interconnected with p53 signaling, the expression profile of activated p53 (S15) after TGM2 silencing was determined by WES (Figure 21C). It could be found that the expression of phosphorylated p53 (S15) was 6-fold increased in cells, lacking TGM2 expression. These results suggest an induction of apoptosis via a TGM2-p53-Caspase3 signal cascade in CRC (Figure 21D). The tumor suppressor p53 is known to be involved in preventing cells from DNA-damage and directs cells in cell cycle arrest or apoptosis [106,254]. This raises the question whether CRC cells are able to evade programmed cell death by a TGM2 mediated inhibition of the tumor suppressor p53 and thus, TGM2 helps CRC cells to circumvent control mechanism and renders them insensitive for growth arrest and apoptosis signals.

4.4.5 P53 knockout prevents cells from loss of TGM2-mediated programmed cell death

The tumor suppressor p53 is one of the best-studied tumor suppressors and one of the most frequently observed mutated genes in cancer [104,254]. Thereby, it can be differentiated between p53 mutations that give raise to a gain of function mutant which in contrast to its wild type counterpart has acquired novel functions and promotes a more aggressive tumor profile, and p53 mutation which leads to a loss of p53 protein activity [108]. Often p53 mutations lead to diminution of the wild type activity but not a complete abolishment, which is also the case for SW480 cells. Although SW480 cells carry two point mutations (R273H and P309S) in the p53 genes, p53 signaling is not fully affected [255]. Nevertheless, to further evaluate the coherence of apoptosis resulting from TGM2 knockdown and p53 expression it was rational to assess next experiments in the HCT116 CRC cell line, because of the p53 wild type status of these cells [256].

As shown previously in this work, lentiviral transduced HCT116 TGM2 knockdown cells showed an equal reduction of expansion ability as SW480 cells (Figure 6C, D). The objective of the next experiments was to compare the expansion kinetics of HCT116 cells which have a p53 wild type (p53^{wt}) or a p53 knockout (p53$^{-/-}$) status upon loss of TGM2. As TGM2 silencing activates p53 signaling, it should be determined whether loss of p53 is sufficient to inhibit loss of TGM2-mediated cell death. In concordance to previous experiments it could be shown that HCT116 p53^{wt} cells undergo apoptosis after TGM2 knockdown within 3 days (Figure 6C, D). In contrast, HCT116 p53$^{-/-}$ cells were not affected in their cell count after TGM2 depletion within the observation period of 3 days (Figure 22B). This rescue indicates the importance of

p53 to convey the apoptosis signal induced by loss of TGM2. These results strongly suggest TGM2 as an upstream regulator of p53.
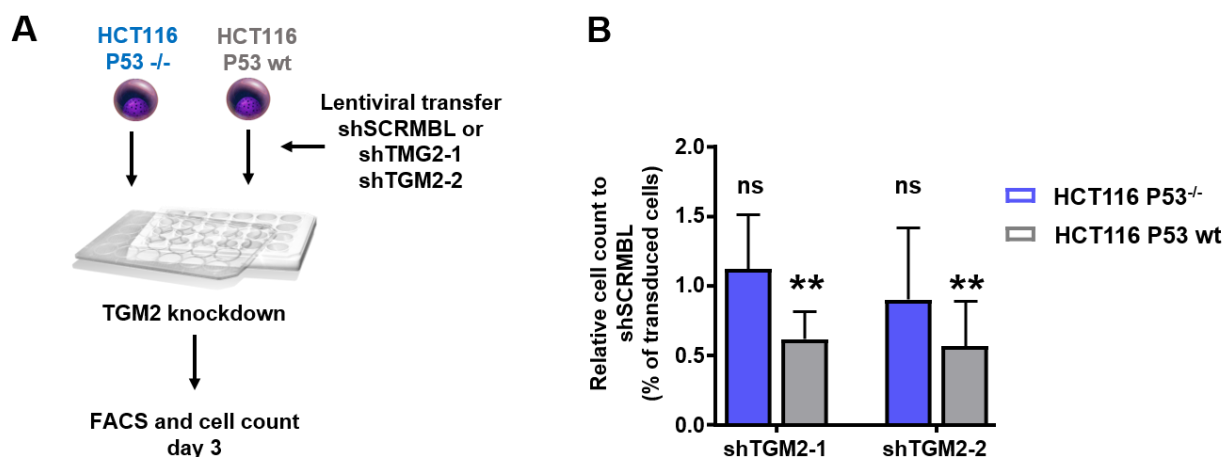
Figure 22 HCT116 p53$^{-/-}$ cells show no significant difference in cell count in comparison to control after TGM2 depletion

(**A**) Scheme of the experimental set up of in vitro expansion of HCT 116 p53 wild type cells (HCT116 p53^{wt}) and HCT116 p53 knockout cells (HCT p53$^{-/-}$). Cells were transduced with either shTM2-1, shTGM2-2 or shSCRMBL and counted after 3 days of transduction.
(**B**) Quantification of cell count of HCT116 p53 ^{wt} and p53 $^{-/-}$ upon TGM2 knockout after 3 days. Cell count was normalized to control. Statistical significance was determined by comparison the relative cell count of HCT116 p53 $^{+/+}$ and p53 $^{-/-}$, upon TGM2 knockdown with shTMG2-1 or shTGM2-2, with shSCRMBL. Statistical significance was determined using Mann-Whitney test. ** p<0.01, ns = not significant

To further assess the molecular mechanism underlying loss of TGM2-induced cell death associated with p53 signaling, continuous single cell tracking based on time-lapse video-microscopy was performed. Focusing at the single cell behavior of either p53 wild type or knockout HCT116 cells after TGM2-knockdown, should reveal a more detailed picture. Therefore, the generation time of an individual cell, was monitored, as well as apoptotic events (Figure 23A). Again, as described previously in this work, dead cells were depicted by their shrunk size and non-refracting appearance with immobility.

HCT116 p53^{wt} and HCT116 p53$^{-/-}$ cells were transduced with shTGM2-1, shTGM2-2 or control scramble and monitored for 3 days. Intriguingly, tracking hundreds of single cells revealed a robust apoptotic response in HCT116 p53^{wt} immediately after TGM2 depletion (Figure 23B). HCT116 p53$^{-/-}$ and TGM2 knockdown cells were significantly more resistant to apoptosis, induced upon TGM2 depletion (Figure 23C,

D). HCT116 p53$^{-/-}$ cells silenced for TGM2 expression revealed no increased occurrence of cell death events compared to control HCT116 p53^{wt} cells transduced with shSCRMBL (Figure 23B, C). Together, these data showed that TGM2 silencing in HCT116 p53$^{-/-}$ cells did not cause an increased occurrence of cell death in contrast to HCT116 p53^{wt} and TGM2 knockout cells, which are showing a strong induction of apoptosis within the observation period of 40 h. These results strongly suggested a mechanism by which TGM2 interacts and blocks p53 to exert its tumor suppressive functions.
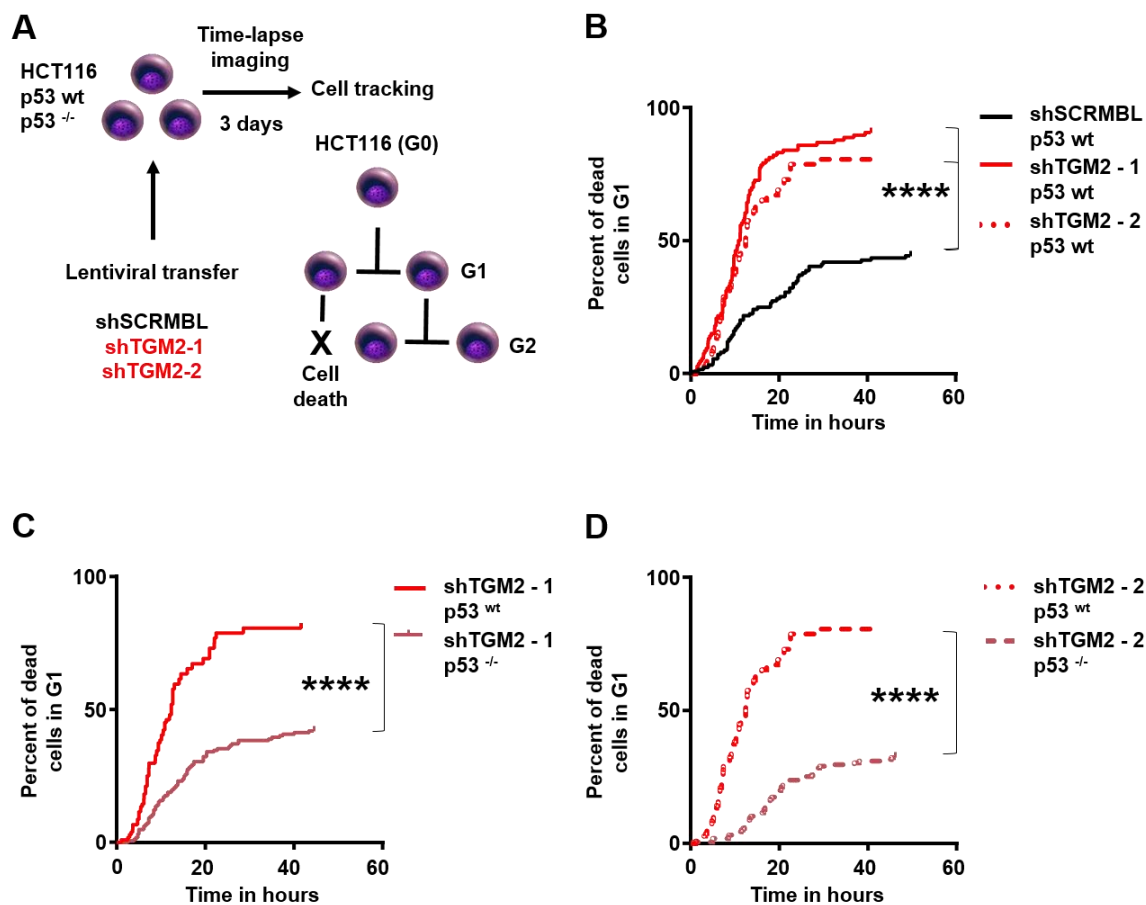
Figure 23 p53 knockout can rescue loss of TGM2 mediated apoptosis

(**A**) Experimental setup of time-lapse imaging analysis and schematic overview of a pedigree including a cell death event in generation 1 (G1).

(**B**) Time-lapse imaging and subsequent single cell tracking of HCT116 p53^{wt} cells after TGM2 silencing together with control shSCRMBL. Cumulative cell death events in % of transduced cells over-time.

(**C**) Time-lapse imaging and subsequent single cell tracking of HCT116 p53^{wt} and HCT116 p53 $^{-/-}$ cells after TGM2 silencing with shTGM2-1. Cumulative cell death events in % of transduced cells over-time. Statistical significance was determined using Log-rank (Mantel-Cox) test. N ~ 100 cells **** p<0.0001

(**D**)Time-lapse imaging and subsequent single cell tracking of HCT116 p53^{wt} and HCT116 p53 $^{-/-}$ cells after TGM2 silencing with shTGM2-2. Cumulative cell death events in % of transduced cells over-time. Statistical significance was determined using Log-rank (Mantel-Cox) test. N ~100 cells **** p<0.0001

4.4.6 TGM2 influences p53 signaling by forming p53-TGM2 complexes

To gain deeper insights into apoptosis induction resulting from TGM2 depletion and to examine whether the activation of p53 signaling pathway is a direct consequence of TGM2 silencing or a secondary event induced by other unknown factors, a proximity ligation assay (PLA) was performed. PLA technology allows the visualization of endogenous protein-protein interaction at the single molecule level [257]. This method relies on the use of combinations of antibodies coupled to complementary oligonucleotides which are amplified and revealed with a fluorescent probe, each spot representing a single protein-protein interaction. First, the specificity of the assay was determined by using mouse-TGM2 antibody alone as negative control. Incubation with two different antibodies from different species directed against TGM2 showed an average of 10.2 fluorescent dots per cell, and represented the positive control. Similar results can be obtained by using two different antibodies from different species, directed against phosphorylated p53(S15), where an average of 7.5 dots per cell could be detected (Figure 24B). These positive controls are useful for validating the presence of the proteins of interest in tested cell lines as well as the functionality of used antibodies and sensitivity of the assay. After the optimization and strict screening of the antibodies, the proximity of TGM2 and p53(S15) was assessed. These results showed that TGM2 interacts directly with p53(S15) and an average of 9.4 dots per cell could be detected (Figure 24B).

Taken together, these results show that a diminished TGM2 expression leads to massive cell death mediated by active caspase 3 induction. TGM2 directly binds to the tumor suppressor p53 and blocks its activity. This enables CRC cells to circumvent stressful conditions and escape cell death. However, it remains to be further determined by which mechanism TGM2 complexes with p53 to promote or inhibit its signaling.
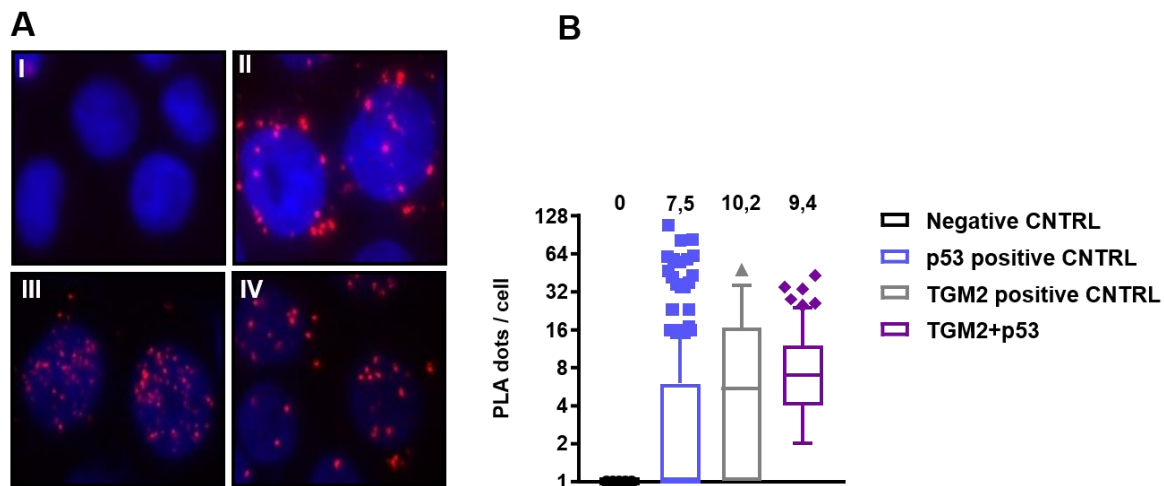
Figure 24 TGM2 functions as a pro-survival molecule via direct interaction with p53

(**A**) Representative picture of a typical cell staining observed in 5 fields randomly chosen.(I) TGM2ms antibody were incubated alone (negative Cntrl) or (II)TGM2rb (TGM2 positive Cntrl). (III) P53(S15)rb antibody were incubated with p53(S15)ms (p53 positive Cntrl) or TGM2ms (IV). Protein-protein interactions were visualized using hybridization probes labeled with Texas Red (red) and the nuclei were stained with DAPI (blue).

(**B**) Quantification of TGM2-p53 interaction and associated technical controls. Technical controls demonstrate the specificity of PLA signals in SW480 cells and the proximity between TGM2 and p53. The data is shown as Tukey boxplot, the box represents 25-75 % of the values and the median with whiskers of 1.5xIQR (interquartile range). Outliers are represented as dots. Mean value of PLA dots per cell is shown above box blots.

(**A-B**) Cntrl = control

5. Discussion

5.1 TGM2 is overexpressed in CRC tissue and provides a promising target for CRC treatment

During the past decade the introduction of new adjuvant chemotherapy regimens led to a significantly increased disease-free survival, however, the 5-year survival rate varies greatly depending on tumor stage and still about 40 % of all CRC patients are dying due to the disease [258,259,260,261]. Hence, there is a considerable medical need for improved CRC therapies and new targets leading to an effective and individual CRC treatment.

Already in existence are targeted therapies combined with chemotherapy regimes in metastatic CRC, in particular Bevacizumab – an antiangiogenic drug and recombinant monoclonal antibody that targets VEGF [262, 263], as well as Panitumumab [264] and Cetuximab [265], both recombinant monoclonal antibodies that target EGFR. Over the past few years, several new targeted antiangiogenic compounds have been developed. Among them Ramucirumab, a fully humanized monoclonal antibody that targets the extracellular domain of VEGF-receptor 2[266] and Ziv-aflibercept a fusion protein which binds to VEGF-A, VEGF-B and placenta growth factor (PIGF) [267,268]. The intention of these therapies is the inhibition of angiogenesis and thus to suppress nutrient supply of the tumor. A new therapeutic approach in targeted therapies of CRC are immune-checkpoint-inhibitors, which show promising results. Anti-tumor immunity is a new line of research for the treatment of patients with solid tumors [269], with the purpose to turn the immune system into a destructive force against tumors. Pembrolizumab and Nivolumab are drugs that target programmed cell death protein 1 (PD-1) and are already in use for CRC treatment [270]. PD-1 interacts with its two ligands PD-L1 and PD-L2, which leads to T-cell inactivation, while blocking PD-1 binding to its ligands results in the reactivation of cytotoxic T-lymphocytes [271].

The need to combine chemotherapy with targeted therapies is revealed by the limitations of conventional chemotherapies. An issue of standard cancer chemotherapy is the preferred interference of the chemotherapeutics with rapidly growing and dividing cells and therefore sparing of non-dividing and quiescent TICs, which bears the risk of chemoresistance and tumor relapse [272]. Besides, chemotherapeutics can provoke severe side effects limiting drug application. Further limitations result from the mechanism of action of the drugs. E.g., the efficacy of 5-FU is inhibited in patients with p53 mutations [273–275] and anti-EGFR inhibitors are ineffective in KRAS mutated CRCs. Therefore, targeted therapy holds great promise

due to the possibility for an individualized cancer therapy, to directly interfere in cancer biology, and to more precisely identify and eradicate cancer cells.

Current study suggests a pivotal role of TGM2 in CRC carcinogenesis due to significantly increased TGM2 protein levels and transamidase activity in patient derived epithelial tumor tissue. This hypothesis is further reinforced by the fact, that preclinical models revealed a severe effect on cell viability, decreased tumor initiation and TIC activity, when TGM2 is depleted or targeted with small molecule inhibitors. Moreover, inhibiting TGM2 sensitizes CRC cells towards apoptosis. Exerted functional roles of TGM2 in CRC renders it as an interesting target for therapeutic CRC intervention. TGM2 inhibition, may eradicate TICs and thus circumvent cancer relapse due to chemoresistance [276]. In this context, TGM2 could serve as a promising target for personalized cancer therapy to support common chemotherapeutics and to minimize side effects to ensure efficient and tolerable cancer therapy. Additionally, TGM2 is known to play a central role in the pathogenesis of different other types of diseases such as celiac disease, Alzheimer´s, Parkinson`s and Huntington`s disease. Thus, great efforts have been made to develop TGM2 inhibitor based-drugs [277]. This has led to a great diversity of potential TGM2 inhibitors. Although, it has to be taken into consideration that TGM2 is an ubiquitously expressed protein, the TGM2-knockout mouse model does not show a general phenotype [278] indicating a compensatory effect of its transaminase family members. Nevertheless, putative TGM2 inhibitors need to act locally and specific to avoid unwanted systemic side effects. ZED1227 probably meets these requirements and is the first TGM2 inhibitor, which entered and successfully completed phase 1 clinical trial for celiac disease therapy. In 2018, ZED1227 entered into phase 2a clinical trial [240]. Additionally, also the first TGM2 inhibitory antibody - UCB7875- has entered in a first-in-men trial with healthy volunteers [241]. These new developments further reinforce the potential of TGM2 as a future drug-target in CRC. In summary, the presented results show that TGM2 is a promising target; its inhibition is pharmacologically feasible and highly effective in the treatment of TGM2-expressing CRCs.

5.2 Discrimination of epithelial and tumor tissue offers new opportunities to investigate CRC and introduces TGM2 as a possible predictive marker

The significance to introduce new molecules as predictive factors, is caused by the polygenic nature of CRC[96,279,280]. The clinical behavior of CRC results from this dynamic processes, therefore one of the central challenge is to determine factors which lead to CRC responsiveness or resistance to antitumor agents [281,282].

One of the main critical issue in CRC treatment is the treatment decision for adjuvant therapy in patients with stage II tumors, as this approach provides survival benefits only for a minor group of patients [283]. 75 % - 80 % of these patients will be cured by surgery alone and the vast majority of remaining patients will relapse despite adjuvant chemotherapy [284].

Although there are several pathologic prognostic factors which provide information on the outcome of patients with CRC, e.g. the depth of tumor invasion into the colon and rectal wall [285], the tumor differentiation status [286,287] as well as lymphovascular and perineural invasion [288]. Although the prognostic value of these pathologic markers is unquestionable, the problem consists in the subjective nature of the evaluation by the pathologist and therefore they all suffer from a great deal of inter- and intra-observer variability [289].

Many efforts have been made to overcome this obstacle and to identify prognostic markers that are less influenced by individual subjectivity and enable a customized diagnostic and treatment regimen. In this context, Miyoshi et al. and Fernández-Aceñero et al. postulate a potential clinical importance of TGM2 as a prognostic marker by linking overexpression of TGM2 mRNA in CRC to a lower overall survival rate in CRC-patients [290, 291]. However, there is a relatively large discrepancy between the two studies regarding the expression of TGM2 mRNA in CRC tissues comparing to normal tissue. While Miyoshi et al. refers to a TGM2 mRNA overexpression of approximately 71 % in CRC samples, Fernández-Aceñero et al. determines only about 34 % of TGM2 high expressing tumors in tested patients. This may be explained by the fact that both groups did not distinguish between stromal and tumor cells since they used whole-tissue sections for RNA analyses. This bears the risk of falsifying the results due to tumor vascularization which was currently shown in a number of independent studies, demonstrating that expression profiles derived from the nonmalignant stromal region can influence assignment of CRC transcriptional subtypes [292,293]. Infiltration of cells of non-tumor origin is dependent on multiple factors and the amount and composition of infiltrating cells is highly variable, which makes accurate molecular analyses difficult [294]. This potentially leads to misclassification of tumors and relativizes the prognostic value of mRNA expression analysis of

whole tissue sections. This, together with the relatively small cohort of tested patients of 91 [290] and 70 [291], collected by Miyoshi et al. and Fernández-Aceñero et al. could lead to misinterpretation of the generated data.

It is known that TGM2 function depends on its localization within the cell and cell-type [295]. Therefore, it is not surprising that TGM2 fulfills various tasks within the tumor microenvironment. In breast cancer, TGM2 is suspected to promote tumor growth due to its overexpression in the secretome of cancer-associated fibroblasts (CAFs) [296], for instance. Simultaneously in epithelial breast cancer cells, TGM2 is reported to be epigenetically silenced due to a suggested tumor suppressive role[297]. Taken together, these findings strongly indicate that stromal and epithelial expression of TGM2 in CRC is independent and designate different tumor parameters. Therefore, to avoid masking effects of stromal cells, a separate consideration of the tumor microenvironment is inevitable.

The present work introduces a new technique to purify CRC cells and therefore provides the opportunity to circumvent stromal-derived intratumoral heterogeneity. The new developed method allows the investigation and quantification of TGM2 protein expression and activity in mucosa-derived tumor and corresponding normal colon cells. First surveys in our laboratory show a correlation between the level of epithelial TGM2 expression and tumor stage (data not shown, manuscript in progress), which highlights the potential of epithelial TGM2 protein expression level as a prognostic marker in CRC. Elevated and quantitatively measured TGM2 expression can now specifically be linked to every individual patient derived sample. The possibility to measure TGM2 expression level and enzymatic activity in a timesaving manner, offers the chance to coordinate additional treatment strategies for an individual therapy. However, the impact of epithelial TGM2 expression levels as a prognostic marker has to be further confirmed by investigation of a larger cohort, retrospective analysis and follow up studies. First data indicate the potential of epithelial TGM2 expression as an important indicator of patient stratification.

5.3 TGM2 signaling in CRC does not contribute to frequently described cancer pathways

This study ought to gain new insights into the molecular mechanisms contributing to the development of CRC. TGM2 has been implicated in a variety of processes like inflammation [298], wound healing [299], apoptosis [228], neurodegenerative disorders [300] and cancer [301]. However, its definitive role remains to be elucidated and is most likely depended on cell type, its location within the cell and available substrates [302]. Very little is known about the contextual roles of TGM2 in promoting or protecting CRC cells from death-induced

signaling and its contributions in promoting drug resistance and metastasis. Several studies have implicated TGM2 in cancer cell growth [229,303] on the other hand multiple publications assign a tumor suppressive role to TGM2 [154,215,304]. Similar to the opposing roles of TGM2 in tumor progression and inhibition, the role of the protein in molecular pathways varies as well, not only concerning signal transduction but also concerning interacting partners and its position within a distinct signaling network.

Existing publications about the TGM2 functions in cancer, give an impression about the manifold roles of TGM2. For example the accumulation of TGM2 in various cell and tissue types could be correlated to induction of apoptosis and tumor growth inhibition. In promonocytic cells for instance, TGM2 was reported to prime cells towards apoptosis due to the posttranslational polymerization of the tumor suppressor pRB [305]. Ectopically overexpression of human TGM2 in hamster fibrosarcoma cells suppresses their ability to form primary tumors [306]. Furthermore, observations have indicated, that TGM2 expression is enhanced by the methylxanthine Theophylline, which is a natural compound, able to induce apoptosis in tumor cells [307]. In hepatocellular carcinomas, TGM2 is predominantly described as a tumor suppressor. In chemically induced hepatocellular carcinomas, the cytosolic transamidase activity was reduced by 65 % when compared to normal livers [308,309]. However, there is no agreement whether the cancer protective function of TGM2 in liver cells is promoted by its transamidation activity. Hence, a transamidation-independent induction of apoptosis was described by Sheresta et al. whereby TGM2 translocates and accumulates in the nucleus [310]. On the other hand, it was also reported for hepatocellular carcinoma cells that the crosslinking activity of TGM2 is essential for the inactivation of the transcription factor Sp1 which leads to the inhibition of EGFR signaling and induction of caspase 3 expression and apoptosis [311]. Similar, it was shown in pancreatic cancer cells, that nuclear TGM2 activates apoptosis in a caspase-dependent manner [312]. In line with this, following reports describe a tumor suppressive function of TGM2 in CRC. The expression of TGM2 in the SW620 metastatic CRC cell line could be increased with 12-tetradecanoyl-phorbol-13-acetate (TPA), this resulted in an inhibition of cell growth and induction of apoptosis [313]. Additionally to this study, n-butyrate and propionate were shown to induce TGM2 expression in SW480 and WiDr CRC cell lines, which in turn induces growth suppression and cell death [314].

In contrast to the above mentioned studies, several publications describe a favorable function of TGM2 in tumor progression. In glioblastoma cells, TGM2 upregulation is linked to poor patient survival by enhancing EGFR signaling and promoting tumor growth [315]. Conversely to the reported function for TGM2 as an upstream modulator of EGFR signaling, in human breast cancer cells, TGM2 expression was found as a downstream event, induced by EGF signaling [316]. At the same time, it is also suggested that EGF promotes TGM2 expression indirectly, via a NF-κB dependent pathway in breast cancer [317]. In ovarian cancer,

extracellular TGM2 is described as an upstream regulator of noncanonical NF-κB signaling which leads to degradation of IκBα and processing of the precursor protein p100 into the active p52/RelB protein and specific activation of target genes [318,319]. Similar, elevated levels of TGM2 were recognized in mantel cell lymphoma in association with increased NF-κB expression and increased chemoresistance [320]. Aberrant regulation of NF-κB is also linked to CRC development and progression by regulating the survival of tumor cells and mediating chemoresistance [321–324]. However, there is little knowledge about the interplay of TGM2 and NF-κB in CRC and an interaction of TGM2 and NF-κB was not shown yet. In the present study, TGM2 cannot be confirmed as an upstream regulator of NF-κB, as depletion of TGM2 does not have any influence on NF-κB signaling in CRC. Probably, similar as reported by Li and coworkers [317], TGM2 acts as a potential downstream target of NF-κB induced by extracellular factors like EGF[250], which needs to be further investigated.

Tumor formation is a multistep process and one of these processes is the adaption to hypoxia. Several studies demonstrated that cellular stressors, such as oxidative stress and inflammation, enhance expression of TGM2 [148, 298]. In glioblastoma cells as well as in embryonic kidney cells HIF-1 activates TGM2 which in turn inhibits caspase 3 by forming insoluble aggregates and activates NF-κB. Thus, TGM2 promotes carcinogenesis and inhibits cell death under hypoxic conditions [148]. Conversely, TGM2 is also known to protect neuronal cells from cell death via negatively regulation of the HIF-1 transcriptional machinery by inhibiting the transcription of the pro-apoptotic gene Bnip3 [147]. Although altered TGM2 expression under hypoxic conditions and interaction with HIF-1 is well documented, in CRC a direct interplay between HIF-1α and TGM2 cannot be detected in the present work. Cultivation of CRC cells under hypoxic conditions altered the HIF-1α expression level, whereas the TGM2 protein expression is not influenced. The independency of HIF-1α and TGM2 signaling in CRC is further reinforced by the fact that TGM2 expression is not affected after HIF-1α knockdown with shRNAs under hypoxic conditions. Nevertheless, it cannot be excluded that TGM2 impinges HIF-1α downstream signaling on the transcriptional level without influencing its protein level. A possible mechanism could be an interaction of TGM2 with HIF-1β, building heterotrimers with HIF-1α, which in turn influences specific target gene transcription, as it was already described by Filliano et al. [147].

Neoblastic transformation is often accompanied by an ECM decomposition which augments cell motility and invasion [325]. Extracellular TGM2 contributes to the ECM network and promotes cell-substrate interaction [326]. However, based on its role in tumor formation and progression, it remains a controversial discussion whether matrix deposition by TGM2 inhibits tumor progression [327] or promotes tumor growth [328]. TGM2, located in the ECM can directly interact with integrins and acts as an integrin associated

coreceptor [329]. In line with this observation, Verma et al. reported an interplay of TGM2 with FAK which plays a critical role in integrin mediated signal transduction in pancreatic ductal adenocarcinomas (PDAC) [330]. Verma and coworkers showed that activation of FAK, induced by TGM2, results in downstream augmentation of PI3K/Akt pathways and thus may contribute to the development of drug resistance and invasive phenotypes in PDAC [227]. In most tumors including CRC, PI3K/Akt hyper-activation are observed at considerable frequency [331,332]. The potential involvement of TGM2 in Akt signaling was particularly intriguing because our laboratory could already show that Akt inhibition in CRC lead to decreased tumorigenicity [10]. Nonetheless, in the present work an interplay between TGM2 and Akt could not be confirmed. As Akt activation via TGM2 is described to be dependent on extracellular signals, this probably indicates an intrinsic TGM2 signaling pathway in CRC, which is independent of extracellular stimuli. Furthermore, by modulating tumor ECM, TGM2 is suggested to inhibit angiogenesis, tumor growth and invasion in mouse CT26 CRC cells[327,333]. This occurs by activation of latent matrix bound TGF β1 that consequently, increases matrix deposition and stabilization probably through a mechanism linked to the ability of TGM2 to interact with β3-integrins and therefore act as a co-receptor for FN. Through an increased cell adhesion, mediated by a TGM2-β3-integrin-FN interaction, cells show a reduced migratory ability [327,333]. However, the same group published completely opposite results in 2017 suggesting a correlation of TGM2 expression with CRC disease progression in vitro. Griffin and coworkers are proposing a key role of TGM2 in EMT due to an increased expression of mesenchymal markers upon ectopic induction of TGM2 expression in the primary CRC cell lines SW480 and RKO. The metastatic cell line SW620 was found to express TGM2 at higher levels compared to SW480 and RKO, indicating an advanced metastatic potential of cells, which express TGM2 at high levels. On the other hand, knockdown of TGM2 reduces mesenchymal marker expression. They propose an induction of EMT probably by enhancing a non-canonical ERK pathway which is activated by TGFβ [145]. Interestingly, others made different observations, reporting a lower level of TGM2 in SW620 in comparison to SW480 cells which is accompanied by a higher ability to metastasize [314,334]. Although Griffin and colleagues use an in vitro TGM2 knockdown model, they do not describe the effect of TGM2 inhibition on cell viability and proliferation nor do they show the migration ability of primary CRC cells after TGM2 induction. Cellura et al. answered the latter question by investigating whether TGM2 expression affects invasive behavior of CRC cells. Unlike Griffins group, they concluded that TGM2 expression correlates inversely with invasive behavior. Knockdown of TGM2 in SW480 cells led to an enhanced invasion and consequently, TGM2 overexpression in SW620 cells resulted in the opposite [335].

The current study demonstrates, by using RNA interference and CRISPR/Cas9 gene editing technologies that a significant reduction or a complete abolishment of TGM2 expression in SW480 and HCT116 CRC cells lead to immediate tumor expansion and cell death in vitro. These findings highly implicate a vital role of TGM2 in CRC cell survival. A more invasive phenotype cannot be observed upon TGM2 depletion. Furthermore, the presented data indicate an involvement of TGM2 in a pro-survival pathway that is independent of extracellular stimuli like ECM mediated signaling, growth factors and hypoxic stimuli. TGM2 is frequently described to be involved in PI3K/Akt signaling as well as in NF-κB and HIF1-α signaling pathways. Interestingly, in the present work, a direct link between these pathways cannot be detected neither by investigating protein expression levels under hypoxic conditions nor by genetic knockdown of potential interacting partners. In conclusion, the generated data of the present work strongly support a pro-survival role of TGM2 in CRC, not via Akt, HIF1-α or NF-κB, but rather via a p53-dependent pathway, which will be discussed in the following chapter.

5.4 The cross-linking function of TGM2-Iso 1 mediates apoptosis escape via modulating p53 signaling

As reported above, TGM2 was found as a pro-survival factor in CRC. This study is the first that systematically investigates the role of TGM2 isoforms and their enzymatic function in CRC. Even in the same cellular compartment, TGM2 function depends on its localization within the cell and on the activation and differentiation status of the cell. This could be shown by its pro-apoptotic function after translocation into the nucleus in hepatocellular carcinoma cells [310], or by the reported intracellular activation of latent TGM2 after perturbation in order to protect the cell from further damage [336,336]. This suggests a tight control mechanism on the transcriptional and translational, as well as on a functional level.

Since different RNA transcripts of TGM2 have been identified in addition to the constitutively spliced full-length TGM2 mRNA, it remains possible that the function of TGM2 in cancer may depend on the pattern of expression of alternative spliced TGM2 molecules, which may be capable of exerting different roles in the cell [152]. In neuroblastoma cells for instance, TGM2 Isoform 1 blocks cell differentiation whereas TGM2 Isoform 2 induces cell differentiation [155]. Full-length TGM2 isoform 1 was found to serve as a ligand for GPR56 in melanoma tumor cells which in turn is known to be involved in suppressing tumor growth and metastasis [154,215]. This study demonstrated that GPR56 binding to the C-terminal β-barrel of TGM2 mediates its inhibitory effect through forming GPR56-TGM2-isoform 1 heterodimers. However, the group

did not mention the role of TGM2-isoform 2 even though an opposite role of TGM2-isoform 2 may be hypothesized due to the lack of the C-terminal β-barrel. How versatile the role of TGM2 is, indicates the next study, implementing the complete opposite functions of TGM2 isoforms in mouse embryonic fibroblast and human breast cancer cells. Here, the authors describe a central role of isoform 2 in the induction of cell death, whereas the isoform 1 displays a protective role against serum deprivation-induced apoptosis [242]. A possible explanation for this contrary roles of TGM2 isoforms is provided by the recently published study of Shresta et al. which describes a nuclear export signal (NES) located in the second β-barrel of TGM2 positioned at the very C-terminus and a nuclear location signal (NLS) in the first β-barrel [310]. While full-length isoform 1 can shuttle between cytosol and nucleus, the truncated isoform 2 lacks NES thereby accumulates in the nucleus and promotes cell signaling, probably by acting as a transcription factor. This possible mechanism was also described in hepatocellular carcinoma cells, where it was shown that treatment with Ethanol (EtOH) or free fatty acids (FFA) provokes TGM2-isoform 2 formation and accumulation in the nucleus mediating cell death [337]. This data was reaffirmed by investigations of Datta et al., which go one step further and assign to all GTP-binding defective TGM2 isoforms, like isoform 2, an pro-apoptotic role [338]. These results are in contradiction to collected data in the current study, which show that in the presence of endogenous TGM2, ectopic overexpression of TGM2-isoform 2 does not have any effect on cell growth or viability. These data suggest a non-apoptotic role of this isoform in CRC. On the other hand, TGM2 isoform 2 is not able to prevent cells from cell death, after knockout of endogenous TGM2. The exact role of TGM2 isoform 2 in CRC remains elusive, but it seems that this isoform does not have any effect on pro- or anti-apoptotic cell fate decisions.

Cellulra et al. propose a control mechanism of TGM2 isoform 1 by miR-19 in CRC and its downregulation is linked to altered CRC invasiveness, whereas TGM2 isoform 2 is not inhibited by the microRNA because of the truncated 3'-end. Therefore, they ascribe a possible role to TGM2 isoform 2 in cell invasion. Interestingly, the investigators attribute the transamidase activity to a restricted invasive behavior of CRC [335]. The present work shows that, ectopic expression of TGM2 isoforms in CRC does not augment cell proliferation, although the invasive behavior was not investigated after overexpression. Here it is reported that only TGM2 isoform 1 was able to rescue TGM2 knockout cells from cell death. Therefore, TGM2 isoform 1 is proposed to participate in the propagation of signals that contribute to cell survival and favorable CRC tumor growth due to its ability to rescue TGM2 knockout cells from cell death. Nevertheless, how TGM2 might orchestrate cell motility, invasion and metastasis in CRC remains elusive and needs further investigations. It is conceivable that CRC cell fate decisions are subjected to fine-tuning mechanism

of TGM2 expression levels by several factors and that a distinct amount of TGM2 protein level and combination of TGM2 isoforms promote either cell death, survival or invasion.

TGM2 is a multifunctional enzyme with pleiotropic functions, but primarily its Ca^{2+}- dependent cross-linking activity and the different posttranslational modifications mediated by TGM2 are investigated in the literature [169]. In a human CRC model, the transamidase activity has been shown to cross-link caspase 3 into nonfunctional oligomers and therefore suppresses apoptosis. Interestingly, this was only seen in Bax-deficient HCT116 cells which are protected from Bax-promoted caspase 3 procession and apoptosis induction [339]. Nevertheless, the mechanism underlying the activation of TGM2 in these cells remains unknown. A similar effect was reported in malignant pleural mesothelioma cells [249]. Contradictory results were observed in neuroblastoma cells, where the cross-linking activity of TGM2 promotes induction of apoptosis [340]. In this work, caspase 3 expression was monitored upon TGM2 depletion, which is most likely activated by an intrinsic apoptosis pathway, due to unaffected levels of components of the extrinsic apoptosis pathway, FADD and Fas/TNFRSF6/CD95 [341]. In contrast to above mentioned publications, in the present work there was no evidence traceable of a direct interaction of TGM2 and caspase 3 in CRC. Although active caspase 3 expression is elevated after TGM2-knockdown in CRC, its activation and thus induction of programmed cell death are more likely a consequence of a signal-cascade provoked of further downstream events.

Interestingly, in several previous studies it was shown that TGM2 function was not dependent on its cross-linking activity and a transamidation inactive protein was able to promote either cell growth or apoptosis, depending on the investigated tumor entity [216,342]. Recent studies indicate a transamidase independent role of TGM2 in regulation of p53 signaling. In renal cell carcinoma (RCC) it was reported that inhibition of TGM2 leads to stabilization of p53 and consequently to apoptosis. In this case, TGM2 acts as an upstream regulator of p53 by inactivating its function by chaperoning p53 via binding to p62 to the autophagosome [342]. This is in complete contrast to the reported ability of TGM2 to act as a kinase and phosphorylate p53 on S15 or S20 residues and thus facilitate apoptosis[177]. On the other hand, in human mammary epithelial cells (HMECs) TGM2 is reported to be a downstream target of p53 and to prevent cells from oncogenic transformation [216]. In the course of this, p53 binds on a promoter element of TGM2 that is located 159 to 78 base pairs upstream of the start codon. Translated TGM2, together with CDKN1A plays a distinct tumor suppressive role in the p53 pathway by promoting, transamidase independently, autophagic flux through autophagic protein degradation and autolysosome clearance in vitro and in vivo [216].

P53 is known as a stress inducible transcription factor, which regulates a large number of diverse downstream genes to exert regulative function in multiple signaling processes [343]. In CRC, p53 mutation is thought to play an important role in disease progression and loss of p53 is a late event in adenoma-carcinoma progression [95,344]. Mutations of p53 occur in approximately 40 % to 50 % of patients with CRC [345] by missense mutations, and patients with mutant p53 gene are often resistant to current therapies, conferring poor prognosis [346]. Tumor-associated p53 mutation appears often not to be simple p53 wild type loss of function mutation; on the contrary, p53 mutation can provoke oncogenic functions [347]. Mechanisms underlying the oncogenic nature of mutant p53 include interaction or regulation of other proteins [348], which promote cancer progression. It is quite conceivable that in this context, TGM2 binding to p53 enhances neomorphic signaling of mutated p53. It could be possible that TGM2 acts as a molecular gatekeeper in CRC, either promoting tumorigenic transition by enhancing mutated p53 signaling or inhibiting p53 wild type signaling. Furthermore, it is possible, that TGM2 binding on p53 wild type is sufficient to deregulate p53 signaling. Deregulated growth control of tumor cells exerted by mutated p53 has been a field of intensive research [349]. Current work provides the evidence that p53-TGM2 protein-protein interaction sustains tumor cell survival and growth. Activation of p53 and subsequent induction of apoptosis in various CRC cells after TGM2 depletion suggest a possibility to sensitize CRC cells to cellular control mechanism and induce programmed cell death.

It is widely accepted that the role of TGM2 in tumorigenesis is context-dependent and the mechanism of TGM2 and p53 interplay may vary cell type-dependent, therefore it is essential to investigate TGM2 function in the coherence of every tumor entity. The present study is the first to investigate TGM2 and p53 regulation in CRC and in concordance to the studies in RCC cells it could be shown that TGM2 directly interacts with p53 and this leads to a deregulated p53 downstream-signaling. The current study showed that TGM2 activity maintained p-p53(S15) levels low, most likely through its transamidase activity. Thus, p53 signaling can be hindered to induce pro-apoptotic pathways such as activating caspase 3 in CRC. Therefore, TGM2 contributes to CRC oncogenic transformation.

Here it could be demonstrated that the TGM2 transamidase activity and protein expression is highly upregulated in primary CRC tissue. Coupled with the fact that it interferes with p53 and leads to CRC tumor progression, raises the interesting possibility to apply approaches that block TGM2 transamidase activity which may offer potential strategies for therapeutic intervention.

6. Publication Bibliography

1. Lee, C.S. & Park, H.H. Structural aspects of transglutaminase 2: functional, structural, and regulatory diversity. *Apoptosis : an international journal on programmed cell death* **22,** 1057–1068 (2017).
2. Ferlay, J. *et al.* Cancer incidence and mortality worldwide. Sources, methods and major patterns in GLOBOCAN 2012. *International journal of cancer* **136,** E359-86 (2015).
3. Robert Koch-Institut. *Bericht zum Krebsgeschehen in Deutschland* (Robert Koch-Institut, Berlin, 2016-).
4. *Krebs in Deutschland. 2005/2006 ; Häufigkeiten und Trends ; eine gemeinsame Veröffentlichung des Robert Koch-Instituts und der Gesellschaft der Epidemiologischen Krebsregister in Deutschland e.V.* 7th ed. (Robert Koch-Inst; GEKID, Berlin, Saarbrücken, 2010).
5. Tariq, K. & Ghias, K. Colorectal cancer carcinogenesis. A review of mechanisms. *Cancer biology & medicine* **13,** 120–135 (2016).
6. Loeb, L.A., Loeb, K.R. & Anderson, J.P. Multiple mutations and cancer. *Proceedings of the National Academy of Sciences of the United States of America* **100,** 776–781 (2003).
7. Reya, T., Morrison, S.J., Clarke, M.F. & Weissman, I.L. Stem cells, cancer, and cancer stem cells. *Nature* **414,** 105–111 (2001).
8. Ricci-Vitiani, L. *et al.* Identification and expansion of human colon-cancer-initiating cells. *Nature* **445,** 111–115 (2007).
9. O'Brien, C.A., Pollett, A., Gallinger, S. & Dick, J.E. A human colon cancer cell capable of initiating tumour growth in immunodeficient mice. *Nature* **445,** 106–110 (2007).
10. Malkomes, P. *et al.* Selective AKT Inhibition by MK-2206 Represses Colorectal Cancer-Initiating Stem Cells. *Annals of surgical oncology* **23,** 2849–2857 (2016).
11. Leblond, C.P. & WALKER, B.E. Renewal of cell populations. *Physiological reviews* **36,** 255–276 (1956).
12. van der Flier, L.G. & Clevers, H. Stem cells, self-renewal, and differentiation in the intestinal epithelium. *Annual review of physiology* **71,** 241–260 (2009).
13. Barker, N. Adult intestinal stem cells. Critical drivers of epithelial homeostasis and regeneration. *Nature reviews. Molecular cell biology* **15,** 19–33 (2014).
14. Bjerknes, M. & Cheng, H. Clonal analysis of mouse intestinal epithelial progenitors. *Gastroenterology* **116,** 7–14 (1999).
15. Cheng, H. Origin, differentiation and renewal of the four main epithelial cell types in the mouse small intestine. II. Mucous cells. *The American journal of anatomy* **141,** 481–501 (1974).
16. Cheng, H. Origin, differentiation and renewal of the four main epithelial cell types in the mouse small intestine. IV. Paneth cells. *The American journal of anatomy* **141,** 521–535 (1974).
17. Cheng, H. & Leblond, C.P. Origin, differentiation and renewal of the four main epithelial cell types in the mouse small intestine. I. Columnar cell. *The American journal of anatomy* **141,** 461–479 (1974).
18. Cheng, H. & Leblond, C.P. Origin, differentiation and renewal of the four main epithelial cell types in the mouse small intestine. III. Entero-endocrine cells. *The American journal of anatomy* **141,** 503–519 (1974).
19. Cheng, H. & Leblond, C.P. Origin, differentiation and renewal of the four main epithelial cell types in the mouse small intestine. V. Unitarian Theory of the origin of the four epithelial cell types. *The American journal of anatomy* **141,** 537–561 (1974).

20. Potten, C.S., Kovacs, L. & Hamilton, E. Continuous labelling studies on mouse skin and intestine. *Cell and tissue kinetics* **7,** 271–283 (1974).

21. Qiu, J.M., Roberts, S.A. & Potten, C.S. Cell migration in the small and large bowel shows a strong circadian rhythm. *Epithelial cell biology* **3,** 137–148 (1994).

22. Cairnie, A.B., Lamerton, L.F. & Steel, G.G. Cell proliferation studies in the intestinal epithelium of the rat. I. Determination of the kinetic parameters. *Experimental cell research* **39,** 528–538 (1965).

23. Barker, N. *et al.* Identification of stem cells in small intestine and colon by marker gene Lgr5. *Nature* **449,** 1003–1007 (2007).

24. Sangiorgi, E. & Capecchi, M.R. Bmi1 is expressed in vivo in intestinal stem cells. *Nature genetics* **40,** 915–920 (2008).

25. Wong, V.W.Y. *et al.* Lrig1 controls intestinal stem-cell homeostasis by negative regulation of ErbB signalling. *Nature cell biology* **14,** 401–408 (2012).

26. Powell, A.E. *et al.* The pan-ErbB negative regulator Lrig1 is an intestinal stem cell marker that functions as a tumor suppressor. *Cell* **149,** 146–158 (2012).

27. Takeda, N. *et al.* Interconversion between intestinal stem cell populations in distinct niches. *Science (New York, N.Y.)* **334,** 1420–1424 (2011).

28. Sato, T. *et al.* Single Lgr5 stem cells build crypt-villus structures in vitro without a mesenchymal niche. *Nature* **459,** 262–265 (2009).

29. Muñoz, J. *et al.* The Lgr5 intestinal stem cell signature. Robust expression of proposed quiescent '+4' cell markers. *The EMBO journal* **31,** 3079–3091 (2012).

30. Potten, C.S. *et al.* Identification of a putative intestinal stem cell and early lineage marker; musashi-1. *Differentiation* **71,** 28–41 (2003).

31. Zhu, L. *et al.* Prominin 1 marks intestinal stem cells that are susceptible to neoplastic transformation. *Nature* **457,** 603–607 (2009).

32. van der Flier, L.G., Haegebarth, A., Stange, D.E., van de Wetering, M. & Clevers, H. OLFM4 is a robust marker for stem cells in human intestine and marks a subset of colorectal cancer cells. *Gastroenterology* **137,** 15–17 (2009).

33. Schuijers, J., van der Flier, L.G., van Es, J. & Clevers, H. Robust cre-mediated recombination in small intestinal stem cells utilizing the olfm4 locus. *Stem cell reports* **3,** 234–241 (2014).

34. van der Flier, L.G. *et al.* Transcription factor achaete scute-like 2 controls intestinal stem cell fate. *Cell* **136,** 903–912 (2009).

35. Schuijers, J. *et al.* Ascl2 acts as an R-spondin/Wnt-responsive switch to control stemness in intestinal crypts. *Cell stem cell* **16,** 158–170 (2015).

36. Yan, K.S. *et al.* The intestinal stem cell markers Bmi1 and Lgr5 identify two functionally distinct populations. *Proceedings of the National Academy of Sciences of the United States of America* **109,** 466–471 (2012).

37. Ginjala, V. *et al.* BMI1 is recruited to DNA breaks and contributes to DNA damage-induced H2A ubiquitination and repair. *Molecular and cellular biology* **31,** 1972–1982 (2011).

38. Ismail, I.H., Andrin, C., McDonald, D. & Hendzel, M.J. BMI1-mediated histone ubiquitylation promotes DNA double-strand break repair. *The Journal of cell biology* **191,** 45–60 (2010).

39. Pan, M.-R., Peng, G., Hung, W.-C. & Lin, S.-Y. Monoubiquitination of H2AX protein regulates DNA damage response signaling. *The Journal of biological chemistry* **286,** 28599–28607 (2011).

40. Breault, D.T. *et al.* Generation of mTert-GFP mice as a model to identify and study tissue progenitor cells. *Proceedings of the National Academy of Sciences of the United States of America* **105,** 10420–10425 (2008).

41. Montgomery, R.K. *et al.* Mouse telomerase reverse transcriptase (mTert) expression marks slowly cycling intestinal stem cells. *Proceedings of the National Academy of Sciences of the United States of America* **108,** 179–184 (2011).

42. May, R. *et al.* Identification of a novel putative gastrointestinal stem cell and adenoma stem cell marker, doublecortin and CaM kinase-like-1, following radiation injury and in adenomatous polyposis coli/multiple intestinal neoplasia mice. *Stem cells (Dayton, Ohio)* **26,** 630–637 (2008).

43. Kusserow, A. *et al.* Unexpected complexity of the Wnt gene family in a sea anemone. *Nature* **433,** 156–160 (2005).

44. Bänziger, C. *et al.* Wntless, a conserved membrane protein dedicated to the secretion of Wnt proteins from signaling cells. *Cell* **125,** 509–522 (2006).

45. Bartscherer, K., Pelte, N., Ingelfinger, D. & Boutros, M. Secretion of Wnt ligands requires Evi, a conserved transmembrane protein. *Cell* **125,** 523–533 (2006).

46. Bhanot, P. *et al.* A new member of the frizzled family from Drosophila functions as a Wingless receptor. *Nature* **382,** 225–230 (1996).

47. Pinson, K.I., Brennan, J., Monkley, S., Avery, B.J. & Skarnes, W.C. An LDL-receptor-related protein mediates Wnt signalling in mice. *Nature* **407,** 535–538 (2000).

48. Tamai, K. *et al.* LDL-receptor-related proteins in Wnt signal transduction. *Nature* **407,** 530–535 (2000).

49. Davidson, G. *et al.* Casein kinase 1 gamma couples Wnt receptor activation to cytoplasmic signal transduction. *Nature* **438,** 867–872 (2005).

50. Zeng, X. *et al.* A dual-kinase mechanism for Wnt co-receptor phosphorylation and activation. *Nature* **438,** 873–877 (2005).

51. Price, M.A. CKI, there's more than one. Casein kinase I family members in Wnt and Hedgehog signaling. *Genes & development* **20,** 399–410 (2006).

52. Clevers, H. Wnt/beta-catenin signaling in development and disease. *Cell* **127,** 469–480 (2006).

53. Fevr, T., Robine, S., Louvard, D. & Huelsken, J. Wnt/beta-catenin is essential for intestinal homeostasis and maintenance of intestinal stem cells. *Molecular and cellular biology* **27,** 7551–7559 (2007).

54. Korinek, V. *et al.* Depletion of epithelial stem-cell compartments in the small intestine of mice lacking Tcf-4. *Nature genetics* **19,** 379–383 (1998).

55. van Es, J.H. *et al.* Dll1+ secretory progenitor cells revert to stem cells upon crypt damage. *Nature cell biology* **14,** 1099–1104 (2012).

56. Hao, H.-X. *et al.* ZNRF3 promotes Wnt receptor turnover in an R-spondin-sensitive manner. *Nature* **485,** 195–200 (2012).

57. Koo, B.-K. *et al.* Tumour suppressor RNF43 is a stem-cell E3 ligase that induces endocytosis of Wnt receptors. *Nature* **488,** 665–669 (2012).

58. Madison, B.B. *et al.* Epithelial hedgehog signals pattern the intestinal crypt-villus axis. *Development (Cambridge, England)* **132,** 279–289 (2005).

59. Kosinski, C. *et al.* Indian hedgehog regulates intestinal stem cell fate through epithelial-mesenchymal interactions during development. *Gastroenterology* **139,** 893–903 (2010).

60. van Dop, W.A. *et al.* Depletion of the colonic epithelial precursor cell compartment upon conditional activation of the hedgehog pathway. *Gastroenterology* **136,** 2195-2203.e1-7 (2009).

61. Lum, L. & Beachy, P.A. The Hedgehog response network. Sensors, switches, and routers. *Science (New York, N.Y.)* **304,** 1755–1759 (2004).

62. Katoh, Y. & Katoh, M. Hedgehog target genes. Mechanisms of carcinogenesis induced by aberrant hedgehog signaling activation. *Current molecular medicine* **9,** 873–886 (2009).

63. Roberts, D.J. *et al.* Sonic hedgehog is an endodermal signal inducing Bmp-4 and Hox genes during induction and regionalization of the chick hindgut. *Development (Cambridge, England)* **121,** 3163–3174 (1995).

64. Roberts, D.J., Smith, D.M., Goff, D.J. & Tabin, C.J. Epithelial-mesenchymal signaling during the regionalization of the chick gut. *Development (Cambridge, England)* **125,** 2791–2801 (1998).

65. Haramis, A.-P.G. *et al.* De novo crypt formation and juvenile polyposis on BMP inhibition in mouse intestine. *Science (New York, N.Y.)* **303,** 1684–1686 (2004).

66. He, X.C. *et al.* BMP signaling inhibits intestinal stem cell self-renewal through suppression of Wnt-beta-catenin signaling. *Nature genetics* **36,** 1117–1121 (2004).

67. Trentesaux, C. & Romagnolo, B. in *Intestinal stem cell niche,* edited by D. Bonnet (Elsevier/Academic Press, Cambridge, MA, 2018), pp. 1–40.

68. Schröder, N. & Gossler, A. Expression of Notch pathway components in fetal and adult mouse small intestine. *Gene expression patterns : GEP* **2,** 247–250 (2002).

69. VanDussen, K.L. *et al.* Notch signaling modulates proliferation and differentiation of intestinal crypt base columnar stem cells. *Development (Cambridge, England)* **139,** 488–497 (2012).

70. Sander, G.R. & Powell, B.C. Expression of notch receptors and ligands in the adult gut. *The journal of histochemistry and cytochemistry : official journal of the Histochemistry Society* **52,** 509–516 (2004).

71. Carulli, A.J. *et al.* Notch receptor regulation of intestinal stem cell homeostasis and crypt regeneration. *Developmental biology* **402,** 98–108 (2015).

72. Vogelstein, B. *et al.* Genetic alterations during colorectal-tumor development. *The New England journal of medicine* **319,** 525–532 (1988).

73. Popat, S., Hubner, R. & Houlston, R.S. Systematic review of microsatellite instability and colorectal cancer prognosis. *Journal of clinical oncology : official journal of the American Society of Clinical Oncology* **23,** 609–618 (2005).

74. Walther, A., Houlston, R. & Tomlinson, I. Association between chromosomal instability and prognosis in colorectal cancer. A meta-analysis. *Gut* **57,** 941–950 (2008).

75. Weisenberger, D.J. *et al.* CpG island methylator phenotype underlies sporadic microsatellite instability and is tightly associated with BRAF mutation in colorectal cancer. *Nature genetics* **38,** 787–793 (2006).

76. Aaltonen, L.A. *et al.* Clues to the pathogenesis of familial colorectal cancer. *Science (New York, N.Y.)* **260,** 812–816 (1993).

77. Ionov, Y., Peinado, M.A., Malkhosyan, S., Shibata, D. & Perucho, M. Ubiquitous somatic mutations in simple repeated sequences reveal a new mechanism for colonic carcinogenesis. *Nature* **363,** 558–561 (1993).

78. WHEELER, J.M.D. DNA mismatch repair genes and colorectal cancer. *Gut* **47,** 148–153 (2000).

79. Vilar, E. & Gruber, S.B. Microsatellite instability in colorectal cancer-the stable evidence. *Nature reviews. Clinical oncology* **7,** 153–162 (2010).

80. Jiricny, J. The multifaceted mismatch-repair system. *Nature Reviews Molecular Cell Biology* **7,** 335 (2006).

81. Aaltonen, L.A. *et al.* Incidence of hereditary nonpolyposis colorectal cancer and the feasibility of molecular screening for the disease. *The New England journal of medicine* **338,** 1481–1487 (1998).

82. Hendriks, Y.M.C. *et al.* Diagnostic Approach and Management of Lynch Syndrome (Hereditary Nonpolyposis Colorectal Carcinoma). A Guide for Clinicians. *CA: A Cancer Journal for Clinicians* **56,** 213–225 (2006).

83. Herman, J.G. *et al.* Incidence and functional consequences of hMLH1 promoter hypermethylation in colorectal carcinoma. *Proceedings of the National Academy of Sciences of the United States of America* **95,** 6870–6875 (1998).

84. Vogelstein, B. *et al.* Allelotype of colorectal carcinomas. *Science (New York, N.Y.)* **244,** 207–211 (1989).

85. Toyota, M. *et al.* CpG island methylator phenotype in colorectal cancer. *Proceedings of the National Academy of Sciences of the United States of America* **96,** 8681–8686 (1999).

86. Lao, V.V. & Grady, W.M. Epigenetics and colorectal cancer. *Nature reviews. Gastroenterology & hepatology* **8,** 686–700 (2011).

87. Gonzalez-Zulueta, M. *et al.* Methylation of the 5' CpG island of the p16/CDKN2 tumor suppressor gene in normal and transformed human tissues correlates with gene silencing. *Cancer research* **55,** 4531–4535 (1995).

88. Graff, J.R. *et al.* E-cadherin expression is silenced by DNA hypermethylation in human breast and prostate carcinomas. *Cancer research* **55,** 5195–5199 (1995).

89. Herman, J.G. *et al.* Silencing of the VHL tumor-suppressor gene by DNA methylation in renal carcinoma. *Proceedings of the National Academy of Sciences of the United States of America* **91,** 9700–9704 (1994).

90. Cunningham, J.M. *et al.* Hypermethylation of the hMLH1 promoter in colon cancer with microsatellite instability. *Cancer research* **58,** 3455–3460 (1998).

91. Schuebel, K.E. *et al.* Comparing the DNA hypermethylome with gene mutations in human colorectal cancer. *PLoS genetics* **3,** 1709–1723 (2007).

92. Sansregret, L., Vanhaesebroeck, B. & Swanton, C. Determinants and clinical implications of chromosomal instability in cancer. *Nature Reviews Clinical Oncology* **15,** 139 (2018).

93. Network, The Cancer Genome Atlas. Comprehensive molecular characterization of human colon and rectal cancer. *Nature* **487,** 330 (2012).

94. Lengauer, C., Kinzler, K.W. & Vogelstein, B. Genetic instability in colorectal cancers. *Nature* **386,** 623–627 (1997).

95. Fearon, E.R. & Vogelstein, B. A genetic model for colorectal tumorigenesis. *Cell* **61,** 759–767 (1990).

96. Cho, K.R. & Vogelstein, B. Genetic alterations in the adenoma--carcinoma sequence. *Cancer* **70,** 1727–1731 (1992).

97. Mann, B. *et al.* Target genes of beta-catenin-T cell-factor/lymphoid-enhancer-factor signaling in human colorectal carcinomas. *Proceedings of the National Academy of Sciences of the United States of America* **96,** 1603–1608 (1999).

98. Sjölander, A., Yamamoto, K., Huber, B.E. & Lapetina, E.G. Association of p21ras with phosphatidylinositol 3-kinase. *Proceedings of the National Academy of Sciences of the United States of America* **88,** 7908–7912 (1991).

99. Rodriguez-Viciana, P. *et al.* Phosphatidylinositol-3-OH kinase as a direct target of Ras. *Nature* **370,** 527–532 (1994).

100. Kyriakis, J.M. *et al.* Raf-1 activates MAP kinase-kinase. *Nature* **358,** 417 (1992).

101. Meylan, E. *et al.* Requirement for NF-kappaB signalling in a mouse model of lung adenocarcinoma. *Nature* **462,** 104–107 (2009).

102.   Vousden, K.H. & Prives, C. Blinded by the Light. The Growing Complexity of p53. *Cell* **137,** 413–431 (2009).

103.   Jenkins, L.M.M., Durell, S.R., Mazur, S.J. & Appella, E. p53 N-terminal phosphorylation. A defining layer of complex regulation. *Carcinogenesis* **33,** 1441–1449 (2012).

104.   Lane, D.P. Cancer. p53, guardian of the genome. *Nature* **358,** 15–16 (1992).

105.   Levine, A.J. p53, the Cellular Gatekeeper for Growth and Division. *Cell* **88,** 323–331 (1997).

106.   Bieging, K.T., Mello, S.S. & Attardi, L.D. Unravelling mechanisms of p53-mediated tumour suppression. *Nature Reviews Cancer* **14,** 359 (2014).

107.   Dittmer, D. *et al.* Gain of function mutations in p53. *Nature genetics* **4,** 42 (1993).

108.   Muller, P.A.J. & Vousden, K.H. Mutant p53 in cancer. New functions and therapeutic opportunities. *Cancer cell* **25,** 304–317 (2014).

109.   Davis, H. *et al.* Aberrant epithelial *GREM1* expression initiates colonic tumorigenesis from cells outside the stem cell niche. *Nature medicine* **21,** 62 (2015).

110.   Barker, N. *et al.* Crypt stem cells as the cells-of-origin of intestinal cancer. *Nature* **457,** 608–611 (2009).

111.   Shmelkov, S.V. *et al.* CD133 expression is not restricted to stem cells, and both CD133+ and CD133- metastatic colon cancer cells initiate tumors. *The Journal of clinical investigation* **118,** 2111–2120 (2008).

112.   Dalerba, P. *et al.* Phenotypic characterization of human colorectal cancer stem cells. *Proceedings of the National Academy of Sciences of the United States of America* **104,** 10158–10163 (2007).

113.   Ginestier, C. *et al.* ALDH1 is a marker of normal and malignant human mammary stem cells and a predictor of poor clinical outcome. *Cell stem cell* **1,** 555–567 (2007).

114.   Lugli, A. *et al.* Prognostic impact of the expression of putative cancer stem cell markers CD133, CD166, CD44s, EpCAM, and ALDH1 in colorectal cancer. *British Journal of Cancer* **103,** 382 (2010).

115.   Ziskin, J.L. *et al.* In situ validation of an intestinal stem cell signature in colorectal cancer. *Gut* **62,** 1012–1023 (2013).

116.   Dylla, S.J. *et al.* Colorectal cancer stem cells are enriched in xenogeneic tumors following chemotherapy. *PloS one* **3,** e2428 (2008).

117.   Lombardo, Y. *et al.* Bone morphogenetic protein 4 induces differentiation of colorectal cancer stem cells and increases their response to chemotherapy in mice. *Gastroenterology* **140,** 297–309 (2011).

118.   Lotti, F. *et al.* Chemotherapy activates cancer-associated fibroblasts to maintain colorectal cancer-initiating cells by IL-17A. *The Journal of experimental medicine* **210,** 2851–2872 (2013).

119.   Colak, S. *et al.* Decreased mitochondrial priming determines chemoresistance of colon cancer stem cells. *Cell death and differentiation* **21,** 1170–1177 (2014).

120.   Grenard, P., Bates, M.K. & Aeschlimann, D. Evolution of transglutaminase genes. Identification of a transglutaminase gene cluster on human chromosome 15q15. Structure of the gene encoding transglutaminase X and a novel gene family member, transglutaminase Z. *The Journal of biological chemistry* **276,** 33066–33078 (2001).

121.   SARKAR, N.K., CLARKE, D.D. & WAELSCH, H. An enzymically catalyzed incorporation of amines into proteins. *Biochimica et biophysica acta* **25,** 451–452 (1957).

122.   Lee, K.N. *et al.* Site-directed mutagenesis of human tissue transglutaminase. Cys-277 is essential for transglutaminase activity but not for GTPase activity. *Biochimica et biophysica acta* **1202,** 1–6 (1993).

123.   Folk, J.E. & Cole, P.W. Identification of a functional cysteine essential for the activity of guinea pig liver transglutaminase. *The Journal of biological chemistry* **241,** 3238–3240 (1966).

124.   Micanovic, R., Procyk, R., Lin, W. & Matsueda, G.R. Role of histidine 373 in the catalytic activity of coagulation factor XIII. *The Journal of biological chemistry* **269,** 9190–9194 (1994).

125.   Pedersen, L.C. *et al.* Transglutaminase factor XIII uses proteinase-like catalytic triad to crosslink macromolecules. *Protein science : a publication of the Protein Society* **3,** 1131–1135 (1994).

126.   Chen, J.S. & Mehta, K. Tissue transglutaminase. An enzyme with a split personality. *The international journal of biochemistry & cell biology* **31,** 817–836 (1999).

127.   Lorand, L., Velasco, P.T., Murthy, S.N., Wilson, J. & Parameswaran, K.N. Isolation of transglutaminase-reactive sequences from complex biological systems. A prominent lysine donor sequence in bovine lens. *Proceedings of the National Academy of Sciences of the United States of America* **89,** 11161–11163 (1992).

128.   Ahvazi, B., Kim, H.C., Kee, S.-H., Nemes, Z. & Steinert, P.M. Three-dimensional structure of the human transglutaminase 3 enzyme. Binding of calcium ions changes structure for activation. *The EMBO journal* **21,** 2055–2067 (2002).

129.   Casadio, R. *et al.* The structural basis for the regulation of tissue transglutaminase by calcium ions. *European journal of biochemistry* **262,** 672–679 (1999).

130.   Noguchi, K. *et al.* Crystal structure of red sea bream transglutaminase. *The Journal of biological chemistry* **276,** 12055–12059 (2001).

131.   Kim, H.C. *et al.* Crystallization and preliminary X-ray analysis of human transglutaminase 3 from zymogen to active form. *Journal of structural biology* **135,** 73–77 (2001).

132.   Liu, S., Cerione, R.A. & Clardy, J. Structural basis for the guanine nucleotide-binding activity of tissue transglutaminase and its regulation of transamidation activity. *Proceedings of the National Academy of Sciences of the United States of America* **99,** 2743–2747 (2002).

133.   Gaudry, C.A. *et al.* Cell surface localization of tissue transglutaminase is dependent on a fibronectin-binding site in its N-terminal beta-sandwich domain. *J. Biol. Chem.* **274,** 30707–30714 (1999).

134.   Hang, J., Zemskov, E.A., Lorand, L. & Belkin, A.M. Identification of a novel recognition sequence for fibronectin within the NH2-terminal beta-sandwich domain of tissue transglutaminase. *J. Biol. Chem.* **280,** 23675–23683 (2005).

135.   Lai, T.S., Slaughter, T.F., Koropchak, C.M., Haroon, Z.A. & Greenberg, C.S. C-terminal deletion of human tissue transglutaminase enhances magnesium-dependent GTP/ATPase activity. *The Journal of biological chemistry* **271,** 31191–31195 (1996).

136.   Kashiwagi, T. *et al.* Crystal structure of microbial transglutaminase from Streptoverticillium mobaraense. *J. Biol. Chem.* **277,** 44252–44260 (2002).

137.   Begg, G.E. *et al.* Mechanism of allosteric regulation of transglutaminase 2 by GTP. *Proceedings of the National Academy of Sciences of the United States of America* **103,** 19683–19688 (2006).

138.   Pinkas, D.M., Strop, P., Brunger, A.T. & Khosla, C. Transglutaminase 2 undergoes a large conformational change upon activation. *PLoS biology* **5,** e327 (2007).

139.   Murtaugh, M.P. *et al.* Induction of tissue transglutaminase in mouse peritoneal macrophages. *J. Biol. Chem.* **258,** 11074–11081 (1983).

140.   Piacentini, M. *et al.* In vivo and in vitro induction of 'tissue' transglutaminase in rat hepatocytes by retinoic acid. *Biochimica et biophysica acta* **1135,** 171–179 (1992).

141.   Singh, U.S. *et al.* Tissue Transglutaminase Mediates Activation of RhoA and MAP Kinase Pathways during Retinoic Acid-induced Neuronal Differentiation of SH-SY5Y Cells. *J. Biol. Chem.* **278,** 391–399 (2003).

142.   Mirza, A. *et al.* A role for tissue transglutaminase in hepatic injury and fibrogenesis, and its regulation by NF-kappaB. *The American journal of physiology* **272,** G281-8 (1997).

143.   Kuncio, G.S. *et al.* TNF-alpha modulates expression of the tissue transglutaminase gene in liver cells. *The American journal of physiology* **274,** G240-5 (1998).

144.   Ghanta, K.S. *et al.* MTA1 coregulation of transglutaminase 2 expression and function during inflammatory response. *The Journal of biological chemistry* **286,** 7132–7138 (2011).

145.   Ayinde, O., Wang, Z. & Griffin, M. Tissue transglutaminase induces Epithelial-Mesenchymal-Transition and the acquisition of stem cell like characteristics in colorectal cancer cells. *Oncotarget* **8,** 20025–20041 (2017).

146.   Zhang, H. & McCarty, N. Tampering with cancer chemoresistance by targeting the TGM2-IL6-autophagy regulatory network. *Autophagy* **13,** 627–628 (2017).

147.   Filiano, A.J., Bailey, C.D.C., Tucholski, J., Gundemir, S. & Johnson, G.V.W. Transglutaminase 2 protects against ischemic insult, interacts with HIF1beta, and attenuates HIF1 signaling. *FASEB journal : official publication of the Federation of American Societies for Experimental Biology* **22,** 2662–2675 (2008).

148.   Jang, G.-Y. *et al.* Transglutaminase 2 suppresses apoptosis by modulating caspase 3 and NF-kappaB activity in hypoxic tumor cells. *Oncogene* **29,** 356–367 (2010).

149.   Gundemir, S., Colak, G., Feola, J., Blouin, R. & Johnson, G.V.W. Transglutaminase 2 facilitates or ameliorates HIF signaling and ischemic cell death depending on its conformation and localization. *Biochimica et biophysica acta* **1833,** 1–10 (2013).

150.   Lu, S. & Davies, P.J.A. Regulation of the expression of the tissue transglutaminase gene by DNA methylation. *Proceedings of the National Academy of Sciences* **94,** 4692–4697 (1997).

151.   Modrek, B. & Lee, C. A genomic view of alternative splicing. *Nature genetics* **30,** 13–19 (2002).

152.   Phatak, V.M. *et al.* Expression of transglutaminase-2 isoforms in normal human tissues and cancer cell lines. Dysregulation of alternative splicing in cancer. *Amino acids* **44,** 33–44 (2013).

153.   Lai, T.-S. & Greenberg, C.S. TGM2 and implications for human disease. Role of alternative splicing. *Frontiers in bioscience (Landmark edition)* **18,** 504–519 (2013).

154.   Xu, L., Begum, S., Hearn, J.D. & Hynes, R.O. GPR56, an atypical G protein-coupled receptor, binds tissue transglutaminase, TG2, and inhibits melanoma tumor growth and metastasis. *Proceedings of the National Academy of Sciences of the United States of America* **103,** 9023–9028 (2006).

155.   Tee, A.E.L. *et al.* Opposing effects of two tissue transglutaminase protein isoforms in neuroblastoma cell differentiation. *The Journal of biological chemistry* **285,** 3561–3567 (2010).

156.   Lai, T.S., Bielawska, A., Peoples, K.A., Hannun, Y.A. & Greenberg, C.S. Sphingosylphosphocholine reduces the calcium ion requirement for activating tissue transglutaminase. *J. Biol. Chem.* **272,** 16295–16300 (1997).

157.   Lai, T.S. *et al.* Calcium regulates S-nitrosylation, denitrosylation, and activity of tissue transglutaminase. *Biochemistry* **40,** 4904–4910 (2001).

158.   Király, R. *et al.* Functional significance of five noncanonical Ca2+-binding sites of human transglutaminase 2 characterized by site-directed mutagenesis. *The FEBS journal* **276,** 7083–7096 (2009).

159.   Mariani, P. *et al.* Ligand-Induced Conformational Changes in Tissue Transglutaminase. Monte Carlo Analysis of Small-Angle Scattering Data. *Biophysical Journal* **78,** 3240–3251 (2000).

160. Stamnaes, J., Pinkas, D.M., Fleckenstein, B., Khosla, C. & Sollid, L.M. Redox regulation of transglutaminase 2 activity. *The Journal of biological chemistry* **285,** 25402–25409 (2010).

161. Siegel, M. *et al.* Extracellular transglutaminase 2 is catalytically inactive, but is transiently activated upon tissue injury. *PloS one* **3,** e1861 (2008).

162. Singh, U.S. & Cerione, R.A. Biochemical effects of retinoic acid on GTP-binding Protein/Transglutaminases in HeLa cells. Stimulation of GTP-binding and transglutaminase activity, membrane association, and phosphatidylinositol lipid turnover. *The Journal of biological chemistry* **271,** 27292–27298 (1996).

163. Singh, U.S., Kunar, M.T., Kao, Y.L. & Baker, K.M. Role of transglutaminase II in retinoic acid-induced activation of RhoA-associated kinase-2. *The EMBO journal* **20,** 2413–2423 (2001).

164. Scarpellini, A. *et al.* Heparan sulfate proteoglycans are receptors for the cell-surface trafficking and biological activity of transglutaminase-2. *The Journal of biological chemistry* **284,** 18411–18423 (2009).

165. Pisano, J.J., Finlayson, J.S. & Peyton, M.P. Cross-link in fibrin polymerized by factor 13. Epsilon-(gamma-glutamyl)lysine. *Science (New York, N.Y.)* **160,** 892–893 (1968).

166. Murthy, S.N., Wilson, J., Zhang, Y. & Lorand, L. Residue Gln-30 of human erythrocyte anion transporter is a prime site for reaction with intrinsic transglutaminase. *The Journal of biological chemistry* **269,** 22907–22911 (1994).

167. Parameswaran, K.N. *et al.* Hydrolysis of gamma:epsilon isopeptides by cytosolic transglutaminases and by coagulation factor XIIIa. *The Journal of biological chemistry* **272,** 10311–10317 (1997).

168. Nemes, Z., Marekov, L.N., Fesus, L. & Steinert, P.M. A novel function for transglutaminase 1. Attachment of long-chain -hydroxyceramides to involucrin by ester bond formation. *Proceedings of the National Academy of Sciences of the United States of America* **96,** 8402–8407 (1999).

169. Lorand, L. & Graham, R.M. Transglutaminases. Crosslinking enzymes with pleiotropic functions. *Nature Reviews Molecular Cell Biology* **4,** 140 (2003).

170. Achyuthan, K.E. & Greenberg, C.S. Identification of a guanosine triphosphate-binding site on guinea pig liver transglutaminase. Role of GTP and calcium ions in modulating activity. *The Journal of biological chemistry* **262,** 1901–1906 (1987).

171. Nakaoka, H. *et al.* Gh. A GTP-binding protein with transglutaminase activity and receptor signaling function. *Science (New York, N.Y.)* **264,** 1593–1596 (1994).

172. Feng, J.F., Readon, M., Yadav, S.P. & Im, M.J. Calreticulin down-regulates both GTP binding and transglutaminase activities of transglutaminase II. *Biochemistry* **38,** 10743–10749 (1999).

173. Lai, T.-S., Slaughter, T.F., Peoples, K.A., Hettasch, J.M. & Greenberg, C.S. Regulation of Human Tissue Transglutaminase Function by Magnesium-Nucleotide Complexes IDENTIFICATION OF DISTINCT BINDING SITES FOR Mg-GTP AND Mg-ATP. *J. Biol. Chem.* **273,** 1776–1781 (1998).

174. Nakano, Y., Forsprecher, J. & Kaartinen, M.T. Regulation of ATPase activity of transglutaminase 2 by MT1-MMP. Implications for mineralization of MC3T3-E1 osteoblast cultures. *Journal of cellular physiology* **223,** 260–269 (2010).

175. Belkin, A.M. *et al.* Matrix-dependent proteolysis of surface transglutaminase by membrane-type metalloproteinase regulates cancer cell adhesion and locomotion. *J. Biol. Chem.* **276,** 18415–18422 (2001).

176. Mishra, S., Melino, G. & Murphy, L.J. Transglutaminase 2 kinase activity facilitates protein kinase A-induced phosphorylation of retinoblastoma protein. *J. Biol. Chem.* **282,** 18108–18115 (2007).

177. Mishra, S. & Murphy, L.J. The p53 oncoprotein is a substrate for tissue transglutaminase kinase activity. *Biochemical and biophysical research communications* **339,** 726–730 (2006).

178. Mishra, S. & Murphy, L.J. Phosphorylation of transglutaminase 2 by PKA at Ser216 creates 14-3-3 binding sites. *Biochemical and biophysical research communications* **347,** 1166–1170 (2006).

179. Peng, X. *et al.* Interaction of tissue transglutaminase with nuclear transport protein importin-α3. *FEBS letters* **446,** 35–39 (1999).

180. Hanahan, D. & Weinberg, R.A. The hallmarks of cancer. *Cell* **100,** 57–70 (2000).

181. Hanahan, D. & Weinberg, R.A. Hallmarks of cancer. The next generation. *Cell* **144,** 646–674 (2011).

182. Evan, G.I. & Vousden, K.H. Proliferation, cell cycle and apoptosis in cancer. *Nature* **411,** 342–348 (2001).

183. Mishra, S. & Murphy, L.J. Tissue transglutaminase has intrinsic kinase activity. Identification of transglutaminase 2 as an insulin-like growth factor-binding protein-3 kinase. *The Journal of biological chemistry* **279,** 23863–23868 (2004).

184. Yi, S.-J., Groffen, J. & Heisterkamp, N. Transglutaminase 2 regulates the GTPase-activating activity of Bcr. *The Journal of biological chemistry* **284,** 35645–35651 (2009).

185. Trahey, M. & McCormick, F. A cytoplasmic protein stimulates normal N-ras p21 GTPase, but does not affect oncogenic mutants. *Science (New York, N.Y.)* **238,** 542–545 (1987).

186. Baek, K.J., Kang, S., Damron, D. & Im, M. Phospholipase Cdelta1 is a guanine nucleotide exchanging factor for transglutaminase II (Galpha h) and promotes alpha 1B-adrenoreceptor-mediated GTP binding and intracellular calcium release. *The Journal of biological chemistry* **276,** 5591–5597 (2001).

187. Park, E.S. *et al.* Phospholipase C-delta1 and oxytocin receptor signalling. Evidence of its role as an effector. *Biochemical Journal* **331,** 283–289 (1998).

188. Feng, J.F., Rhee, S.G. & Im, M.J. Evidence that phospholipase delta1 is the effector in the Gh (transglutaminase II)-mediated signaling. *The Journal of biological chemistry* **271,** 16451–16454 (1996).

189. Kang, S.K., Kim, D.K., Damron, D.S., Baek, K.J. & Im, M.-J. Modulation of intracellular Ca2+ via α1B-adrenoreceptor signaling molecules, Gαh (transglutaminase II) and phospholipase C-δ1. *Biochemical and biophysical research communications* **293,** 383–390 (2002).

190. Wu, J. *et al.* Roles of tissue transglutaminase in ethanol-induced inhibition of hepatocyte proliferation and alpha 1-adrenergic signal transduction. *The Journal of biological chemistry* **275,** 22213–22219 (2000).

191. Lee, K.-H. *et al.* Calreticulin inhibits the MEK1,2-ERK1,2 pathway in α1-adrenergic receptor/Gh-stimulated hypertrophy of neonatal rat cardiomyocytes. *The Journal of Steroid Biochemistry and Molecular Biology* **84,** 101–107 (2003).

192. Coussens, L.M. & Werb, Z. Inflammation and cancer. *Nature* **420,** 860–867 (2002).

193. Mantovani, A., Allavena, P., Sica, A. & Balkwill, F. Cancer-related inflammation. *Nature* **454,** 436–444 (2008).

194. Bernstein, C.N., Blanchard, J.F., Kliewer, E. & Wajda, A. Cancer risk in patients with inflammatory bowel disease. *Cancer* **91,** 854–862 (2001).

195. Grivennikov, S.I., Greten, F.R. & Karin, M. Immunity, Inflammation, and Cancer. *Cell* **140,** 883–899 (2010).

196.   Kim, Y. *et al.* Transglutaminase II interacts with rac1, regulates production of reactive oxygen species, expression of snail, secretion of Th2 cytokines and mediates in vitro and in vivo allergic inflammation. *Molecular immunology* **47,** 1010–1022 (2010).

197.   Jacobs, M.D. & Harrison, S.C. Structure of an IκBα/NF-κB Complex. *Cell* **95,** 749–758 (1998).

198.   Mann, A.P. *et al.* Overexpression of tissue transglutaminase leads to constitutive activation of nuclear factor-kappaB in cancer cells. Delineation of a novel pathway. *Cancer research* **66,** 8788–8795 (2006).

199.   Barsigian, C., Stern, A.M. & Martinez, J. Tissue (type II) transglutaminase covalently incorporates itself, fibrinogen, or fibronectin into high molecular weight complexes on the extracellular surface of isolated hepatocytes. Use of 2-(2-oxopropyl)thio imidazolium derivatives as cellular transglutaminase inactivators. *J. Biol. Chem.* **266,** 22501–22509 (1991).

200.   Forsprecher, J., Wang, Z., Nelea, V. & Kaartinen, M.T. Enhanced osteoblast adhesion on transglutaminase 2-crosslinked fibronectin. *Amino acids* **36,** 747 (2008).

201.   Barsigian, C., Fellin, F.M., Jain, A. & Martinez, J. Dissociation of fibrinogen and fibronectin binding from transglutaminase-mediated cross-linking at the hepatocyte surface. *J. Biol. Chem.* **263,** 14015–14022 (1988).

202.   Aeschlimann, D. & Paulsson, M. Cross-linking of laminin-nidogen complexes by tissue transglutaminase. A novel mechanism for basement membrane stabilization. *J. Biol. Chem.* **266,** 15308–15317 (1991).

203.   Verma, A. *et al.* Therapeutic significance of elevated tissue transglutaminase expression in pancreatic cancer. *Clinical cancer research : an official journal of the American Association for Cancer Research* **14,** 2476–2483 (2008).

204.   Craene, B. de & Berx, G. Regulatory networks defining EMT during cancer initiation and progression. *Nature reviews. Cancer* **13,** 97–110 (2013).

205.   Herz, J. & Strickland, D.K. LRP. A multifunctional scavenger and signaling receptor. *The Journal of clinical investigation* **108,** 779–784 (2001).

206.   Zemskov, E.A., Mikhailenko, I., Strickland, D.K. & Belkin, A.M. Cell-surface transglutaminase undergoes internalization and lysosomal degradation. An essential role for LRP1. *Journal of cell science* **120,** 3188–3199 (2007).

207.   Zhong, H. *et al.* Modulation of hypoxia-inducible factor 1alpha expression by the epidermal growth factor/phosphatidylinositol 3-kinase/PTEN/AKT/FRAP pathway in human prostate cancer cells: implications for tumor angiogenesis and therapeutics. *Cancer research* **60,** 1541–1545 (2000).

208.   Kim, D.-S. *et al.* Cancer cells promote survival through depletion of the von Hippel-Lindau tumor suppressor by protein crosslinking. *Oncogene* **30,** 4780–4790 (2011).

209.   Faye, C. *et al.* Transglutaminase-2. A new endostatin partner in the extracellular matrix of endothelial cells. *The Biochemical journal* **427,** 467–475 (2010).

210.   Zemskov, E.A. *et al.* Regulation of platelet-derived growth factor receptor function by integrin-associated cell surface transglutaminase. *J. Biol. Chem.* **284,** 16693–16703 (2009).

211.   Min, B. *et al.* CHIP-mediated degradation of transglutaminase 2 negatively regulates tumor growth and angiogenesis in renal cancer. *Oncogene* **35,** 3718 (2016).

212.   Lewis, T.E. *et al.* Tissue transglutaminase interacts with protein kinase A anchor protein 13 in prostate cancer. *Urologic oncology* **23,** 407–412 (2005).

213.   Aoudjit, F. & Vuori, K. Integrin Signaling in Cancer Cell Survival and Chemoresistance. *Chemotherapy Research and Practice* **2012** (2012).

214. Verma, A. & Mehta, K. Tissue transglutaminase-mediated chemoresistance in cancer cells. *Drug resistance updates : reviews and commentaries in antimicrobial and anticancer chemotherapy* **10,** 144–151 (2007).

215. Xu, L. & Hynes, R.O. GPR56 and TG2. Possible roles in suppression of tumor growth by the microenvironment. *Cell cycle (Georgetown, Tex.)* **6,** 160–165 (2007).

216. Yeo, S.Y. *et al.* Transglutaminase 2 contributes to a TP53-induced autophagy program to prevent oncogenic transformation. *eLife* **5,** e07101 (2016).

217. Yee, J.K., Friedmann, T. & Burns, J.C. Generation of high-titer pseudotyped retroviral vectors with very broad host range. *Methods in cell biology* **43 Pt A,** 99–112 (1994).

218. Zufferey, R., Nagy, D., Mandel, R.J., Naldini, L. & Trono, D. Multiply attenuated lentiviral vector achieves efficient gene delivery in vivo. *Nature biotechnology* **15,** 871–875 (1997).

219. Dull, T. *et al.* A Third-Generation Lentivirus Vector with a Conditional Packaging System. *Journal of Virology* **72,** 8463–8471 (1998).

220. Schambach, A. *et al.* Lentiviral vectors pseudotyped with murine ecotropic envelope: increased biosafety and convenience in preclinical research. *Experimental hematology* **34,** 588–592 (2006).

221. Sürün, D. *et al.* High Efficiency Gene Correction in Hematopoietic Cells by Donor-Template-Free CRISPR/Cas9 Genome Editing. *Molecular Therapy. Nucleic Acids* **10,** 1–8 (2017).

222. Subramanian, A. *et al.* Gene set enrichment analysis: a knowledge-based approach for interpreting genome-wide expression profiles. *Proceedings of the National Academy of Sciences* **102,** 15545–15550 (2005).

223. Kreso, A. & O'Brien, C.A. Colon cancer stem cells. *Current protocols in stem cell biology* **Chapter 3,** Unit 3.1 (2008).

224. Oellerich, T. *et al.* The B-cell antigen receptor signals through a preformed transducer module of SLP65 and CIN85. *The EMBO journal* **30,** 3620–3634 (2011).

225. Shevchenko, A., Tomas, H., Havlis, J., Olsen, J.V. & Mann, M. In-gel digestion for mass spectrometric characterization of proteins and proteomes. *Nature protocols* **1,** 2856–2860 (2006).

226. Yin, A.H. *et al.* AC133, a novel marker for human hematopoietic stem and progenitor cells. *Blood* **90,** 5002–5012 (1997).

227. Verma, A. *et al.* Increased expression of tissue transglutaminase in pancreatic ductal adenocarcinoma and its implications in drug resistance and metastasis. *Cancer research* **66,** 10525–10533 (2006).

228. Zhang, H., Chen, Z., Miranda, R.N., Medeiros, L.J. & McCarty, N. TG2 and NF-κB Signaling Coordinates the Survival of Mantle Cell Lymphoma Cells via IL6-Mediated Autophagy. *Cancer research* **76,** 6410–6423 (2016).

229. Agnihotri, N., Kumar, S. & Mehta, K. Tissue transglutaminase as a central mediator in inflammation-induced progression of breast cancer. *Breast cancer research : BCR* **15,** 202 (2013).

230. Karpuj, M.V. *et al.* Transglutaminase aggregates huntingtin into nonamyloidogenic polymers, and its enzymatic activity increases in Huntington's disease brain nuclei. *Proceedings of the National Academy of Sciences of the United States of America* **96,** 7388–7393 (1999).

231. Litvinov, S.V. *et al.* Epithelial cell adhesion molecule (Ep-CAM) modulates cell-cell interactions mediated by classic cadherins. *The Journal of cell biology* **139,** 1337–1348 (1997).

232. Mehta, K., Kumar, A. & Im Kim, H. Transglutaminase 2. A multi-tasking protein in the complex circuitry of inflammation and cancer. *Biochemical pharmacology* **80,** 1921–1929 (2010).

233. Boutros, M. & Ahringer, J. The art and design of genetic screens. RNA interference. *Nature reviews. Genetics* **9,** 554–566 (2008).

234.   Boyce, S.T. & Ham, R.G. Calcium-regulated differentiation of normal human epidermal keratinocytes in chemically defined clonal culture and serum-free serial culture. *The Journal of investigative dermatology* **81,** 33s-40s (1983).

235.   Tan, S.H., Bertulfo, F.C. & Sanda, T. Leukemia-Initiating Cells in T-Cell Acute Lymphoblastic Leukemia. *Frontiers in Oncology* **7** (2017).

236.   Pastrana, E., Silva-Vargas, V. & Doetsch, F. Eyes wide open. A critical review of sphere-formation as an assay for stem cells. *Cell stem cell* **8,** 486–498 (2011).

237.   Lai, T.-S. *et al.* Identification of chemical inhibitors to human tissue transglutaminase by screening existing drug libraries. *Chemistry & biology* **15,** 969–978 (2008).

238.   Case, A. & Stein, R.L. Kinetic analysis of the interaction of tissue transglutaminase with a nonpeptidic slow-binding inhibitor. *Biochemistry* **46,** 1106–1115 (2007).

239.   Denayer, T., Stöhr, T. & van Roy, M. Animal models in translational medicine: Validation and prediction. *European Journal of Molecular & Clinical Medicine* **2,** 5 (2017).

240.   Dr. Falk Pharma und Zedira. *Dr. Falk Pharma und Zedira geben den Start der Phase 2a Wirksamkeitsstudie für ZED1227 zur Zöliakie* (2018).

241.   UCB Biopharma S.P.R.L. *A First-In-Human Study With a Single Ascending Dose of UCB7858 in Healthy Volunteers. Available at* https://www.clinicaltrials.gov/ct2/show/record/NCT02879877?term=tgm2&rank=3 (2018).

242.   Antonyak, M.A. *et al.* Two isoforms of tissue transglutaminase mediate opposing cellular fates. *Proceedings of the National Academy of Sciences of the United States of America* **103,** 18609–18614 (2006).

243.   Tatsukawa, H., Furutani, Y., Hitomi, K. & Kojima, S. Transglutaminase 2 has opposing roles in the regulation of cellular functions as well as cell growth and death. *Cell death & disease* **7,** e2244 (2016).

244.   Hitomi, K., Ikura, K. & Maki, M. GTP, an inhibitor of transglutaminases, is hydrolyzed by tissue-type transglutaminase (TGase 2) but not by epidermal-type transglutaminase (TGase 3). *Bioscience, biotechnology, and biochemistry* **64,** 657–659 (2000).

245.   Lai, T.-S., Liu, Y., Li, W. & Greenberg, C.S. Identification of two GTP-independent alternatively spliced forms of tissue transglutaminase in human leukocytes, vascular smooth muscle, and endothelial cells. *FASEB journal : official publication of the Federation of American Societies for Experimental Biology* **21,** 4131–4143 (2007).

246.   Vermes, I., Haanen, C., Steffens-Nakken, H. & Reutelingsperger, C. A novel assay for apoptosis. Flow cytometric detection of phosphatidylserine expression on early apoptotic cells using fluorescein labelled Annexin V. *Journal of immunological methods* **184,** 39–51 (1995).

247.   Rieger, M.A., Hoppe, P.S., Smejkal, B.M., Eitelhuber, A.C. & Schroeder, T. Hematopoietic cytokines can instruct lineage choice. *Science (New York, N.Y.)* **325,** 217–218 (2009).

248.   Schroeder, T. Tracking hematopoiesis at the single cell level. *Annals of the New York Academy of Sciences* **1044,** 201–209 (2005).

249.   Zonca, S. *et al.* Tissue transglutaminase (TG2) enables survival of human malignant pleural mesothelioma cells in hypoxia. *Cell death & disease* **8,** e2592 (2017).

250.   Li, Q. & Verma, I.M. NF-kappaB regulation in the immune system. *Nature reviews. Immunology* **2,** 725–734 (2002).

251.   Cairns, R.A., Harris, I.S. & Mak, T.W. Regulation of cancer cell metabolism. *Nature Reviews Cancer* **11,** 85 (2011).

252.   Kumar, S. & Mehta, K. Tissue transglutaminase constitutively activates HIF-1α promoter and nuclear factor-κB via a non-canonical pathway. *PloS one* **7,** e49321 (2012).

253.   Earnshaw, W.C., Martins, L.M. & Kaufmann, S.H. Mammalian caspases. Structure, activation, substrates, and functions during apoptosis. *Annual review of biochemistry* **68,** 383–424 (1999).

254.   Kastan, M.B., Onyekwere, O., Sidransky, D., Vogelstein, B. & Craig, R.W. Participation of p53 protein in the cellular response to DNA damage. *Cancer research* **51,** 6304–6311 (1991).

255.   Rochette, P.J., Bastien, N., Lavoie, J., Guérin, S.L. & Drouin, R. SW480, a p53 double-mutant cell line retains proficiency for some p53 functions. *Journal of molecular biology* **352,** 44–57 (2005).

256.   Waldman, T., Kinzler, K.W. & Vogelstein, B. p21 is necessary for the p53-mediated G1 arrest in human cancer cells. *Cancer research* **55,** 5187–5190 (1995).

257.   Söderberg, O. *et al.* Direct observation of individual endogenous protein complexes in situ by proximity ligation. *Nature methods* **3,** 995–1000 (2006).

258.   Siegel, R.L., Miller, K.D. & Jemal, A. Cancer statistics, 2018. *CA: A Cancer Journal for Clinicians* **68,** 7–30 (2018).

259.   Lee, K.-C., Ou, Y.-C., Hu, W.-H., Liu, C.-C. & Chen, H.-H. Meta-analysis of outcomes of patients with stage IV colorectal cancer managed with chemotherapy/radiochemotherapy with and without primary tumor resection. *OncoTargets and therapy* **9,** 7059–7069 (2016).

260.   Barrier, A. *et al.* Stage II colon cancer prognosis prediction by tumor gene expression profiling. *Journal of clinical oncology : official journal of the American Society of Clinical Oncology* **24,** 4685–4691 (2006).

261.   O'Connor, E.S. *et al.* Adjuvant chemotherapy for stage II colon cancer with poor prognostic features. *Journal of clinical oncology : official journal of the American Society of Clinical Oncology* **29,** 3381–3388 (2011).

262.   Hurwitz, H. *et al.* Bevacizumab plus irinotecan, fluorouracil, and leucovorin for metastatic colorectal cancer. *The New England journal of medicine* **350,** 2335–2342 (2004).

263.   Emmanouilides, C. *et al.* Front-line bevacizumab in combination with oxaliplatin, leucovorin and 5-fluorouracil (FOLFOX) in patients with metastatic colorectal cancer. A multicenter phase II study. *BMC cancer* **7,** 91 (2007).

264.   Douillard, J.-Y. *et al.* Randomized, phase III trial of panitumumab with infusional fluorouracil, leucovorin, and oxaliplatin (FOLFOX4) versus FOLFOX4 alone as first-line treatment in patients with previously untreated metastatic colorectal cancer. The PRIME study. *Journal of clinical oncology : official journal of the American Society of Clinical Oncology* **28,** 4697–4705 (2010).

265.   Martín-Martorell, P. *et al.* Biweekly cetuximab and irinotecan in advanced colorectal cancer patients progressing after at least one previous line of chemotherapy. Results of a phase II single institution trial. *British Journal of Cancer* **99,** 455–458 (2008).

266.   Spratlin, J.L. *et al.* Phase I pharmacologic and biologic study of ramucirumab (IMC-1121B), a fully human immunoglobulin G1 monoclonal antibody targeting the vascular endothelial growth factor receptor-2. *Journal of clinical oncology : official journal of the American Society of Clinical Oncology* **28,** 780–787 (2010).

267.   Lockhart, A.C. *et al.* Phase I study of intravenous vascular endothelial growth factor trap, aflibercept, in patients with advanced solid tumors. *Journal of clinical oncology : official journal of the American Society of Clinical Oncology* **28,** 207–214 (2010).

268.   Mody, K., Baldeo, C. & Bekaii-Saab, T. Antiangiogenic Therapy in Colorectal Cancer. *Cancer journal (Sudbury, Mass.)* **24,** 165–170 (2018).

269.   Pardoll, D.M. The blockade of immune checkpoints in cancer immunotherapy. *Nature Reviews Cancer* **12,** 252 (2012).

270.   National Comprehensive Cancer Network. *NCCN Guideline with NCCN Evidence Blocks™ - Colon Cancer Version 2.2018. Available at*
https://www.nccn.org/store/login/login.aspx?ReturnURL=https://www.nccn.org/professionals/physician_gls/pdf/colon_blocks.pdf (2018).

271.   He, J., Hu, Y., Hu, M. & Li, B. Development of PD-1/PD-L1 Pathway in Tumor Immune Microenvironment and Treatment for Non-Small Cell Lung Cancer. *Scientific Reports* **5,** 13110.

272.   Todaro, M., Francipane, M.G., Medema, J.P. & Stassi, G. Colon cancer stem cells: promise of targeted therapy. *Gastroenterology* **138,** 2151–2162 (2010).

273.   Petak, I., Tillman, D.M. & Houghton, J.A. p53 dependence of Fas induction and acute apoptosis in response to 5-fluorouracil-leucovorin in human colon carcinoma cell lines. *Clinical cancer research : an official journal of the American Association for Cancer Research* **6,** 4432–4441 (2000).

274.   Longley, D.B. *et al.* The role of thymidylate synthase induction in modulating p53-regulated gene expression in response to 5-fluorouracil and antifolates. *Cancer research* **62,** 2644–2649 (2002).

275.   Ahnen, D.J. *et al.* Ki-ras mutation and p53 overexpression predict the clinical behavior of colorectal cancer. A Southwest Oncology Group study. *Cancer research* **58,** 1149–1158 (1998).

276.   Ishiguro, T. *et al.* Tumor-derived spheroids. Relevance to cancer stem cells and clinical applications. *Cancer science* **108,** 283–289 (2017).

277.   Keillor, J.W. & Apperley, K.Y.P. Transglutaminase inhibitors: a patent review. *Expert opinion on therapeutic patents* **26,** 49–63 (2016).

278.   Iismaa, S.E., Mearns, B.M., Lorand, L. & Graham, R.M. Transglutaminases and disease: lessons from genetically engineered mouse models and inherited disorders. *Physiological reviews* **89,** 991–1023 (2009).

279.   Sousa e Melo, F. de *et al.* Poor-prognosis colon cancer is defined by a molecularly distinct subtype and develops from serrated precursor lesions. *Nature medicine* **19,** 614–618 (2013).

280.   Wang, Y. *et al.* Gene expression profiles and molecular markers to predict recurrence of Dukes' B colon cancer. *Journal of clinical oncology : official journal of the American Society of Clinical Oncology* **22,** 1564–1571 (2004).

281.   Markowitz, S.D. & Bertagnolli, M.M. Molecular origins of cancer. Molecular basis of colorectal cancer. *The New England journal of medicine* **361,** 2449–2460 (2009).

282.   André, T. *et al.* Oxaliplatin, fluorouracil, and leucovorin as adjuvant treatment for colon cancer. *The New England journal of medicine* **350,** 2343–2351 (2004).

283.   Group, Q.C. Adjuvant chemotherapy versus observation in patients with colorectal cancer. A randomised study. *The Lancet* **370,** 2020–2029 (2007).

284.   Benson, A.B. New approaches to the adjuvant therapy of colon cancer. *The oncologist* **11,** 973–980 (2006).

285.   Edge, S.B. & Compton, C.C. The American Joint Committee on Cancer. The 7th edition of the AJCC cancer staging manual and the future of TNM. *Annals of surgical oncology* **17,** 1471–1474 (2010).

286.   Griffin, M.R., Bergstralh, E.J., Coffey, R.J., Beart, R.W. & Melton, L.J. Predictors of survival after curative resection of carcinoma of the colon and rectum. *Cancer* **60,** 2318–2324 (1987).

287.   Wiggers, T., Arends, J.W. & Volovics, A. Regression analysis of prognostic factors in colorectal cancer after curative resections. *Diseases of the colon and rectum* **31,** 33–41 (1988).

288.   Betge, J. *et al.* Intramural and extramural vascular invasion in colorectal cancer. Prognostic significance and quality of pathology reporting. *Cancer* **118,** 628–638 (2012).

289.   Wei, J.T., Miller, E.A., Woosley, J.T., Martin, C.F. & Sandler, R.S. Quality of colon carcinoma pathology reporting. A process of care study. *Cancer* **100,** 1262–1267 (2004).

290.   Miyoshi, N. *et al.* TGM2 is a novel marker for prognosis and therapeutic target in colorectal cancer. *Annals of surgical oncology* **17,** 967–972 (2010).

291.   Fernández-Aceñero, M.J., Torres, S., Garcia-Palmero, I., Díaz Del Arco, C. & Casal, J.I. Prognostic role of tissue transglutaminase 2 in colon carcinoma. *Virchows Archiv : an international journal of pathology* **469,** 611–619 (2016).

292.   Dunne, P.D. *et al.* Challenging the Cancer Molecular Stratification Dogma. Intratumoral Heterogeneity Undermines Consensus Molecular Subtypes and Potential Diagnostic Value in Colorectal Cancer. *Clinical cancer research : an official journal of the American Association for Cancer Research* **22,** 4095–4104 (2016).

293.   Dunne, P.D. *et al.* Cancer-cell intrinsic gene expression signatures overcome intratumoural heterogeneity bias in colorectal cancer patient classification. *Nature Communications* **8,** 15657 (2017).

294.   Maman, S. & Witz, I.P. A history of exploring cancer in context. *Nature Reviews Cancer* **18,** 359 (2018).

295.   Kuo, T.-F., Tatsukawa, H. & Kojima, S. New insights into the functions and localization of nuclear transglutaminase 2. *The FEBS journal* **278,** 4756–4767 (2011).

296.   Hernandez-Fernaud, J.R. *et al.* Secreted CLIC3 drives cancer progression through its glutathione-dependent oxidoreductase activity. *Nature Communications* **8,** 14206 (2017).

297.   Ai, L. *et al.* The transglutaminase 2 gene (TGM2), a potential molecular marker for chemotherapeutic drug sensitivity, is epigenetically silenced in breast cancer. *Carcinogenesis* **29,** 510–518 (2008).

298.   Mehta, K. & Han, A. Tissue Transglutaminase (TG2)-Induced Inflammation in Initiation, Progression, and Pathogenesis of Pancreatic Cancer. *Cancers* **3,** 897–912 (2011).

299.   Telci, D. & Griffin, M. Tissue transglutaminase (TG2)--a wound response enzyme. *Frontiers in bioscience : a journal and virtual library* **11,** 867–882 (2006).

300.   Oono, M. *et al.* Transglutaminase 2 accelerates neuroinflammation in amyotrophic lateral sclerosis through interaction with misfolded superoxide dismutase 1. *Journal of neurochemistry* **128,** 403–418 (2014).

301.   Ashour, A.A. *et al.* Elongation factor-2 kinase regulates TG2/β1 integrin/Src/uPAR pathway and epithelial-mesenchymal transition mediating pancreatic cancer cells invasion. *Journal of cellular and molecular medicine* **18,** 2235–2251 (2014).

302.   Chhabra, A., Verma, A. & Mehta, K. Tissue transglutaminase promotes or suppresses tumors depending on cell context. *Anticancer research* **29,** 1909–1919 (2009).

303.   Herman, J.F., Mangala, L.S. & Mehta, K. Implications of increased tissue transglutaminase (TG2) expression in drug-resistant breast cancer (MCF-7) cells. *Oncogene* **25,** 3049–3058 (2006).

304.   Akar, U. *et al.* Tissue transglutaminase inhibits autophagy in pancreatic cancer cells. *Molecular cancer research : MCR* **5,** 241–249 (2007).

305.   Oliverio, S. *et al.* Tissue transglutaminase-dependent posttranslational modification of the retinoblastoma gene product in promonocytic cells undergoing apoptosis. *Molecular and cellular biology* **17,** 6040–6048 (1997).

306.   Johnson, T.S. *et al.* Transfection of tissue transglutaminase into a highly malignant hamster fibrosarcoma leads to a reduced incidence of primary tumour growth. *Oncogene* **9,** 2935–2942 (1994).

307.   Caraglia, M. *et al.* Theophylline-induced apoptosis is paralleled by protein kinase A-dependent tissue transglutaminase activation in cancer cells. *Journal of biochemistry* **132,** 45–52 (2002).

308.   Knight, C.R.L., Rees, R.C. & Griffin, M. Apoptosis: a potential role for cytosolic transglutaminase and its importance in tumour progression. *Biochimica et Biophysica Acta (BBA) - Molecular Basis of Disease* **1096,** 312–318 (1991).

309.   Hand, D., Elliott, B.M. & Griffin, M. Expression of the cytosolic and particulate forms of transglutaminase during chemically induced rat liver carcinogenesis. *Biochimica et biophysica acta* **970,** 137–145 (1988).

310.   Shrestha, R. *et al.* Molecular mechanism by which acyclic retinoid induces nuclear localization of transglutaminase 2 in human hepatocellular carcinoma cells. *Cell death & disease* **6,** e2002 (2015).

311.   Tatsukawa, H. *et al.* Dual induction of caspase 3- and transglutaminase-dependent apoptosis by acyclic retinoid in hepatocellular carcinoma cells. *Molecular cancer* **10,** 4 (2011).

312.   Fok, J.Y. & Mehta, K. Tissue transglutaminase induces the release of apoptosis inducing factor and results in apoptotic death of pancreatic cancer cells. *Apoptosis : an international journal on programmed cell death* **12,** 1455–1463 (2007).

313.   Kósa, K., Rosenberg, M.I., Chiantore, M.V. & Luca, L.M. de. TPA induces transglutaminase C and inhibits cell growth in the colon carcinoma cell line SW620. *Biochemical and biophysical research communications* **232,** 737–741 (1997).

314.   Fukuda, K. Induction of tissue transglutaminase expression by propionate and n-butyrate in colon cancer cell lines. *The Journal of nutritional biochemistry* **10,** 397–404 (1999).

315.   Zhang, J., Antonyak, M.A., Singh, G. & Cerione, R.A. A mechanism for the upregulation of EGF receptor levels in glioblastomas. *Cell reports* **3,** 2008–2020 (2013).

316.   Antonyak, M.A. *et al.* Augmentation of tissue transglutaminase expression and activation by epidermal growth factor inhibit doxorubicin-induced apoptosis in human breast cancer cells. *The Journal of biological chemistry* **279,** 41461–41467 (2004).

317.   Li, B. *et al.* EGF potentiated oncogenesis requires a tissue transglutaminase-dependent signaling pathway leading to Src activation. *Proceedings of the National Academy of Sciences of the United States of America* **107,** 1408–1413 (2010).

318.   Yakubov, B. *et al.* Extracellular Tissue Transglutaminase Activates Noncanonical NF-κB Signaling and Promotes Metastasis in Ovarian Cancer12. *Neoplasia (New York, N.Y.)* **15,** 609–619 (2013).

319.   Park, S.-S., Kim, J.-M., Kim, D.-S., Kim, I.-H. & Kim, S.-Y. Transglutaminase 2 mediates polymer formation of I-kappaBalpha through C-terminal glutamine cluster. *The Journal of biological chemistry* **281,** 34965–34972 (2006).

320.   Jung, H.J. *et al.* Calcium blockers decrease the bortezomib resistance in mantle cell lymphoma via manipulation of tissue transglutaminase activities. *Blood* **119,** 2568–2578 (2012).

321.   Sakamoto, K. *et al.* Constitutive NF-kappaB activation in colorectal carcinoma plays a key role in angiogenesis, promoting tumor growth. *Clinical cancer research : an official journal of the American Association for Cancer Research* **15,** 2248–2258 (2009).

322.   Caccamo, D. *et al.* Nuclear factor-kappab activation is associated with glutamate-evoked tissue transglutaminase up-regulation in primary astrocyte cultures. *Journal of neuroscience research* **82,** 858–865 (2005).

323.   Jana, A. *et al.* NFkB is essential for activin-induced colorectal cancer migration via upregulation of PI3K-MDM2 pathway. *Oncotarget* **8,** 37377–37393 (2017).

324.   Voboril, R. & Weberova-Voborilova, J. Constitutive NF-kappaB activity in colorectal cancer cells. Impact on radiation-induced NF-kappaB activity, radiosensitivity, and apoptosis. *Neoplasma* **53,** 518–523 (2006).

325.   Kumar, S., Kapoor, A., Desai, S., Inamdar, M.M. & Sen, S. Proteolytic and non-proteolytic regulation of collective cell invasion: tuning by ECM density and organization. *Scientific Reports* **6,** 19905.

326.   Aeschlimann, D. & Thomazy, V. Protein crosslinking in assembly and remodelling of extracellular matrices: the role of transglutaminases. *Connective tissue research* **41,** 1–27 (2000).

327.   Jones, R.A. *et al.* Matrix changes induced by transglutaminase 2 lead to inhibition of angiogenesis and tumor growth. *Cell death and differentiation* **13,** 1442–1453 (2006).

328.   Mangala, L.S., Fok, J.Y., Zorrilla-Calancha, I.R., Verma, A. & Mehta, K. Tissue transglutaminase expression promotes cell attachment, invasion and survival in breast cancer cells. *Oncogene* **26,** 2459–2470 (2007).

329.   Akimov, S.S. & Belkin, A.M. Cell surface tissue transglutaminase is involved in adhesion and migration of monocytic cells on fibronectin. *Blood* **98,** 1567–1576 (2001).

330.   Zhao, X. & Guan, J.-L. Focal adhesion kinase and its signaling pathways in cell migration and angiogenesis. *Advanced drug delivery reviews* **63,** 610–615 (2011).

331.   Danielsen, S.A. *et al.* Portrait of the PI3K/AKT pathway in colorectal cancer. *Biochimica et biophysica acta* **1855,** 104–121 (2015).

332.   Luo, J., Manning, B.D. & Cantley, L.C. Targeting the PI3K-Akt pathway in human cancer. *Cancer cell* **4,** 257–262 (2003).

333.   Kotsakis, P., Wang, Z., Collighan, R.J. & Griffin, M. The role of tissue transglutaminase (TG2) in regulating the tumour progression of the mouse colon carcinoma CT26. *Amino acids* **41,** 909–921 (2011).

334.   Zirvi, K.A., Keogh, J.P., Slomiany, A. & Slomiany, B.L. Transglutaminase activity in human colorectal carcinomas of differing metastatic potential. *Cancer letters* **60,** 85–92 (1991).

335.   Cellura, D. *et al.* miR-19-Mediated Inhibition of Transglutaminase-2 Leads to Enhanced Invasion and Metastasis in Colorectal Cancer. *Molecular cancer research : MCR* **13,** 1095–1105 (2015).

336.   Lai, T.-S., Lin, C.-J., Wu, Y.-T. & Wu, C.-J. Tissue transglutaminase (TG2) and mitochondrial function and dysfunction. *Frontiers in bioscience (Landmark edition)* **22,** 1114–1137 (2017).

337.   Kojima, S., Kuo, T.-F. & Tatsukawa, H. Regulation of transglutaminase-mediated hepatic cell death in alcoholic steatohepatitis and non-alcoholic steatohepatitis. *Journal of gastroenterology and hepatology* **27 Suppl 2,** 52–57 (2012).

338.   Datta, S., Antonyak, M.A. & Cerione, R.A. GTP-binding-defective forms of tissue transglutaminase trigger cell death. *Biochemistry* **46,** 14819–14829 (2007).

339.   Yamaguchi, H. & Wang, H.-G. Tissue transglutaminase serves as an inhibitor of apoptosis by cross-linking caspase 3 in thapsigargin-treated cells. *Molecular and cellular biology* **26,** 569–579 (2006).

340.   Melino, G. *et al.* Tissue transglutaminase and apoptosis. Sense and antisense transfection studies with human neuroblastoma cells. *Molecular and cellular biology* **14,** 6584–6596 (1994).

341.   Elmore, S. Apoptosis: A Review of Programmed Cell Death. *Toxicologic pathology* **35,** 495–516 (2007).

342.   Kang, J.H. *et al.* Renal cell carcinoma escapes death by p53 depletion through transglutaminase 2-chaperoned autophagy. *Cell death & disease* **7,** e2163 (2016).

343.   Li, X.-L., Zhou, J., Chen, Z.-R. & Chng, W.-J. P53 mutations in colorectal cancer - molecular pathogenesis and pharmacological reactivation. *World journal of gastroenterology* **21,** 84–93 (2015).

344.   Baker, S.J. *et al.* Chromosome 17 deletions and p53 gene mutations in colorectal carcinomas. *Science (New York, N.Y.)* **244,** 217–221 (1989).

345.   Iacopetta, B. TP53 mutation in colorectal cancer. *Human mutation* **21,** 271–276 (2003).

346.   Goh, H.S., Yao, J. & Smith, D.R. p53 point mutation and survival in colorectal cancer patients. *Cancer research* **55,** 5217–5221 (1995).

347.   Muller, P.A.J. & Vousden, K.H. p53 mutations in cancer. *Nature cell biology* **15,** 2–8 (2013).

348.   Coffill, C.R. *et al.* Mutant p53 interactome identifies nardilysin as a p53R273H-specific binding partner that promotes invasion. *EMBO reports* **13,** 638–644 (2012).

349.   Di Agostino, S. *et al.* Gain of function of mutant p53. The mutant p53/NF-Y protein complex reveals an aberrant transcriptional mechanism of cell cycle regulation. *Cancer cell* **10,** 191–202 (2006).

350.   Debaize, L., Jakobczyk, H., Rio, A.-G., Gandemer, V. & Troadec, M.-B. Optimization of proximity ligation assay (PLA) for detection of protein interactions and fusion proteins in non-adherent cells: application to pre-B lymphocytes. *Molecular cytogenetics* **10,** 27 (2017).

7. Appendix

7.1 Abbreviations

°C	Degree Celcius
µ	Micro
7AAD	7-Aminoactinomycin D
ADP	Adenosin Diphosphate
AKAP13	Protein kinase A protein anchor protein 13
APC	Adenomatous-polyposis-coli-Protein
ATP	Adenosin Triphosphate
BFP	blue fluorescent protein
BMP	Bone Morphogenetic protein
BSA	Bovine Serum Albumin
CAFs	cancer associated fibroblasts
Cas9	CRISPR-associated protein 9
CBC	Crypt basal columnar cells
CC-ICs	Colon cancer initiating cells
cDNA	Complementary DNA
CDS	Coding sequence
CHIP	Carboxyl-terminus of Hsp70-interacting protein
CIMP	CpG island methylator phenotype
CIN	Chromosomal instability
CMV	Cytomegalovirus
CRC	Colorectal carcinoma
CRISPR	Clustered regularly interspaced short palindromic repeats
Cys	Cystein
DEGs	Differentially expressed genes
DMEM	Dulbecco's Modified Eagle Medium
DMSO	Dimethyl sulfoxide
DNA	Deoxyribonucleic acid
Dsh	Dishevelled
E.coli	Escherichia coli
ECL	Enhanced chemiluminescence
ECM	Extracellular matrix
EDTA	Ethylenediaminetetraacetic acid
EGFR	Epidermal growth factor receptor
EMT	Epithelial to mesenchymal transition
EMT	Epithelial to mesenchymal transition
ERK	Extracellular signal regulated kinase

EtBr	Ethidiumbromide
EtOH	Ethanol
FACS	Fluorescence activated cell sorting
FAK	Focal Adhesion Kinase
FBS	Fetal bovine serum
FCS	Fetal calf serum
FDR	False discovery rate
FFA	Free fatty acids
FN	Fibronectin
Fz	Fizzled
g	Gramm
GAPs	GTPase-activating proteins
GDP	Guanosin Diphosphate
GO	Gene ontology
GPCR	G protein coupled receptor
GSEA	Gene set enrichment analysis
GSK3	Glycogen synthase 3
GTP	Guanosin Triphosphate
h	Hour
HBSS	Hanks balanced salt solution
HDAC3	Histone deacetlyase-3
HDR	High-Dynamic-Range
HEK	Human embryonic kidney
Hh	Hedgehog
HIF-1α	Hypoxia-inducible factor 1-alpha
HIV-1	Human immunodeficiency virus type-1
HMECs	Human mammary epithelial cells
i.p.	intraperitoneal
IGF	Insulin-like growth factor
IGFBP-3	Insulin-like growth factor-binding protein 3
IHh	Indian hedgehog
IL	Interleukin
IRES	Internal ribosome entry site
ISC	Intestinal stem cell
IκBα	Nuclear factor of kappa light polypeptide gene enhancer in B-cells inhibitor, alpha
K	Kilo
L	Liter
LB	Lysogeny broth
LDL	Low Density Lipoprotein
Lgr5	Leu-rich repeat-containing G protein-coupled receptor 5
LPS	Lipopolysaccharide binding protein
LRP	Low Density Lipoprotein Receptor-related Protein
m	Milli

M	molar
MACS	Magnetic activated cell sorting
min	Minute
miRNA	Micro Ribonucleic acid
MMR	DNA mismatch repair
MOI	Multiplicity of infection
MPM	Malignant pleural mesothelioma
mRNA	Messenger RNA
MS	Mass spectrometry
MSI	Microsatellite instability
MTI-MMP	Membrane Type 1 Matrix Metalloproteinase
n	Nano
NES	Nuclear export signal
NF-κB	Nuclear factor 'kappa-light-chain-enhancer' of activated B-cells
NICD	Notch intracellular domain
NLS	Nuclear localization signal
o.	Oral
ORF	Open reading frame
p	Pico
PBS	Phosphate buffered saline
PCNA	Proliferating Cell Nuclear Antigen
PCR	Polymerase chain reaction
PD-1	Cell death protein 1
PDAC	Pancreatic ductal adenocarcinomas
PDGF	Platelet derived growth factor
PDGFR	Platelet Derived Growth Factor Receptor
PDI	Protein disulfide isomerase
PEG	Polyethylene glycol
Pi	Inorganic phosphate
PI3K	Phosphatidylinositol 3 kinase
PIGF	Placenta growth factor
PKA	Protein kinase A
PLA	Proximity ligation assay
PTCH	Patched
RA	Retinoic acid
RCC	Renal cell carcinoma
RNA	Ribonucleic acid
RNAi	RNA interference
ROS	Reactive oxygen species
RTKs	Receptor tyrosine kinases
RT-PCR	RT-PCR
SFFV	Spleen focus-forming virus
sgRNA	Small guide RNAs

|	
SHh	Sonic hedgehog
shRNA	Short hairpin RNA
SILAC	Stable isotope labeling by amino acids
SMO	Smoothened
STAT3	Signal transducer and activator of transcription 3
STK36	Serin/threonine kinase 36
TA	Transit-amplifying cells
TAE	TRIS-Acetat-EDTA
TE	TRIS-EDTA
TFT	Transcription factor targets
TGF	Transforming growth factor
TGM2	Tissue Transglutaminase 2
TICs	Tumor initiating cells
TNF	Tumor Necrosis Factor
TPA	12-tetradecanoyl-phorbol-13acetate
Tris	Tris(hydroxymethyl)aminomethane
TTT	Timm's tracking tool
V	Volt
VEGF	Vascuar endothelial growth factor
VHL	von Hippel-Lindau
VSV	Vesicular stomatitis virus
VSV-G	Glycoprotein G of VSV
W	Watt
w/v	Weight per volume
WB	Western Blot
WLS	Wntless
WT	Wild type
YFP	Yellow fluorescent protein

7.2 Vector maps
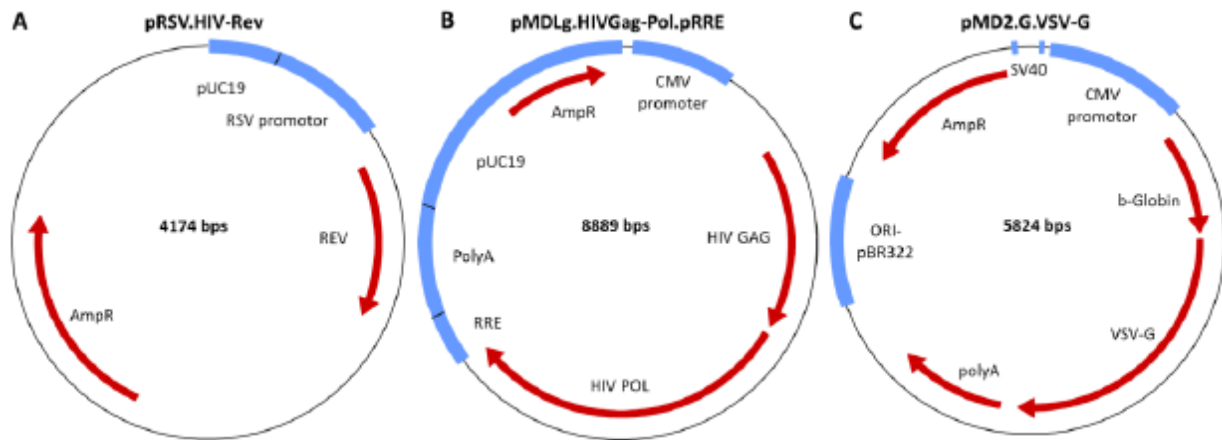
Figure 25 Plasmids for virus production

(**A**) Expression plasmid pRSV.HIV-Rev for lentiviral reverse transcriptase (*REV*) of HIV-1; driven by RSV promoter

(**B**) Expression plasmid pMDLg.HIVGag-Pol.pRRE for structural genes (*gag/pol*) of HIV-1 for lentiviral particle assembly.

(**C**) Expression plasmid pMD2.G.VSV-G for VSV-G (*env*) for pseudo typing of lentiviral particles. RSV: Rous sarcoma virus promoter; CMV: cytomegalo virus promoter; Amp: Ampicillin Resistence gene; HIV: human immunodeficiency virus; RRE: Rev response element; VSV-G: glycoprotein G of VSV. Provided by Axel Schambach, Hannover Medical School.
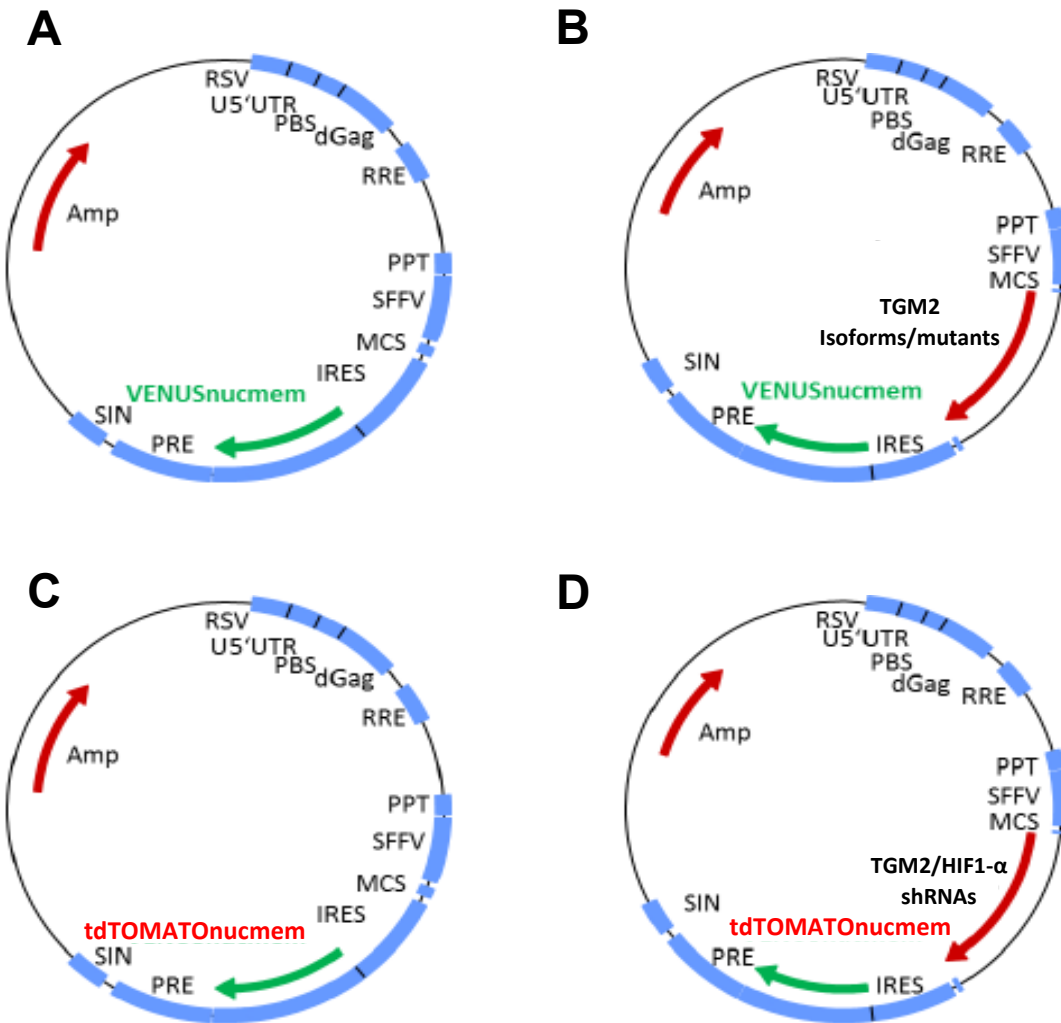
Figure 26 Lentiviral plasmids

(**A**) pRRL.PPT.SFFV MCS IRES-Venusnucmem pre

(**B**) pRRL.PPT.SFFV TGM2 Isoforms/mutants IRES-Venusnucmem pre

(**C**) pRRL.PPT.SFFV MCS IRES-tdTOMATOnucmem pre

(**D**) pRRL.PPT.SFFV TGM2/HIF1-α shRNAs IRES- tdTOMATOnucmem pre

(**A-B**) Lentiviral expression vectors for the ectopic expression of control, TGM2 Isoforms and mutants

(**C-D**) Lentiviral expression vectors for shRNA expression to silence TGM2 or HIF1 expression
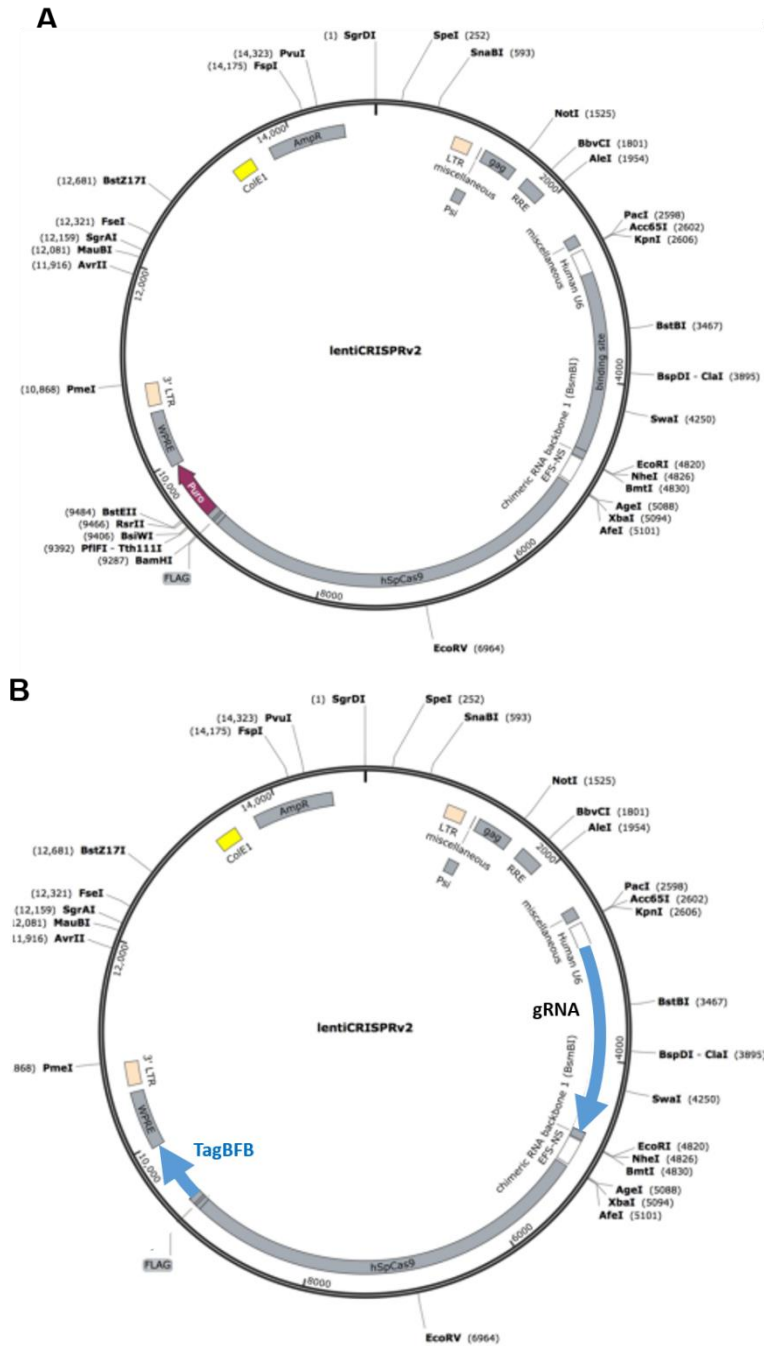
Figure 27 Lentiviral CRISPR plasmids

 (**A**) LentiCRISPRv2-MCS-TagBFB
(**B**) LentiCRISPRv2-TGM2-sgRNA a/b-TagBFB
(**A-B**) Lentiviral expression vectors for the CRISPR expression of control, and TGM2-sgRNAs to knockout TGM2 expression

7.3 ImageJ Macro for PLA analysis

```
imageName = getTitle();
run("Split Channels");
selectWindow(imageName + " (blue)");
selectWindow(imageName + " (red)");
selectWindow(imageName + " (blue)");
run("Smooth");
run("Median...", "radius = 2");
setAutoThreshold("Default dark");
//run("Threshold...");
setOption("BlackBackground", false);
run("Convert to Mask");
selectWindow(imageName + " (blue)");
run("Close-");
run("Open");
run("Watershed");
run("Sharpen");
run("Clear Results");
run("Analyze Particles...", "size = 75Ð550 show = [Overlay Outlines] exclude clear add");
selectWindow(imageName + " (red)");
run ("Find Maxima...", "noise = 60 output = [Single Points] exclude");
selectWindow (imageName + " (red) Maxima");
run ("Divide...", "value=255");
run ("Set Measurements...", "area integrated redirect = None decimal = 3");
roiManager("Measure");
String.copyResults();
selectWindow (imageName + " (red) Maxima");
close();
```

Adapted from Debaize et al.[350]

7.4 Curriculum vitae

M.Sc. Ilaria Lunger

Contact

Anna-Beyer-Str. 6

60435 Frankfurt am Main

ilaria_lunger@hotmail.com

Personal data

Date of birth	19. 03 1985
Place of birth	Meran
Nationality	Italian

Academic education

04/2015-06/2018	**PhD student in the group of Prof. Dr. Michael A. Rieger at the LOEWE Center for Cell and Gene Therapy, University hospital Frankfurt –** Department for Hematology/Oncology, Frankfurt am Main: "Transglutaminase 2 is required for the survival and tumorigenicity of colorectal cancer cells through its transamidase activity by blocking p53 signaling"
01/2014 - 04/2015	**Research assistant in the group of Prof. Dr. Michael A. Rieger and Dr. Patrizia Malkomes, LOEWE Center for Cell and Gene Therapy** - Department for Hematology/Oncology, Frankfurt am Main
09/2013	**Thesis Master of Science in molecular cell- and developmental biology** - Leopold Franzens University Innsbruck
08/2011 - 09/2013	**Research visit in the group of Prof. Dr. Volknandt** – Department for neurochemistry, Institute for cell biology and neuroscience, Goethe University Frankfurt
09/2010 - 02/2011	**Master of Science - Studies molecular cell and developmental biology** - Leopold Franzens University Innsbruck
10/2006 - 09/2010	**Bachelor of Science Biology - Leopold-Franzens-University Innsbruck**
09/1999 - 06/2004	**Matura (Abitur) – Gymnasium "Marie Curie"; Fachrichtung Biotechnologie**

Honors and Awards

09/2014	**Best Poster research award**, LOEWE Institute for Cell and Gene-therapy
09/2014	**Best Poster Award**, University Center for Tumor diseases (UCT)

Skills

Training courses	"**Leadership for young scientists**" with Rob Thomson, RTTA **-** soft skills for real results
	"**Advanced Project management**" with Dr. Thomas Teichler, Lead to Trust
	"**Science communication**" Science in dialogue with the Ludwig Boltzmann society and the Vienna University of Technology
Languages	**German**, native
	Italian, business fluent
	English, business fluent

Publications

Single cell-analyses to reveal hematopoietic stem cell fate decision
Lunger I, Fawaz M, Rieger MA. FEBS Lett. 08/2017, DOI: 10.1002/1873-3468.12712

Selektive AKT inhibition by MK-2206 Represses Colorectal Cancer-Initiating Stem Cells
Malkomes P, **Lunger I**, Luetticke A, Oppermann E, Haetscher N, Serve H, Holzer K, Bechstein WO, Rieger MA. Annals of Surgical Oncology 04/2016 DOI: 10.1245/s10434-016-5218-z

The Proteome of the presynaptic active zone from mouse brain
Weingarten J, Lassek M, Mueller BF, Rohmer M, **Lunger I**, Baeumlisberger D, Dudek S, Gogesch P, Karas M, Volknandt W. 02/2014 Molecular and Cellular Neuroscience DOI: 10.1016/j.mcn.2014.02.003